Universitetet i Stavanger

**DET TEKNISK-NATURVITENSKAPELIGE FAKULTET**

# MASTEROPPGAVE

| | |
|---|---|
| Studieprogram/spesialisering:<br><br>Environmental technology, specialization offshore environmental engineering | Vår semesteret, 2012<br><br>Åpen / Konfidensiell |
| Forfatter:<br>Anne Kristine Norland | ……<br>(signatur forfatter) |
| Fagansvarlig: Malcolm Kelland<br><br>Veileder(e): Anders Grinrød | |
| Tittel på masteroppgaven:<br><br>Engelsk tittel:<br>Organic flow assurance<br>- Pour point depressant development through experimental design | |
| Studiepoeng: 30 | |
| Emneord:<br>Wax<br>Pour point depressants<br>Design of experiments<br>Design Expert<br>Viscosity measurements | Sidetall: 92<br><br>Stavanger, 29.06/2012<br>dato/år |

# Organic flow assurance

## Pour point depressant development through Experimental Design

**Anne Kristine Norland**

**Vår 2012**

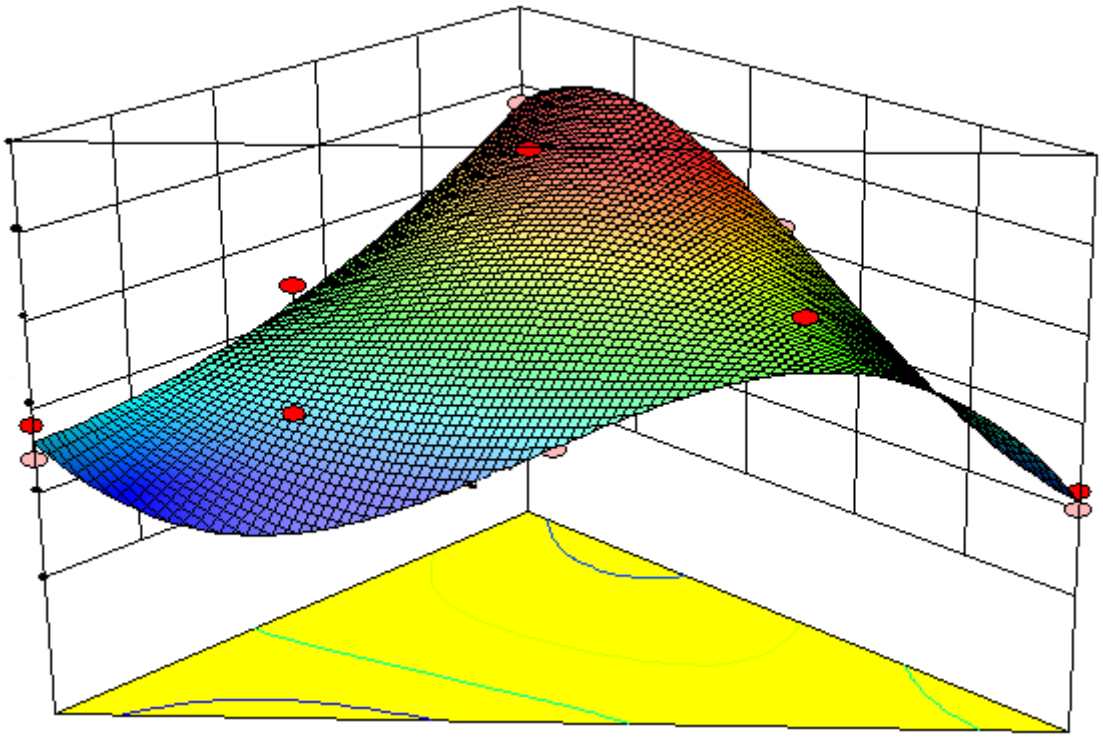

# *Abstract*

Flow assurance is of great importance in the oil and gas industry, where the main objective is to provide and secure the transport of the well stream fluid from the reservoir to the process facilities. The main challenges in flow assurance are solid depositions in the pipelines, which can lead to reduction in the production, or in worst case completely block the pipelines.
Wax deposition is a common problem in the oil industry, especially with cold and deep offshore fields. Waxes are long alkane chains found in the crude oil, which can begin to precipitate and form deposits in the pipelines when the temperature decreases during production.
There are applied different methods for preventing and removing wax depositions, such as mechanical removing, heat application or chemical prevention.
The application of wax inhibitors is an effective method to prevent wax depositions, and in this thesis a common group of chemicals called pour-point depressants (PPDs) are tested. The PPDs are polymers consisting of a polymer backbone with long alkyl side chains attached, which are meant to interfere with the wax crystals and prevent further growth.
The focus of the thesis is to use a statistical method called design of experiments (DOE) to find the best formulation for a group of PPDs known as acrylate ester polymers. There were performed two analyses with one mixture containing acrylate ester polymers where there were synthesized different percentages of alkyl side chains of 16 carbons, 18 carbons, and 22 carbons length on the polymer backbone. The other mixture contains different percentages of acrylate ester polymers, which had alkyl side chains of either 16 carbons, 18 carbons or 22 carbons length.
A software program called Design-Expert was used to perform the two DOE analyses. Design-Expert managed to quick and simple come up with a systematic plan for the minimum number experiments needed, to find the optimal formulations for the two mixture analyses.
The performances of the different PPDs were measured by a viscometer, where the effect of the PPDs was how well they managed to displace the temperature for then the wax started to precipitate and cause gelling of the crude oil. The results from the viscosity measurements were analysed in Design-Expert, which provided a response surface graph where the optimum effects of the different PPDs combinations could be easily found from.
The results from the response surface graphs and the optimization points for the two analyses showed similar results. The best interaction of the different alkyl side chains length on the polymers were in general found to be with different percentages of 16 carbons and 18 carbons, with an increasing optimum towards polymers containing only 18 carbons. The optimal formulations were made and their effect tested on the viscometer. However, none of the results corresponded well to what the response surface graphs had indicated, and were in general much lower than expected. Overall the different DOE analysis did not manage to find an optimal combination for the different components in the mixtures, which were any better than acrylate ester polymers with 18 carbons alkyl side chains alone.

# *Acknowledgments*

I wish to thank all those who helped me with the work in my master thesis.
I like to especially thank my supervisor, Anders Grinrød, who has given me this great opportunity to work at Mi SWACO for my thesis project, and for being there through the whole process giving me help and guidance.
I would also like to thank, Malcolm Kelland, for his incredible commitment to his students, and for helping me in the process in writing the thesis.
I would also like to thank, Astrid Lone, for taking the time to help and assist in the laboratory work.
I really appreciate all the support you all have given me to complete this thesis.

# Table of Contents

# *1. Introduction to organic deposition- Petroleum wax*

Flow assurance is a critical and costly task in the oil and gas industry, especially when operating offshore. Flow assurance means to provide and secure the transport of the well stream fluid from the reservoir to the process facilities. The well stream fluid is a multiphase mixture fluid that mainly consists of oil (liquid hydrocarbons), gas (gaseous hydrocarbons) and water [1]. During the production the transport of the multiphase fluid can cause different problems downhole and in the flow lines, such as:

- Organic depositions, such as wax and asphaltene.
- Scale deposits caused by different inorganic salts.
- Formation of gas hydrates, due to mixing of water and hydrocarbons.
- Corrosion damage to the pipelines and associated equipment, due to high water cut.

Flow assurance is designed to identify, quantify and reduce the challenges with the flow risks, such as solid depositions, to avoid the reduction of the well stream flow, or in worst case complete clogging of the flow lines leading to production stop [2]. A severe deposition problem can have an enormous economic effect on the oil companies, hence different prevention and remediation methods for the deposition problems have been developed, and still being further improved as new and more difficult oil fields are being exploited.
This thesis focuses on the organic deposition of wax, and the prevention of this problem with the use of chemical wax inhibitors, mainly as pour-point depressants.

**Figure 1 Subsea production system [3].**

## *1.1 Organic deposition*

The wax and asphaltene make up the organic deposition of the petroleum fluid, and is a common problem that has created many challenges for the oil industry. Most of the problems arise with the transport of the well stream fluid from the reservoir through the processing systems, where the depositions can lead to formation damages, and clogging to the tubular string, wellhead, flow lines and surface equipment.

In recent years the development of new oil fields have become more challenging due to the exploration in more difficult climates, which especially applies for offshore operations with increasing water depth and colder environments. The new oil fields are often tied back to exiting platforms through subsea multiphase flow lines (figure 1), which creates longer distances for the well stream fluid to be transported. These conditions can lead to a higher temperature decline and pressure drop in the well stream fluid over a longer time period, and thereby challenges the flow assurance. When the well stream fluid is transported from the reservoir, and up to the surface these physical changes occurring can alter the chemical characteristics of the well stream fluid, such leading to serve organic deposition problems as seen in figure 2 below[4].

**Figure 2 Wax deposition in pipeline (Hydrafact)**

## *1.2 Asphaltene*

Asphaltene is a heavy organic component in the crude oil, and can present a big challenge to the oil production if it deposits in the flow lines. The asphaltene in the crude oil consists of various polyaromatic structures with aliphatic chains, which contains heteroatoms such as sulphur, nitrogen, oxygen and different metals such as nickel, vanadium and iron. A general definition used for asphaltene in crude oil is that it is insoluble in light aliphatic hydrocarbons such as pentane and heptanes, but soluble in aromatic solvents such as toluene [1].

Asphaltene can be present in crude oil in different amount, depending on the crude oil. However the deposition of asphaltene is not dependent on how much asphaltene there is present in the crude oil, but on the stability of the asphaltenes in the crude oil and on the crude oil itself [5]. In the reservoir the asphaltene will exists as individual asphaltene molecules or aggregates, and be soluble in the crude oil due to the high pressure. Disturbance to the stability of asphaltene can for example be the

pressure drop created when the oil production starts. When the pressure drops, the lighter hydrocarbons and other gases, which acts as solvent for the asphaltene in the crude oil, will go out from the solution and into the gas phase. This will leave the remaining crude oil less polar, which can then cause the asphaltene to associate and flocculent together, causing severe deposition problems. Compared with wax deposition the mechanism and control methods for asphaltene deposition are quite different, but both components are often found deposited together. However a small amount of asphaltene present in the crude oil can actually reduce the wax deposition significantly [6].

## *1.3 Wax*

The wax deposition problems have over the years gained more importance in the oil industry, as new oil fields are being developed in more hostile environments. The challenges with the wax deposition are the transport of the crude oil in deepwater pipelines, where the temperatures are low. In the reservoir the waxes will exist in the liquid phase of the crude oil, due to the high pressure and temperature, however under standard conditions waxes will be present as solids. When the production starts the pressure and especially the temperature changes can lead to wax precipitation inside the wall of the flow lines. If not treated the wax deposition can eventually reduce or in worst case block the well stream flow [2, 7].

### 1.3.1 Wax Characterization

The petroleum wax/paraffin are long hydrocarbon chains found naturally in crude oils and condensate, and contain at least 15 or more carbon atoms. These molecules can be either straight or branched hydrocarbon chains, and can contain some cyclic and/or aromatic hydrocarbons, as seen in the wax molecule examples in figure 3 below [1].

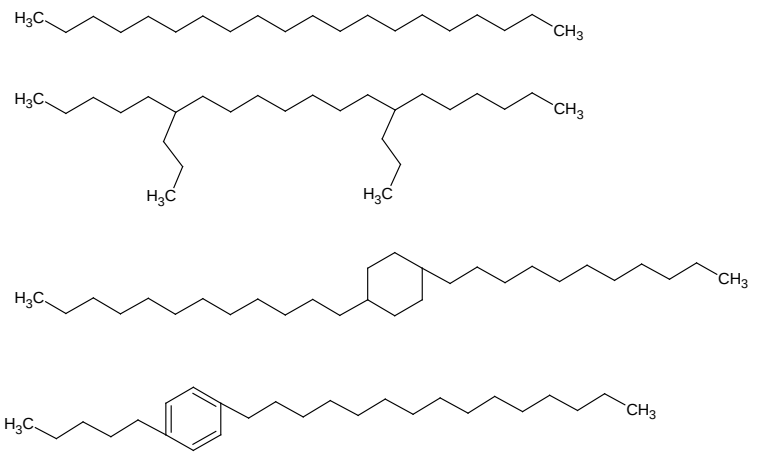


**Figure 3 Different wax molecule structures, straight, branched, cyclic and aromatic.**

The severity of the wax deposition problems are related to the crude oil and the molecular composition of the wax molecules. The waxes in crude oils are often more difficult to control compared to those found in condensate, because the alkane chains are often longer in the crude oil than in the condensate, which consists of lighter hence shorter hydrocarbons.

It is generally the long straight hydrocarbon chain (*n*-paraffin) in the crude oil that causes deposition problems in the production pipelines. These are wax molecules with 25-50 or even longer carbon chains, which forms clearly defined and needle-shaped macrocrystalline waxes when precipitated. These hard crystalline waxes are difficult to remove, and are the main components responsible for the blocking of the pipelines.
When the crude oil contains wax molecules with 16-25 carbon atoms or branched wax molecules, it will generally form a microcrystalline structure. This will result in a more soft mushy wax, which is the major contributing factor to tank bottom sludge.
The structure of the wax molecules, straight or branched, and the presence of cyclic and aromatic hydrocarbon rings, will have a significant effect on the melting point, boiling point and solubility of the waxes in the crude oil. However in general the melting point of the waxes is normally increasing as the molecular size of the waxes increases. Thus as higher melting point a wax have, the more difficult it is to keep the wax from depositing [1, 6, 7].

### 1.3.2 Wax crystallization process

The precipitation of the wax molecules occurs when the temperature of the crude oil decreases below the wax appearance temperature (WAT), or sometimes called cloud point. This is the temperature when the first wax crystal begins to precipitate out from the crude oil. The crystallization of the wax molecules can further develop an ordered solid structure, which traps the crude oil causing it to experience a gel consistence with low flow ability. The crystallization process can be divided into two stages called nucleation and growth.
When the temperature decreases the molecular motion of the molecules in the crude oil are being hindered, due to less energy to move around freely. This will make it easier for the wax molecules to come closer and aligned together, and eventually attached to each other and reach a critical and stable size. The cluster of the wax molecules is called nuclei, and the formation process nucleation. The nuclei will be stable as long as the temperature is below the melting point for the wax, however increasing the temperature the nuclei structure will be disrupted by thermal motion. Once the nuclei is formed and the temperature is kept low, more wax molecules will precipitate and continue to grow on the nucleation site, which is referred to as the growth process.
The nucleation process can be further characterized as either homogeneous or heterogeneous. Homogeneous nucleation refers to the formation of a pure nuclei cluster, which means that the wax molecules have spontaneously and randomly crystallized together forming a stable wax nucleus. Heterogeneous nucleation happens when there are provided an active site for the nucleation process to occur, caused by impurities in the solution. The latter process is the most common nucleation process for crude oil, because crude oils normally contains a lot of impurities such as asphaltenes, formation fines, clay and corrosion products, which can act as a nucleation site for the wax crystals[8]. However asphaltenes present in the crude oil have also shown to inhibited wax deposition, because they will disrupt the growth process of the wax crystallization network, and thereby increase the mobility of the crude oil [6].

### *1.3.3 Wax deposition mechanisms*

The most important factor governing the wax deposition is the reduction in the temperature of the crude oil, due to the cooling of the flow lines by the cold seawater. The flow rate of the well stream fluid in the flow line is important to the settling of the wax crystals on the wall surface, and the stripping of wax depositions off the pipeline walls. The surface properties of the pipeline also play an important role. If the surface material is rough this can lead to more wax crystal adhering to the surface wall, and thereby increasing the deposition [7].

There have been done a lot of studies to explain the mechanisms for the wax deposition. It is important to get a better understanding of the wax deposition process, and be able to manage and control the wax deposition problems that may occur. Many different wax deposition mechanisms have been proposed, such as molecular diffusion, Brownian diffusion, shear dispersion and gravitational settling [9]. However the mechanisms are still not fully confirmed, but molecular diffusion and shear dispersion are regarded as the primary wax deposition mechanisms [1, 10]:

- Molecular diffusion mechanism:
  The wax starts to precipitate when the temperature of the pipeline surface becomes lower than the WAT of the crude oil. The crude oil near the wall surface will crystallize and adhere to the surface wall, which will create a concentration gradient between the wax concentration near the pipeline wall and wax concentration in the bulk liquid. The concentration gradient means that the wax molecules will move from high concentration to low concentration. The low wax concentration is towards the pipe wall, due to the wax precipitating out of the solution and deposits on the pipe wall. The molecular diffusion mechanism has widely been accepted as the dominant wax deposition mechanism.

- Shear dispersion mechanism:
  The well stream flow does normally experience a difference in the velocity, depending on where in the fluid it is being measured. The bulk fluid will often have a higher velocity compared to the fluid near the pipe wall, due to the friction between the fluid and the wall. Already precipitated wax near the pipe wall will therefore move to the pipe wall where the velocity are lower and deposit. However increasing the pumping pressure will increase the shear rate, thus decreasing the wax deposition rate. Figure 4 below shows an illustration of the concept of the different velocity profiles that can be experienced in the flow lines, laminar flow and turbulent flow, which depend on the pressure applied to the well stream flow. High shear environment, found in turbulent flow, will disrupt the adhering and growing of wax deposits on the pipe wall. While low shear environment, laminar flow, will cause the wax molecules to easily adhere to the pipe wall, and cluster together [8].

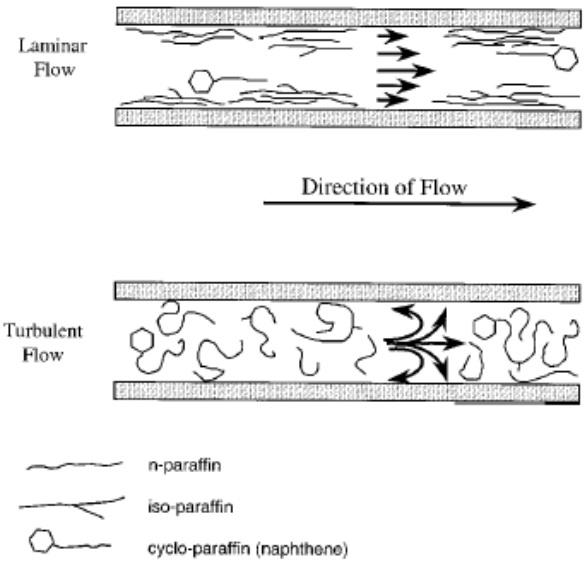


**Figure 4 The velocity profile for laminar and turbulent flow for the crude oil in the pipelines [8].**

## *1.3.4 Wax causing problems*

The wax deposition problems occur when the temperature of the crude oil decreases below the WAT. The WAT is different for each crude oil, and is dependent on the pressure and the crude oil composition. The concentrations of light ends in the crude oil have a significant effect on the WAT, because they act as a solvent for the wax in the crude oil. The light ends are light hydrocarbons, such as methane and ethane, and other gases, such as $CO_2$ and $N_2$. When the pressure is reduced this can lead to the release of the light ends to the gaseous phase [11]. A decrease in the light ends can thereby reduce the solubility of the wax in the crude oil, resulting in an increase in the WAT.
When the WAT increases the temperature at which wax begins to precipitate gets higher, and it can be as high as 50 °C for some oils. In deepwater flow lines the temperature is usually low, and if the distance from the reservoir to the process facilities is long, the cold seawater will eventually start to cool the well stream flow, leading to wax precipitation inside the flow line walls. The three major problems associated with the wax crystallization of the crude oil are [1, 7]:

- High viscosity and pressure loss of the crude oil flow.
  When the wax begins to crystallize this will result in higher viscosity of the crude oil and loss of the pressure in the pipeline, which can reduce the effective capacity of the line. A high viscosity and wax deposition in the flow lines will require a higher pumping pressure to ensure flow of the crude oil, however severe gelling of the crude oil can in worst case lead to production stop.

- High yield stress for restoring the flow.
  When the crude oil is allowed to be stored in the pipeline over a time period, such as during shut-in, the crude oil can be cooled down to below the pour-point. The pour point is the temperature at which the crude oil begins to gel, causing no movement of the crude oil. At the pour-point a high extent of wax crystallization has resulted in a wax crystal matrix, which traps the liquid crude oil and prevents it from flowing. The wax crystal matrix is formed when

the waxes precipitate out as plate like crystals, which interact with each other and form a 3-dimensional structure. The temperature where the crude oil begins to gel is often 10-30 °C below the WAT. To restore the flow of the crude oil a high pressure must be applied to break the gel. However sometimes the pressure needed to resume the flow is not great enough, leaving the pipeline chocked.

- Deposition of wax crystals on surfaces.
  If the flow lines are cooled to the temperature below the WAT, the wax in the crude oil near the pipeline can start to precipitate and deposit on the wall surface. The build up of the wax deposit inside the pipeline wall will cause a reduction in the well stream flow, due to a smaller pipeline diameter and roughness of the pipeline surface (figure 5).

**Figure 5 Wax precipitation inside pipeline wall [12].**

## *1.4 Wax treatment techniques*

In flow assurance the most important task is to maintain the well stream flow, and prevent any blockage from occurring that can stop the production. In order to sustain an optimal production at all time, thoroughly analysis and research have to be implemented in the planning phase of a field, to achieve better understanding and predict any possible challenges that can occur. This include important knowledge about pressures, temperatures, flows, fluid samplings, solid samplings and laboratory testing, which will all be helpful in determining the processes that can take place in the flow lines, and be able to come up with solutions to the challenges that may arise. In most cases the flow assurance solutions would add a substantial amount of cost for the project, however these costs would be small compared to loss caused by reduction or shutdown of the production due to pipeline blockage [13].
The problems related to wax deposition are often associated with deepwater flow lines, and tend to involve more difficult flow assurance challenges. However there have been evolved numerous techniques to remove and reduce the build-up of wax deposition downhole and in the flow lines. Many of the methods have achieved great results when applied, however their success rate is dependent on the wax composition and crude oil found in the specific reservoir, and therefore will vary for the different fields. In many cases a combination of two or more treatment methods have been used to more efficiently remove and reduce the wax depositions.

The wax treatments techniques are divided into two categories, the wax removal techniques and the wav prevention techniques [12].

## *1.5 Wax removal techniques*

The most common methods used for removing already deposit wax are by mechanical removal, heat application, and chemical removal. However some of these techniques are also regarded as wax preventive techniques, such as with heat application.

### *1.5.1 Mechanical removal*

Pigging is the first widely used mechanical removal technique used to remove wax deposits formed at the pipeline walls, and is a good and cost effective method. However in recent years more difficult offshore fields have been exploited, where deep and long tieback pipelines are being applied, which have lead to more extensive wax problems. These conditions have required more frequent cleanings, thereby making pigging a difficult and costly operation. In many fields it is therefore usual to perform pigging in combination with for example wax inhibitor chemicals or hot oil [2, 12].
The pigging operations are performed by using a scraper or cutter, which will scrape the wax deposition of the walls inside the pipelines. There are developed different types of pigs with different shapes and materials, which will have profound effect on the wax removal performance. The most conventional used pigs are disc, cup and polly, which all have different wax removal performance depending on the wax hardness and thickness. The frequency of the pigging operations depends on the severity of the wax depositions, and can vary from weeks to months. However to much wax deposition in the flow lines will require more pressure to operate the pig, and too much wax cuttings in the flow lines can reduce or block the well stream fluid [14].

### *1.5.2 Heat application*

Different thermal solutions for removing or reducing wax deposition have shown to be successful for flow lines in deepwater fields. Active heating has especially been regarded as an efficient flow assurance solution against wax, due to the advantages to control the temperature above the formation region [15]. Figure 6 below shows an overview of the different thermal management systems used to control the temperature of the well stream flow in the flow lines. The thermal management system is normally broken down to passive insulation and active heating. Passive insulation is mainly techniques used to prevent the warm well stream fluid to lose it heat by using different insulation methods. Active heating use external sources to heat the flow lines to keep the temperature of the well stream fluid above the wax deposition temperature, with the use of electrical heating or hot fluid. Active heating makes it possible to maintain the temperature through the production, however in long flow lines the operational cost can become very high [16].

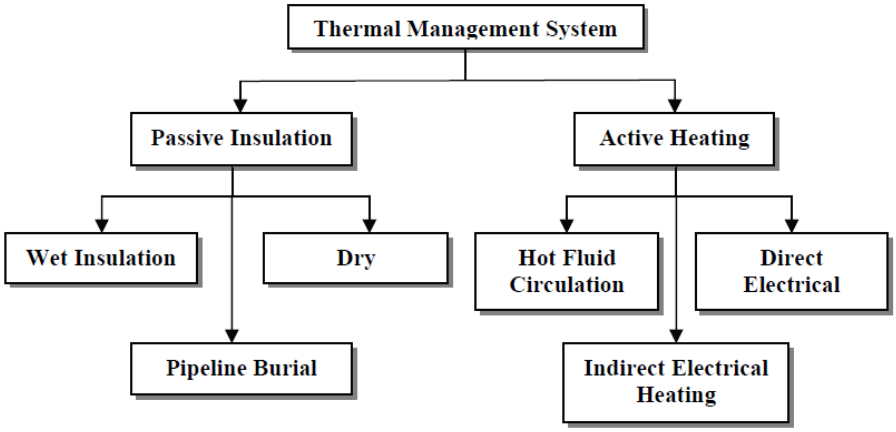


**Figure 6 The different heating methods used for oil and gas fields [16].**

## *1.5.3 Wax removing chemicals*

There are many different types of chemicals that can be used to remove wax depositions, and several methods on how to apply them. The most common chemical methods used in the oil and gas industry as a removal technique are hot oiling and wax solvents. The application of thermochemical packages are a more controversial wax removal technique.

### *Hot oiling*

The hot oiling is a technique that has been used a lot in the early days in the oil and gas industry for removing wax depositions downhole and in the flow lines. In the process hot oil is heated to a temperature above the melting point for wax and then pumped into the well, normally through the annulus space. The heated oil will circulate around the tubing and melt the wax deposits inside the tubing, and then be brought back to the surface via a heating system in the production tubing. As a result of the process the melted wax inside the tubing will be transported with the well stream fluids through the flow lines to the production facilities. During the hot-oil process a wax dispersant is usually added to the crude oil, to enhance the dispersion of the melted wax with the crude oil.
The hot-oil technique is a fast and simple method, which will effectively remove the wax deposition. However this method can be dangerous, especially when applied to wells that have crude with low flash point. There have been operations where the hot-oil has been replaced with steam or hot water to melt the wax, but is rarely used due to risk of corrosion and emulsion problems.
The hot-oiling method is not usually used in subsea flow lines, due to the high expenses related to heating the oil. There have also been reports showing formation damage due to the hot-oiling [1, 17, 18].

### *Wax Solvent*

The adding of solvent downhole and to the flow lines have shown to be effective to remove wax depositions, as it will help to resolve the precipitated wax and make it easier to transport the crude oil to the surface [19].

The different solvents have different abilities to dissolve wax deposits, which depends on the wax, the location in the system and the temperature. Normally the solvents are applied in frequent batch treatments or continuously. Aliphatic and aromatic solvents are the two main groups of solvent used on the oilfields. The aliphatic solvents are straight or ring formed hydrocarbons, and the most common aliphatic solvent used are diesel, kerosene and condensate. The aromatic solvents are chemical containing a carbon ring with delocalized electron double bonding, such as xylene and toluene, which are the most popular solvents used today (figure 7)[20]. A mixture of xylene or toluene together with an aliphatic solvent has shown to increase the wax removal. Adding a surfactant can also enhance the performance of the solvent by helping it to disperse the waxes [21]. In sub-sea systems or cold climates solvents alone may not be effective, and usually have to be used in combination with other methods, such as hot oiling. More faster and effective wax removal has been achieved by heating the xylene and toluene solvent when employed [1, 18].
Other solvent that have been applied with good success are benzene, chlorinated hydrocarbons, and carbon disulfide. However many of the solvents used are not environmental friendly and some highly toxic. Many also possess dangerous risks related to low flash points, such as the aromatic solvents, and corrosion problems, as seen with chlorinated hydrocarbons [22].

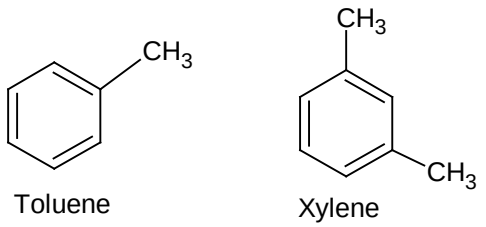


**Figure 7 Aromatic wax solvent, toluene and xylene.**

## *Thermochemical packages*

Thermochemical packages are wax removal methods that utilizes the heat of an exothermic reaction to melt the wax deposits downhole or in subsea flow lines. A common reaction used is the acid-catalyzed decomposition of ammonium nitrate. The reaction starts by mixing a sodium nitrate and ammonium nitrate or chloride in an aqueous solution, in the presence of HCl as catalyst, as shown in the reaction equation in figure 8. There will be developed huge amount of heat as the reaction rate increases, which will be transported upwards the pipelines and melt the waxes. The reaction is controlled by keeping the pH in range between 5.0 and 8.0. However keeping the reaction under control is very important, as the reaction can cause great risks to the pipelines and materials, or worst case damage the pipeline system [1, 23].

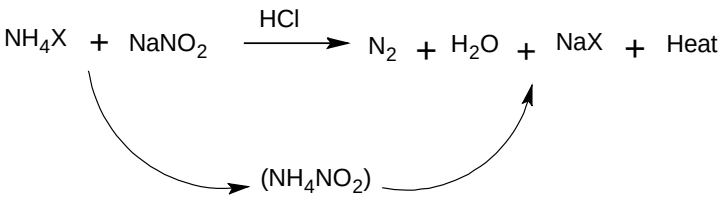


**Figure 8 The thermochemical reaction used as wax deposition removal.**

## *1.6 Wax preventive techniques*

The wax preventive techniques are different solutions intended to prevent the wax from precipitate and deposit in the flow lines. The preventive solutions can be as simples as [12]:

- Increasing the pipeline pressure, which will lead to an increase in the shear rate, thereby making it harder for the wax to deposit inside the pipeline walls.
- Insulate or bury the flow lines, so that no heat will be lost from the well stream fluid, thereby keeping the temperature above the WAT. Different insulation materials used are polypropylene foam, rubber, glass and plastic, which have all low heat transfer coefficients, assuring less heat lost to the surroundings. Burying the flow lines will be effective due to the high heat capacity of the soil, which will absorbed and store the heat from the flow lines [16].
- Coating the inside of the flow lines with a material that will keep the wax from adhering on the pipeline wall. Types of coating material that have been proposed are plastic pipes or plastic-coated pipes. These have shown to decrease the deposition rate on the pipeline walls. However when a layer of wax deposition have covered the pipe, the growing rate will be the same as for steel pipelines [2].

Besides from the preventive techniques mention above there are also other preventive techniques which are more controversial methods, such as cold flow, magnetic fluid conditioning and microbial prevention. Some of these methods have given varied results when applied, therefore more research is needed. However these methods are more environmental friendly as there are no chemicals released.

- Cold flow
  Cold flow is a new technology that is being exploited as a method for removing wax deposition in deepwater and cold oilfields. The method approach is to decrease the temperature of the bulk fluid, to prevent the temperature gradient in the flow lines, and thereby stop the wax precipitate from depositing on the pipeline walls. The whole well stream fluid will be cooled down to the temperature of the surrounding seawater, thereby making the wax precipitate inside the bulk fluid and be transported as solid dispersion within the well stream fluid [24].However further investigation needs to be done to work out how to effectively cool down the well stream fluid, and how to transport the cold well stream fluid to the surface without causing severe gelling in the flow lines [25].

- Magnetic fluid conditioning (MFC)
  The MFC technology uses magnets and electromagnets to prevent wax depositions, usually downhole. The techniques utilizes a magnetic field to alter the kinetics of the precipitated wax, which disturbs the wax crystal agglomeration process, making it harder for wax to precipitated and grow into larger crystals [26]. Studies have shown that the WAT have not been change by the MFC technique, but it had an effect on the viscosity of the crude oil. There is still little information about the mechanisms for this technique, and there have been a variety of claims about the success rate for the method [27].

- Microbial prevention
  The use of selectively isolated bacteria have shown to be an effective and environmental friendly method to both remove and prevent wax deposition in flow lines [28]. The selected microbes used are called paraffin degrading bacterial (PDB). These are tough bacteria that can survive the extreme conditions found in the reservoir, well tubular, and surface flow lines, with the varying temperatures, pressures and anaerobic environment (no oxygen present). The microorganisms mechanism are to biodegrade the long wax molecules into smaller components, which thereby prevents wax precipitation or deposition in the flow lines. The mechanism will cause a decrease in the WAT as a result of the breakdown of the wax molecules, which will decrease of the wax content in the crude oil. The breakdown into smaller hydrocarbons will also reduce the viscosity of the crude oil, and increase the API of the oil. The API is a measurement of how light or heavy oil is compared to water. The bacteria can also form a bio-film layer inside the pipeline wall, which will avoid wax from adhering to the pipeline wall [29].

## *1.7 Chemical wax prevention*

In the recent years there has been more focus on using chemical prevention against wax deposition to minimize transportation problems with waxy crude oils. These wax reducing chemicals are added early to the well stream fluid, normally by injection at the wellhead or downhole. Here their present will affect the wax crystallization and growth process of the crude oils, which will occur as the temperature of the well stream fluid decreases during the transportation in flow lines.
In many cases the application of wax preventive chemicals alone will not fully manage to prevent wax depositions in the whole flow lines, however they can reduce the frequency of other wax removing techniques, such as mechanical removal [1].
There are mainly three different preventive chemicals used against wax deposition:

- Wax dispersants
- Inhibitors or wax crystal modifiers
- Pour-point depressants (PPDs) or flow improvers

Wax dispersants are surface active chemicals, which prevent wax deposition by reducing their tendency to adhere to the pipeline walls, and by keeping the precipitated wax dispersed as separated particles [30].The preventive mechanisms for wax dispersants are quite different compared to the mechanisms for the wax inhibitors and PDDs.
The wax inhibitors are chemicals referred to as wax crystals modifiers, and will affect the WAT for the crude oil. While the PPDs are chemical that affects the pour-point, which will reduce the gelling of the crude oil as the temperature decreases, and thereby improve the flow. However for both of these classes to be able to reduce the wax deposition they have to be applied before the temperatures are below the WAT, so that they can interfere with the crystallization process of the waxes. There are a lot of similarity between the two chemical classes in both the chemistry and mechanisms, and in most cases the wax inhibitors will also function as PPDs [1]. The wax inhibitors and PPDs chemicals will therefore be summarized together further on.

## *1.7.1 Wax dispersants*

Wax dispersants as a preventive technique alone are rarely used in the oilfields, however in combination with other wax inhibitors, such as PPDs, their present have given better results in preventing wax depositions.

Wax dispersants are surfactants, which are amphiphilic chemicals that possess both a hydrophobic part, which is water repelling, and a hydrophilic part, which is water attractive. Usually the dispersant molecules consist of a long hydrocarbon chain, the hydrophobic part, with a hydrophilic head. Figure 9 below shows an example of a common wax dispersant group called alkyl sulphonates.

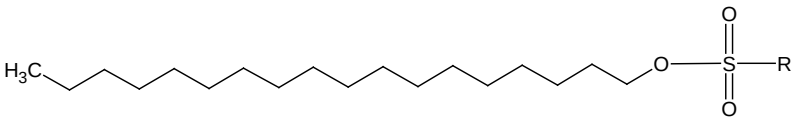


**Figure 9 An example of a wax dispersant, alkyl sulphonate. The R-group is usually an alkyl or aryl group.**

The wax dispersants ability to reduce wax depositions are mainly by adhering into the pipeline wall and creating a surface film, which make it difficult for the precipitated wax to stick to the wall. Some wax dispersants can also create a surface film which will let the precipitated wax bind weakly to the wall, but this bond will easily break off with the turbulent fluid flow, thereby preventing wax deposition build-up inside the pipelines. Wax dispersant will also absorb to growing wax crystal, and prevent them to agglomerate together, which will make it easier to transport the precipitated wax with the well stream flow [31].

Other common wax dispersants are alkyl aryl sulphonates, fatty amine ethoxylates, other alkoxylated products, and imidazolines. Imidazolines dispersants are good surface coating chemicals, which can also prevent gelling of the crude oil in cold climates and acts as a good corrosion inhibitor [1, 32].

## *1.7.2 Wax inhibitors and pour-point depressants (PPDs)*

The chemicals used as wax inhibitors and PPDs are normally polymers with long alkyl chains, which are intended to interfere with the wax crystallization and growth process. However the mechanisms for the wax inhibitors and PPDs are not fully understood and different mechanisms have been proposed. The general mechanism is that wax inhibitor polymers contain a structure similar to the wax structure, which will allow the polymer to be incorporated into the wax crystal growth. Beside the similar structure the polymer can also contain a structural part, which will cover the wax site, and thereby prevent new wax molecules to attach to the wax and continuing further growth [33]. The effect of this alternation causes a reduction in the three dimensional network the wax deposition can form, and promote the formation of smaller wax aggregates. The overall effect will give a lower pour-point and a reduction in the viscosity of the crude oil, which makes it easier to transport the crude oil [30].

The wax inhibitor chemicals are often waxy materials and solid at room temperature, and therefore must be dissolved before they are applied in the field [34]. The wax inhibitors are usually dissolved in aromatic solvents when they are applied in cold deepwater fields. The use of a good solvent in cold climates can also avoid gelling of the wax inhibitor, such as toluene, xylene and cyclopentane.

In general good wax inhibitors, with concentration of 50-200 ppm, have shown to prevent wax deposition at temperatures from 10-15 °C below the WAT. While the PPDs, with relatively high dosage, have shown to reduce the pour point temperature with up to 30 °C [1, 30].
The main chemical groups used as wax inhibitors and PPDs are:

- Ethylene copolymers
- Miscellaneous polymers
- Comb polymers

## *Ethylene copolymers*

Different types of polyethylene polymers copolymerized with larger monomers are common and effective wax inhibitors. These copolymers will consist of monomers of ethylene, and another larger monomer, which will contain branches or side chain that can interfere with the wax molecules in the crude oil, thereby preventing them from aligning together and form larger wax deposits.
Polyethylene polymers alone can crystallize together with the wax molecules of similar structure, and therefore have limited success preventing wax deposition [1].
The most successful copolymer are ethylene/vinyl acetate (EVA), shown in the figure 10 below. It is the percentage of vinyl acetate in EVA, which determines how effective the polymer will inhibit the wax crystallization growth. Increasing the vinyl acetate content will interrupt the crystallization process and lower the WAT, and also make the polymer more polar, which will enhance the solubility. However to much vinyl acetate will limit the co-crystallization with the wax, and cause a negative effect on the wax inhibition [35]. The optimum vinyl acetate in EVA polymers are around 25-30 percent [36].
Other ethylene copolymers used as wax inhibitors are ethylene/small alkene copolymers, such as poly(ethylene butene) and poly(ethylene-*b*-propylene), and ethylene/acrylonitrile copolymers [37, 38].

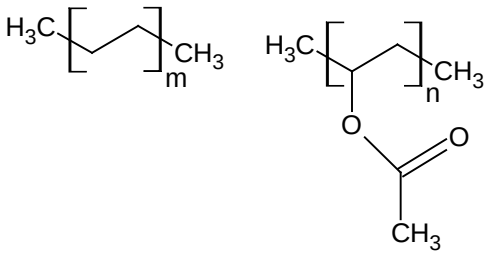


**Figure 10 Ethylene/vinyl acetate (EVA).**

## *Miscellaneous polymers*

The miscellaneous polymers are chemicals that have shown to be good wax inhibitors or have synergetic effective with PPDs against wax deposition, which means their present will enhance the wax deposition removal. Some chemicals that have been used against wax deposition are alkyl phenol-formaldehyde resins (figure 11), long chain phosphoric ester surfactants with sodium aluminate, and branched polymer, such as polyethyleneimine with pendant carbon 18 groups and dendrimeric hyperbranched polyesteramides with long alkyl chains [39-42].

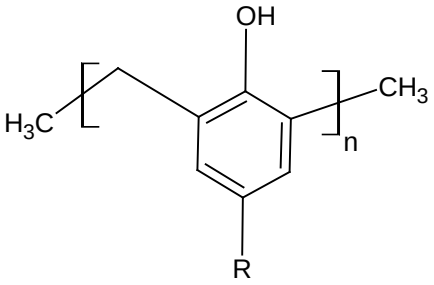


**Figure 11 Alkyl phenol-formaldehyde resins.**

## *Comb polymers*

The comb polymers are regarded as the most effective wax inhibitor class used today. These polymers have got their name as a result of their chemical structure, because they look like a comb, as the figure 12 shows below. The comb polymer consists of a polyvinyl backbone with different pendant chains, which are normally long alkyl chains.

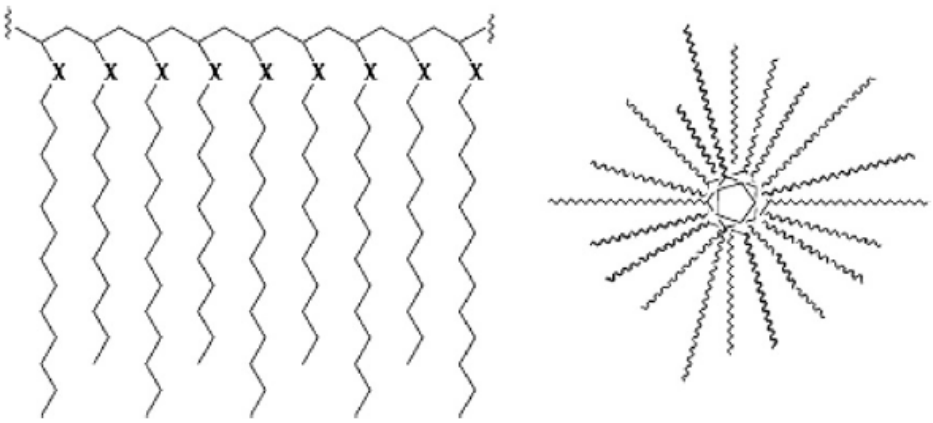

**Figure 12 A general structure of comb polymers [1].**

The structural designs of the PPDs normally contain three variable characteristic, which can influence their performance, and should be chosen in relation to the wax structures in the specific crude (figure 13) [34, 43]:

- The length on the polymers pendent chains is the most important variable, since the interaction between the wax in the crude oil and the PPD should be of similar length to get the best wax inhibition.
- The polymer backbone have shown little affect on the performance of the wax PPDs, but provides a structure for where the pendant chains are suspended from.
- A polar part on the backbone will prevent the whole polymer to be co-crystallized with the wax alkane chains. This part on the polymer will prevent further agglomerating, and thereby prevent the wax growth.

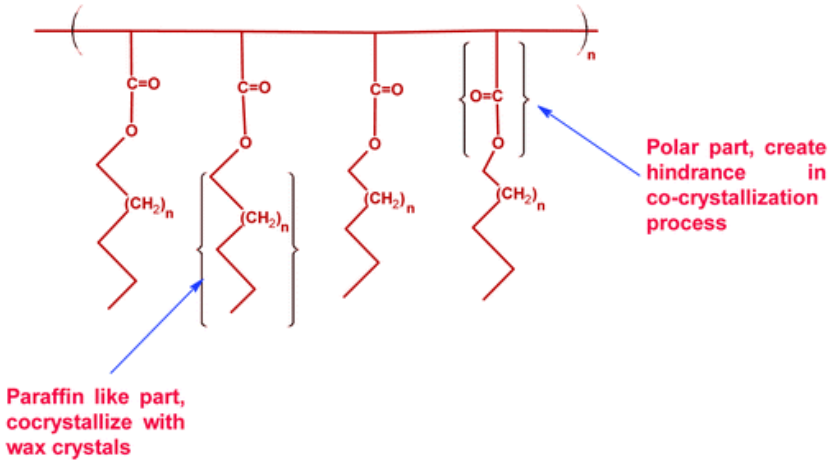


**Figure 13 The general structural characteristics for the comb polymers [43].**

The polymer molecular weight may also influence the PPDs performance in the way the polymer interacts with the wax. A short and low molecular weight polymer may cause to little disruption to wax crystallization, while a very long and high molecular weight polymer can interact with itself instead of with the wax.

The inhibition mechanism for the PPDs involves having a long alkyl side chain that can be embedded into the wax crystal by binding to the waxes of similar size. This interaction will thereby decrease the rate of wax formation, leading to a more soft wax that can be easier transported [44]. The high specificity of crude oils makes it difficult to develop universal PPDs that can be used in the different fields. The PPDs have to be developed to interact with wax alkane chains length and portions for the specific crude treated. It can therefore be wise to have a range of comb polymers available for wax treatment in case of changes in the crude oil composition. Comb polymers containing a range of alkyl chains have been proposed to get a better cover of the different wax alkane chains and improved performance [45].

The comb polymers are usually divided into two different polymer classes, which are the maleic copolymers and (meth)acrylate ester polymers.

### *Maleic copolymers*

Maleic anhydride monomers are often used to make effective comb polymers. The maleic anhydride monomers can be polymerized together with other vinyl comonomers, and then added a long alkyl side chain by reacting the anhydride with various alcohols of different length, alkyl mercaptans or alkylamines to from monoester, diester, thioester or imides [1, 46].

The chemical structure in figure 14 shows a copolymer of long chain α-olefin and maleic anhydride, where the maleic anhydride can be further derivatized to get another long side chain group [43].

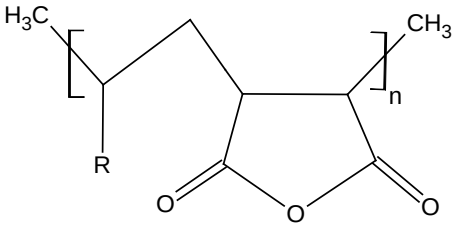


**Figure 14 Chemical structure of α-olefin maleic anhydride copolymer.**

The α-olefin maleic anhydride copolymer structure will then have an alternating structure of the two monomers, which can improve the polymer as a wax inhibitor.
The side chain groups on the maleic anhydride copolymer should be of long alkyl chains, preferably of similar size as the wax molecules. A maleic anhydride/α-olefin copolymer reacted with carbon 18 alkylamines to make a maleimide have been used as PPDs (figure 14) [1].

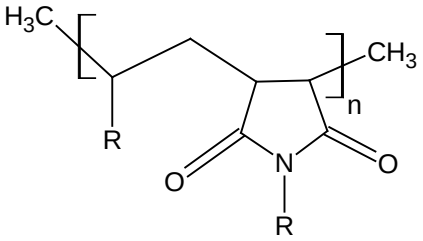


**Figure 15 Alkyl maleimide/α-olefin copolymers.**

Other chemicals claimed as good flow improvers as copolymers of maleic anhydride are methacrylate and styrene [47, 48]. Figure 16 below shows a monoester of maleic anhydride/(meth)acrylate ester copolymer.

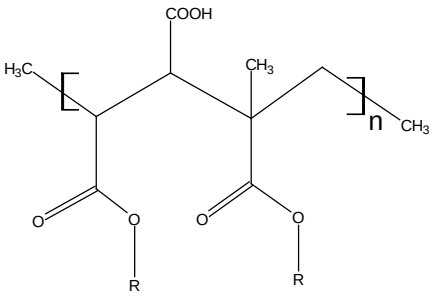


**Figure 16 Monoester of maleic/(meth)acrylate ester copolymers.**

## *(Meth)acrylate ester polymers*

Polymers of acrylate or methacrylate ester are the other class of comb polymers commonly been used as wax inhibitors or PPDs. These polymers are made up by (meth)acrylic acid monomers, where the ester groups are made from long-chain alcohols. The length on the alkyl side chain should be longer than 18 carbons length, to get the best interaction with the waxes in the crude and inhibit further wax growth. The optimum alkyl ester chain have been found to be between 20-24 carbons length, except the cost of alcohols over 18 carbons are high [49]. The difference between methacrylate polymers and acrylate polymers are a methyl group or a hydrogen atom on the

backbone of the polymer (figure 17). The methacrylate polymers have shown to give the best wax inhibition [50].

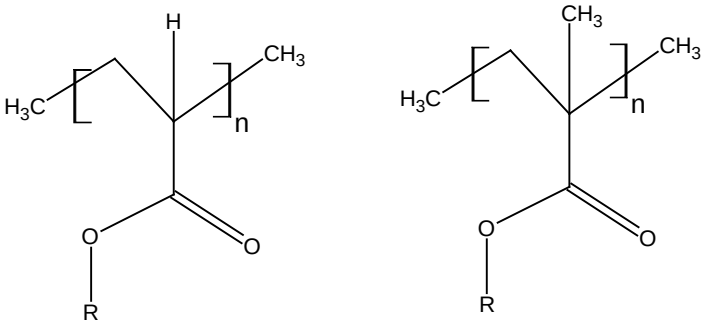


**Figure 17 Structure of acrylate ester and methacrylate ester polymers, the R-group is normally a long alkyl chain.**

The frequency of the alkyl side chains on the polyacrylate ester polymers is also important for the wax inhibition performance, but this will be dependent on the wax composition in that specific crude. One study for a specific crude oil showed the optimum performance with 60% of 18 carbons length side chains, where the rest of the acrylate ester groups where methyl side chains [51].
A blend of two polyalkyl(meth)acrylate have shown to give a better performance as PPDs [45]. This can be two poly(meth)acrylate polymers with different length in their side chains [41]. There is comercially avalaible a poly(meth)acrylate polymer with a mix of 7% C18, 58% C20, 30% C22 and 6% C24 alkanols. A polymer with a mixture of different alkyl side chains will cover a broader range of wax molecule lengths, and thereby give a better chance to interact with the wax and prevent further wax growth.
Other wax inhibition improvments on the polyalkylmethacrylate ester polymer class have been discovered by using different copolymers, such as copolymers of (meth)acrylic acid ester of 16 carbons alcohols with a small percentage of hydrophilic (meth)acrylic acid, vinyl pyridine, or N-vinyl pyrrolodone [45, 49, 52].

## *1.8 Wax test methods*

In order to reduce wax deposition problems laboratory measurements are needed to get knowledge about the wax behaviour and composition of the specific crude oil. This information is especially important for application with wax inhibitors and PPDs, since their effectiveness greatly relays on the chemical properties of the wax.
It is very important to know the temperature when the wax begins to crystallize, which is the WAT. The WAT can be determined by letting a warm crude oil flow over a cold surface and measure the temperature at which the wax deposits [53].
There have been developed many different test methods for determining the WAT and the wax behaviour, which all have their advantages and speciality in their use. Some these methods that are normally applied are [54]:

- Cold finger [55]
- Cloud point determination (ASTM-D2500)[56]
- Differential scanning calorimetry (DSC) [57]

- Cross-polarization microscopy [19, 58]
- Filter plugging [59]
- Fourier transform infrared spectroscopy [60]

The temperature at which the crude oil movement is reduced by gelling is also a typically test performed. This is a standard method from the American Society for Testing and Materials (ASTM), which is a simple test to find the pour-point of a crude [61]. The method involves periodically tilting a tube containing sample of crude oil at decreasing temperatures, to find the temperature where there is no movement of the crude. This method is also used when testing PPDs, to compare the crude oil pour point differences with and without inhibitor addictives.

Another good test method for finding the WAT and to observe the effect of the PPDs is by using viscosity measurements [62]. A viscometer is used to measure the viscosity for a crude oil as the temperature is decreased at constant rate. As the temperature goes down the viscosity increases, and will eventually reach the WAT, which leads to an exponential growth in the viscosity measurement. The difference in viscosity at the different temperatures can be further used to evaluate the effectiveness of PPDs, to see if the exponential growths of the viscosity are delayed at lower temperatures. The viscosity measurement for analyzing PPDs performance in crude oil is the experimental study in this thesis.

## *References:*


1. Kelland, M.A., *Production Chemicals for the Oil and Gas Industry*2009: CRC Press, Boca Raton, Fl, 2009..
2. Al-Yaari, M., *Paraffin Wax Deposition: Mitigation and Removal Techniques*, in *SPE Saudi Arabia section Young Professionals Technical Symposium*2011, Society of Petroleum Engineers: Dhahran, Saudi Arabia.
3. *International wins for oil and gas company*. 2012; Available from: http://pipelinesinternational.com/news/international_wins_for_oil_and_gas_company/065986/.
4. Gao, S., *Investigation of interactions between gas hydrates and several other flow assurance elements.* Energy & Fuels, 2008. **22**(5): p. 3150-3153.
5. Buckley, J.S. *Asphaltenes*. 2007 [cited 2012 30.04]; Available from: http://baervan.nmt.edu/Petrophysics/group/intro-2-asphaltenes.pdf.
6. Dobbs, J.B., *A Unique Method of Paraffin Control in Production Operations*, in *SPE Rocky Mountain Regional Meeting*1999, 1999,. Society of Petroleum Engineers Inc.: Gillette, Wyoming.
7. Misra, S., S. Baruah, and K. Singh, *Paraffin Problems in Crude Oil Production And Transportation: A Review.* SPE Production & Operations, 1995(1): p. 50-54.
8. Hammami, A. and M.A. Raines, *Paraffin Deposition From Crude Oils: Comparison of Laboratory Results With Field Data.* SPE Journal, 1999. **4**(1): p. 9-18.
9. Burger, E.D., T.K. Perkins, and J.H. Striegler, *Studies of Wax Deposition in the Trans Alaska Pipeline.* SPE Journal of Petroleum Technology, 1981(6): p. 1075-1086.
10. Leiroz, A.T. and L.F.A. Azevedo, *Studies On The Mechanisms Of Wax Deposition In Pipelines*, in *Offshore Technology Conference*2005: Houston, Texas.
11. Carnahan, N.F., *Paraffin Deposition in Petroleum Production.* SPE Journal of Petroleum Technology, 1989(10): p. 1024-1025, 1106.
12. Mokhatab, S. *Wax prevention and remediation in subsea pipelines and flow lines*. 2009. **230**.
13. Abney, L., et al., *Flow Remediation Solutions for Pipelines*, in *Offshore Technology Conference*2003: Houston, Texas.
14. Wang, Q., C. Sarica, and T.X. Chen, *An Experimental Study on Mechanics of Wax Removal in Pipeline*, in *SPE Annual Technical Conference and Exhibition*2001, Copyright 2001, Society of Petroleum Engineers Inc.: New Orleans, Louisiana.
15. Esaklul, K.A., et al., *Active Heating For Flow Assurance Control in Deepwater Flow lines*, in *Offshore Technology Conference*2003: Houston, Texas.
16. Thant, M.M.M., et al., *Mitigating Flow Assurance Challenges in Deepwater Fields using Active Heating Methods*, in *SPE Middle East Oil and Gas Show and Conference*2011, Society of Petroleum Engineers: Manama, Bahrain.
17. Barker, K.M., *Formation Damage Related to Hot Oiling.* SPE Production Engineering, 1989. **4**(4): p. 371-375.
18. Straub, T.J., S.W. Autry, and G.E. King, *An Investigation Into Practical Removal of Downhole Paraffin by Thermal Methods and Chemical Solvents*, in *SPE Production Operations Symposium*1989, 1989 Copyright 1989, Society of Petroleum Engineers, Inc.: Oklahoma City, Oklahoma.
19. Ferworn, K.A., A. Hammami, and H. Ellis, *Control of Wax Deposition: An Experimental Investigation of Crystal Morphology and an Evaluation of Various Chemical Solvents*, in *International Symposium on Oilfield Chemistry*1997, Copyright 1997, Society of Petroleum Engineers Inc.: Houston, Texas.

20. Barker, K.M., M.E. Newberry, and Y.R. Yin, *Paraffin Solvation in the Oilfield*, in *SPE International Symposium on Oilfield Chemistry*2001, Copyright 2001, Society of Petroleum Engineers Inc.: Houston, Texas.
21. Thierheimer Jr, C.L., *Solvent for paraffin removal from oilfield equipment*, 1990, Google Patents.
22. Woo, G.T., S.J. Garbis, and T.C. Gray, *Long-Term Control of Paraffin Deposition*, in *SPE Annual Technical Conference and Exhibition*1984, 1984 Copyright 1984 Society of Petroleum Engineers of AIME: Houston, Texas.
23. Ashton, J.P., et al., *In-Situ Heat System Stimulates Paraffinic-Crude Producers in Gulf of Mexico.* SPE Production Engineering, 1989. **4**(2): p. 157-160.
24. Aiyejina, A., et al., *Wax formation in oil pipelines: A critical review.* International Journal of Multiphase Flow, 2011. **37**(7): p. 671-694.
25. Argo, C.B., et al., *Method and system for transporting flows of fluid hydrocarbons containing wax, asphaltenes, and/or other precipitating solids*, 2007, Google Patents.
26. Tung, N.P., et al., *Studying the Mechanism of Magnetic Field Influence on Paraffin Crude Oil Viscosity and Wax Deposition Reductions*, in *SPE Asia Pacific Oil and Gas Conference and Exhibition*2001, Copyright 2001, Society of Petroleum Engineers Inc.: Jakarta, Indonesia.
27. Chow, R., et al., *Precipitation of Wax From Crude Oil Under the Influence of a Magnetic Field.* Journal of Canadian Petroleum Technology, 2000. **39**(6).
28. Sadeghazad, A. and N. Ghaemi, *Microbial Prevention of Wax Precipitation in Crude Oil by Biodegradation Mechanism*, in *SPE Asia Pacific Oil and Gas Conference and Exhibition*2003, Society of Petroleum Engineers: Jakarta, Indonesia.
29. Rana, D.P., et al., *Novel Microbial Process for Mitigating Wax Deposition in Down Hole Tubular and Surface Flow Lines*, in *SPE Oil and Gas India Conference and Exhibition*2010, Society of Petroleum Engineers: Mumbai, India.
30. Pedersen, K.S. and H.P. Rønningsen, *Influence of Wax Inhibitors on Wax Appearance Temperature, Pour Point, and Viscosity of Waxy Crude Oils.* Energy & Fuels, 2003. **17**(2): p. 321-328.
31. Ahn, S., et al., *Paraffin Crystal and Deposition Control By Emulsification*, in *SPE International Symposium on Oilfield Chemistry*2005, 2005,. Society of Petroleum Engineers Inc.: The Woodlands, Texas.
32. Martin, R.L., H.L. Becker, and D. Galvan, *Method of reducing paraffin deposition with imidazolines*, 2010, Google Patents.
33. Jennings, D.W. and M.E. Newberry, *Paraffin Inhibitor Applications in Deepwater Offshore Developments*, in *International Petroleum Technology Conference*2008, International Petroleum Technology Conference: Kuala Lumpur, Malaysia.
34. Manka, J.S. and K.L. Ziegler, *Factors Affecting the Performance of Crude Oil Wax-Control Additives*, in *SPE Production and Operations Symposium*2001, Society of Petroleum Engineers: Oklahoma City, Oklahoma.
35. Lindeman, O.E. and S.J. Allenson, *Theoretical Modeling of Tertiary Structure of Paraffin Inhibitors*, in *SPE International Symposium on Oilfield Chemistry*2005, 2005,. Society of Petroleum Engineers Inc.: The Woodlands, Texas.
36. Machado, A.L.C., E.F. Lucas, and G. González, *Poly(ethylene-co-vinyl acetate) (EVA) as wax inhibitor of a Brazilian crude oil: oil viscosity, pour point and phase behavior of organic solutions.* Journal of Petroleum Science and Engineering, 2001. **32**(2–4): p. 159-165.
37. Tinsley, J.F., et al., *Novel Laboratory Cell for Fundamental Studies of the Effect of Polymer Additives on Wax Deposition from Model Crude Oils†.* Energy & Fuels, 2007. **21**(3): p. 1301-1308.
38. Motz, K.L., R.A. Latham, and R.J. Statz, *Low pour crude oil compositions*, 1990, Google Patents.

39. Martella, D.J. and J.J. Jaruzelski, *Alkyl phenol-formaldehyde condensates as fuel and lubricating oil additives*, 1993, EP Patent 0,311,452.
40. Gentili, D.O., et al., *Evaluation of Polymeric Phosphoric Ester-Based Additives as Wax Deposition Inhibitors*, in *SPE Latin American and Caribbean Petroleum Engineering Conference*2005, Society of Petroleum Engineers: Rio de Janeiro, Brazil.
41. Duncum, S.N., K. James, and C.G. Osborne, *Wax deposit inhibitors*, 2000, Google Patents.
42. Van Bergen, P.F., M.A. Van Dijk, and A.J. Zeeman, *Method For Improving the Flow Ability of a Mixture That Contains Wax and Other Hydrocarbons*, 2005, Google Patents.
43. Soni, H.P., Kiranbala, and D.P. Bharambe, *Performance-Based Designing of Wax Crystal Growth Inhibitors.* Energy & Fuels, 2008. **22**(6): p. 3930-3938.
44. Jang, Y.H., et al., *Wax Inhibition by Comb-like Polymers: Support of the Incorporation−Perturbation Mechanism from Molecular Dynamics Simulations.* The Journal of Physical Chemistry B, 2007. **111**(46): p. 13173-13179.
45. Wirtz, H., et al., *New copolymers, mixtures thereof with poly (meth) acrylate esters and the use thereof for improving the cold fluidity of crude oils*, 1994, Google Patents.
46. Son, A.J., R.B. Graugnard, and B.J. Chai, *The Effect of Structure on Performance of Maleic Anhydride Copolymers as Flow Improvers of Paraffinic Crude Oil*, in *SPE International Symposium on Oilfield Chemistry*1993, 1993 Copyright 1993, Society of Petroleum Engineers, Inc.: New Orleans, Louisiana.
47. Al-Sabagh, A.M., et al., *Styrene-maleic anhydride copolymer esters as flow improvers of waxy crude oil.* Journal of Petroleum Science and Engineering, 2009. **65**(3–4): p. 139-146.
48. Han, S., Y. Song, and T. Ren, *Impact of Alkyl Methacrylate−Maleic Anhydride Copolymers as Pour Point Depressant on Crystallization Behavior of Diesel Fuel.* Energy & Fuels, 2009. **23**(5): p. 2576-2580.
49. Gateau, P., A. Barbey, and J.F. Brunelli, *Acrylic copolymers as additives for inhibiting paraffin deposit in crude oil, and compositions containing same*, 2004, Google Patents.
50. Mcdougall, L.A., *CH, CHY*, 1972, Google Patents.
51. D. M. Duffy, C.M., J. L. Irwin, A. F.Di Salvo, P.C. Taylor, M. Arjmandi, A. Danesh, S. R. Ren, A. Todd, B. Tohidi, M. T. Storr, L. Jussaume, J.-P. Montfort, and P.M. Rodger, *Chemistry in the Oil Industry*, in *Symposium* 2003: Manchester.
52. Shmakova-Lindeman, O.E., *Paraffin inhibitors*, 2008, Google Patents.
53. Kruka, V., E. Cadena, and T. Long, *Cloud-point determination for crude oils.* Journal of Petroleum Technology, 1995. **47**(8): p. 681-687.
54. Monger-McClure, T.G., J.E. Tackett, and L.S. Merrill, *Comparisons of Cloud Point Measurement and Paraffin Prediction Methods.* SPE Production & Operations, 1999. **14**(1): p. 4-16.
55. Weispfennig, K., *Advancements in Paraffin Testing Methodology*, in *SPE International Symposium on Oilfield Chemistry*2001, 2001,. Society of Petroleum Engineers Inc.: Houston, Texas.
56. international, A., *ASTM D2500-11*, in *Standard test method for cloud point of petroleum products*.
57. Letoffe, J., et al., *Crude oils: characterization of waxes precipitated on cooling by dsc and thermomicroscopy.* Fuel, 1995. **74**(6): p. 810-817.
58. Karan, K., J. Ratulowski, and P. German, *Measurement of Waxy Crude Properties Using Novel Laboratory Techniques*, in *SPE Annual Technical Conference and Exhibition*2000, 2000,. Society of Petroleum Engineers Inc.: Dallas, Texas.
59. Leontaritis, K.J. and J.D. Leontaritis, *Cloud Point and Wax Deposition Measurement Techniques*, in *International Symposium on Oilfield Chemistry*2003, Society of Petroleum Engineers: Houston, Texas.

60. Roehner, R. and F. Hanson, *Determination of wax precipitation temperature and amount of precipitated solid wax versus temperature for crude oils using FT-IR spectroscopy.* Energy & Fuels, 2001. **15**(3): p. 756-763.
61. international, A., *ASTM D97-11*, in *Standard test method for pour point of petroleum products*.
62. Pedersen, K.S. and H.P. Rønningsen, *Effect of Precipitated Wax on ViscosityA Model for Predicting Non-Newtonian Viscosity of Crude Oils.* Energy & Fuels, 1999. **14**(1): p. 43-51.

# 2. Design of Experiments

In studies where the main purpose is to find the best formulation involving more than one variable can require a lot of experiments and be time consuming. Design of experiments (DOE) is a statistical method commonly used to more efficiently carry out an experiment.
An example of where the use of DOE is helpful can be as simple as finding the right ratio of mixing orange, apple and grape juice in a drink, to get the best taste. DOE can be a useful technique in many different industries involving optimization of mixtures, such as in food, pharmaceuticals, paint, and with production chemical for the oil and gas industry, as will be presented in this thesis.
When designing an experiment it will normally be broken down into three steps [1]:

- the planning of the experiment
- the performance of the experiment
- the analysis and interpretation of the results and data

In DOE the most important step is the planning phase, where the objective is to systematic ally plan each experiment such that the greatest amount of information can be obtained, and thereby minimize the number of experiments, the cost of materials, and the time required [2].
When starting the DOE process it is important to clearly define the inputs or factors used in the formulation. In the method the inputs are those being varied, and their results will give the output of the analysis, which are the responses that are measured. When this information is available a systematic design, such as mixture design, can be made to find the best formulation of the different factors. Mixture design may be used when the proportions of the factors in an experiment are applied, rather than the amount of each factor, hence the total sum of factors adds to a fix total. This means that if one of the factors is increased, then the portion of another factor has to decrease, such as the total sum of factors is always the same [3].
In the example with the juice mix, this means the sum of orange, apple and grape juice adds up to a 100% mixture. However all the components have their one percentage value in the mixture, for example 40% orange juice, 20% apple juice and 20% grape juice. Changing the proportion of one of the juices will therefore lead to change in the proportion of the other juices.
Mixture design is used in this thesis, where the purpose is to find the best wax inhibitor formulation by mixing of three different chemicals. A software program called Design Expert is used to more easily perform statistical DOE, and find the optimization of the formulation. The program allows to visualize the optimization point, by plotting the experiments in a response surface graph, which will give a 3-dimensional curve where the best formulation point can be easily read of.

## 2.1 The simplex-lattice design

In mixture design all the variables are being considered simultaneously by using a systematic approach, which will give the minimum number of experiments necessary to find the optimal mixture formulation. The layout for the experiments required are found by using a simplex-lattice, which is just a triangle marked with points representing different proportions of the three components in the mixture (figure 1). The simplex-lattice design will provide a good overview of all the experiments needed to cover the different mixture possibilities, which will make it easy and quick to indicate which interaction between the components will give the best formulation. The simplex will create a

systematic plan, where the components are varied between zero and hundred percent, in a hundred percent total mixture.

A simplex is defined as a geometric figure, which have one more vertex than the number of dimension [4]. The simplex in figure 1 below is a 2-dimensional triangle. Each corner in the triangle represents each of the components in the pure state, and here their value is 100 percent, which is their maximum value. The binary blends are the half and half mixture of two of the components, and they are located mid-point on the edges of the simplex. The point in the middle of the simplex is the point where all the components are mixed equally. Each component in the simplex will increase in the percent value towards the left in a circle motion. To read of the percent value of each component in a given point in the simplex, can be done by first drawing a vertical line to the right from the point, and then drawing the parallel lines out from the point for the two other sides. The points where the three lines intersect the edges on the simplex are the percent values for each component in the given point. The figure 1 shows how to read of the percent value of each component for the middle point, which has a percent value of 33.33 for each component.

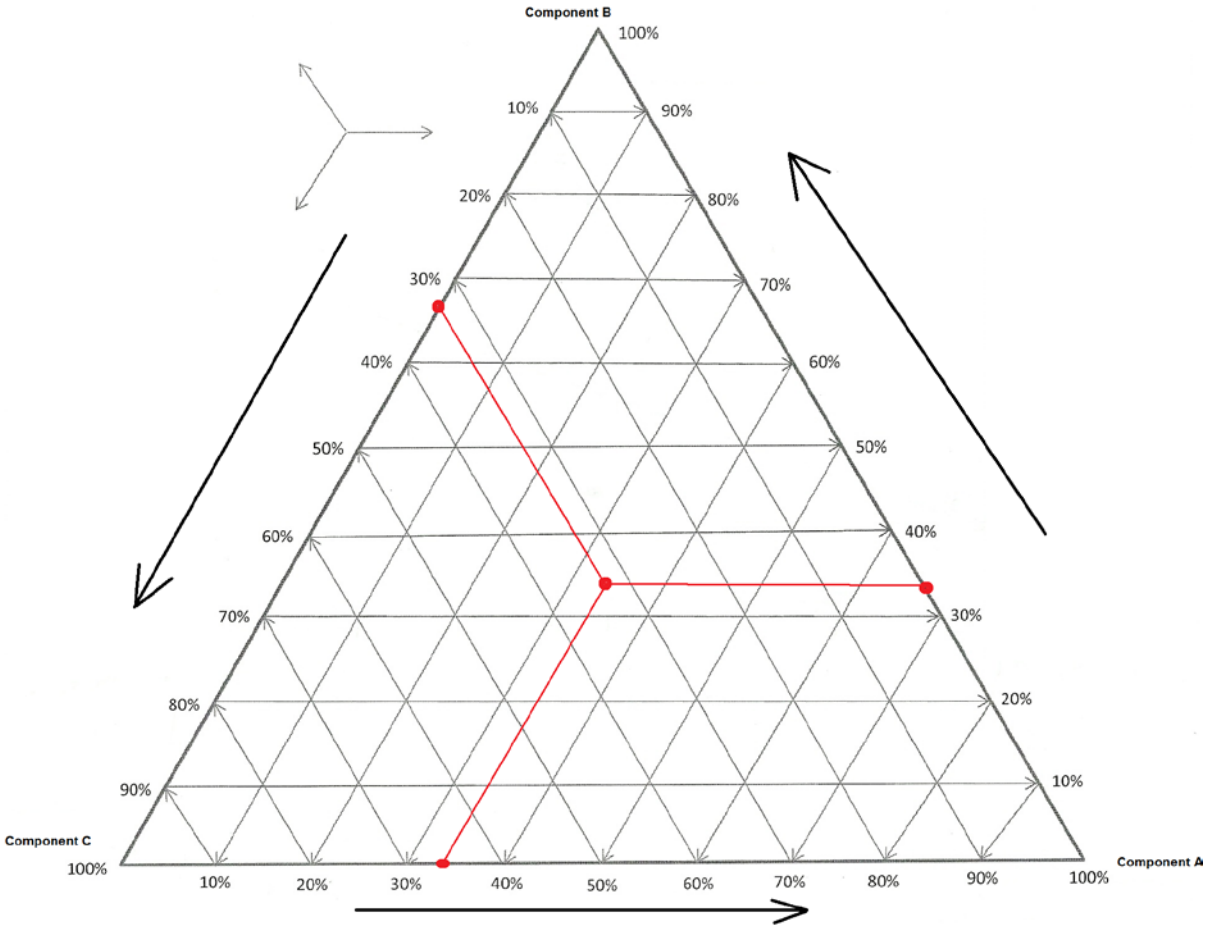


**Figure 1 Simplex-lattice design.**

## *2.2 Mixture design models*

When the experiments from the simplex design are performed and the data collected, these responses will be further treated by finding a model to functionally describe them. The purpose of the model is to graphically represent a response surface for the mixture blends in the simplex. The models are based on mathematical equations used to develop a response surface of the measured values, which reflects the portions of the components in the mixture [5].

The most common regression models used for experiments are polynomial functions, which are set of mathematical equations. For mixture design the regression model called Scheffè canonical polynomials are mostly used, and are applied in many technical articles, books, and in software packages, such as design expert.

The equations in figure 2 below show the different Scheffè polynomials [6]. The degree of the polynomials is dependent on the number of data collected in the experiments. Polynomials of degree one is called linear polynomials, and as shown in figure 2, these equations contain no exponents. Polynomials with a degree of two are called quadratic, degree of three, cubic, and degree of four, quartic. In mixture designs with three components the polynomials usually are of second, third, and fourth degree [7]. The polynomials of second and higher order are often referred to as response surface models.

Linear:

$$\hat{y} = \sum_{i=1}^{q} \beta_i x_i$$

Linear + Squared:

$$\hat{y} = \sum_{i=1}^{q} \beta_i x_i + \sum_{i=1}^{q} \beta_i x_i^2$$

Quadratic:

$$\hat{y} = \sum_{i=1}^{q} \beta_i x_i + \sum_{i<j}^{q-1} \sum_{j}^{q} \beta_{ij} x_i x_j$$

Special cubic:

$$\hat{y} = \sum_{i=1}^{q} \beta_i x_i + \sum_{i<j}^{q-1} \sum_{j}^{q} \beta_{ij} x_i x_j + \sum_{i<j}^{q-2} \sum_{j<k}^{q-1} \sum_{k}^{q} \beta_{ijk} x_i x_j x_k$$

Full cubic:

$$\hat{y} = \sum_{i=1}^{q} \beta_i x_i + \sum_{i<j}^{q-1} \sum_{j}^{q} \beta_{ij} x_i x_j + \sum_{i<j}^{q-1} \sum_{j}^{q} \delta_{ij} x_i x_j (x_i - x_j) + \sum_{i<j}^{q-2} \sum_{j<k}^{q-1} \sum_{k}^{q} \beta_{ijk} x_i x_j x_k$$

Special quartic:

$$\hat{y} = \sum_{i=1}^{q} \beta_i x_i + \sum_{i<j}^{q-1} \sum_{j}^{q} \beta_{ij} x_i x_j + \sum_{i<j}^{q-2} \sum_{j<k}^{q-1} \sum_{k}^{q} \beta_{iijk} x_i^2 x_j x_k + \sum_{i<j}^{q-2} \sum_{j<k}^{q-1} \sum_{k}^{q} \beta_{ijjk} x_i x_j^2 x_k + \sum_{i<j}^{q-2} \sum_{j<k}^{q-1} \sum_{k}^{q} \beta_{ijkk} x_i x_j x_k^2$$

Full quartic:

$$\hat{y} = \sum_{i=1}^{q} \beta_i x_i + \sum_{i<j}^{q-1} \sum_{j}^{q} \beta_{ij} x_i x_j + \sum_{i<j}^{q-1} \sum_{j}^{q} \delta_{ij} x_i x_j (x_i - x_j) + \sum_{i<j}^{q-1} \sum_{j}^{q} \gamma_{ij} x_i x_j (x_i - x_j)^2 + \sum_{i<j}^{q-2} \sum_{j<k}^{q-1} \sum_{k}^{q} \beta_{iijk} x_i^2 x_j x_k$$
$$+ \sum_{i<j}^{q-2} \sum_{j<k}^{q-1} \sum_{k}^{q} \beta_{ijjk} x_i x_j^2 x_k + \sum_{i<j}^{q-2} \sum_{j<k}^{q-1} \sum_{k}^{q} \beta_{ijkk} x_i x_j x_k^2 + \sum_{i<j}^{q-3} \sum_{j<k}^{q-2} \sum_{k<l}^{q-1} \sum_{l}^{q} \beta_{ijkl} x_i x_j x_k x_l$$

**Figure 2 The Scheffè polynomial equations used in design expert.**

## *2.3 Design Expert*

Design Expert is a software program especially designed for analysing the performance for a process or formulation. The main function of the program is to simple and quick model DOE, to get the best formulation of the components in a mixture. It provides in-depth analysis of the mixture components, and applies important statistical methods for finding the best model to describe the response data. The suggested model will provide a 3-dimensional surface graph for the responses, where the optimization point can easily be found from.
Design Expert can be applied when the information about the experiments design, number of components and response measures are defined. In mixture design the software program will incorporate the gathered information into simplex-lattice design, which will come up with an experiment plan. This plan will give the number of experiments needed, made of the different mixture blends of the components, and how many replicates needed to estimate the pure error. The pure error is the minimum variation expected from the performance of each experiment [8]. When all the experimental data is collected this will be put into the simplex-lattice design plan, and the program can start the calculations and statistical analysis of the response data. Based on the results from these tests the program will suggest the best fitted model, and provide a response graph for the measured responses.
The analysis section of the response data in the program has six sections, which are briefly described below [8, 9] :

- **Transform**
  Transformation means to apply a mathematical function to all the response data, to make them meet the assumptions of being normally distributed with a constant variance. Experimental data that are normally distributed means the data collected follow a bell shaped distribution, where the data are randomly spread around a mean value. The variance describe have far the data are spread around the mean value.
  When starting Design Expert the program sets the transformation as none by default, which means the response data are analysed as entered. However later in the analysis, if the diagnostic plots show abnormalities, this may indicate that the response data need a transformation. Some of the transformations used for the response data are square root, natural Log, natural 10 Log, and power.

- **Fit summary**
  In fit summary the program will start the regression calculations to fit all the different polynomial models to the response data selected, and use different important statistics for comparing the different models against each other. The model with a statistically significant will be the suggested model for the mixture design, which implies that model has little variation in the data and therefore unlikely they have occurred by chance.

- **Model**
  The suggested model given in fit summary is selected, and will be used further in the analysis. However in the model section it is possible to change the model option if needed.

- **ANOVA (analysis of variance)**
  Based on the results found from the fit summary analysis, the program goes deeper into the statistics for the suggested model in the analysis of variance section.
  In the analysis of variance more statistical models and tests are applied to the response data, such as mean, variance, and standard deviation. Details of the analysis will be given and comments about the statistics, and the polynomials equations used for the suggested model will be provided.

- **Diagnostics**
  In diagnostics there are made graphical plots for the different statistic analysis applied, to make it easier to see how the measured data points fits the selected model. The plots will show how well the model satisfies the assumptions from the analysis of variance.

- **Model graphs**
  In the last section of the analysis, the response data are plotted as a function of the different components in the mixture. The program will illustrate the response surface graph in a contour plot and in a 3-dimensional plot, to make it easy to observe the best interaction between the different components in the mixture.

### *2.3.1. Analysis of Diagnostic plots*

In the diagnostics section in Design-Expert the residuals are studied in more detail by looking at different plots to check for trends and deviant points. The residual is the difference in the actual measured points from the experiments, and the estimated points from the selected model. The diagnostics plot is therefore used to help uncover problems such as; departures from the model assumptions, outliers or suspect data points, and high influence data points [1]. The program shows the studentized form of residuals, which means that the residual are divided by the estimated standard deviation of that residual [8].
The plots of the residuals are of great importance when checking the adequacy of the selected model, and the different plots used by Design-Expert have been briefly described below.

**The normal plot of residuals**

In the normal probability plot of the actual data point found from the experiments are compared with the model to check if they are normally distributed, in which case the measured point follows a straight line, as shown in figure 3.
It is common to see small variation from the straight line, where the residuals are randomly scattered around the line. However when the points start to deviate from the straight line and forms a S-shaped pattern, shown in the right plot in figure 3, this may indicate a need of transformation of the response data.

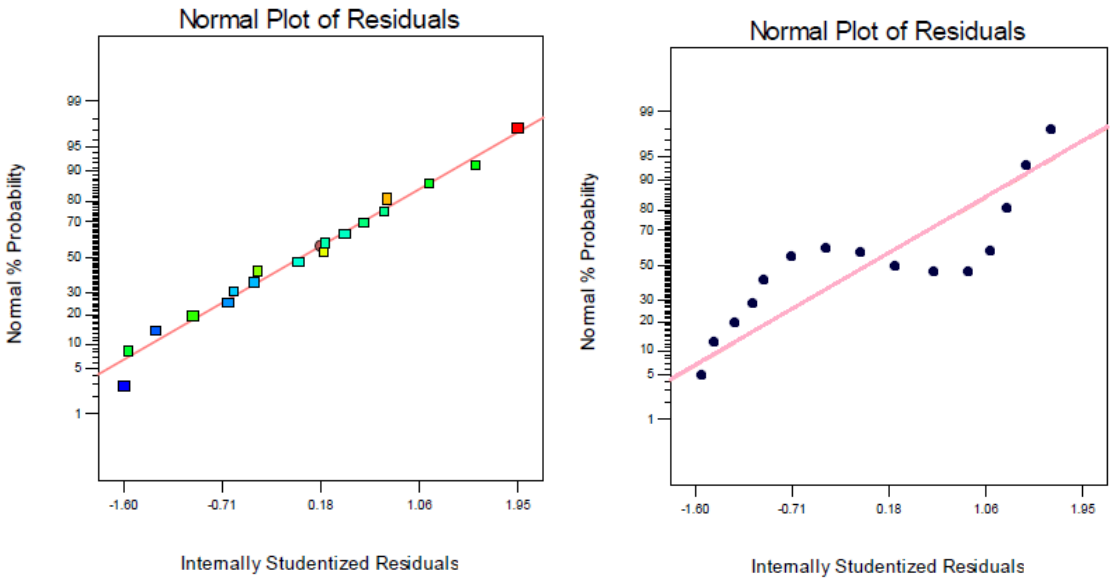


**Figure 3 The normal plot of residuals.**

**The residuals vs. predicted plot**

In the residuals versus predicted plot the difference in the actual data points from the experiments and the predicted points from the model are compared, and it confirms if the assumption about a constant variance is valid. The plot should show a random scatter of the actual data points around the graph, as seen in the left plot in figure 4, which indicates that the residuals are independent of the size of the predicted values. If the residuals show an increasing trend of points from the left to right (funnel shaped pattern, see right plot in figure 4), that is the residuals increases in size together with the predicted values, this can indicate that the variance is not constant and a transformation should be preformed.

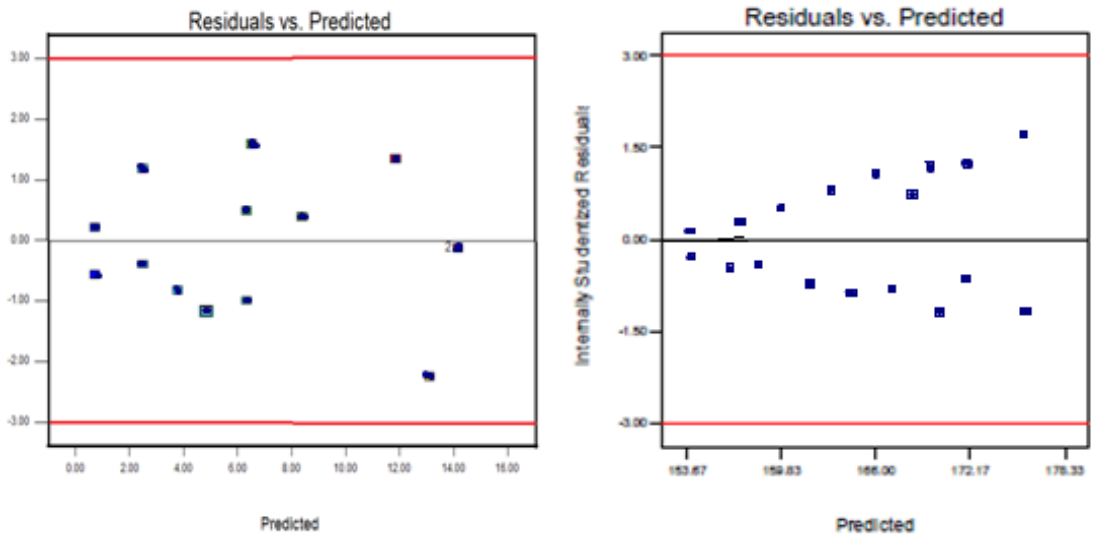


**Figure 4 The residuals versus predicted plots**

**The residuals vs. run plot**

The residuals versus run plot shows the residual points in the experimental run order, and is used to check if there have happened any systematic variations during the experiments, which can influence the response. This can be variables such as temperature changes, time during the day when the experiments were performed, or any variation in the performance of the experiments. The plot should show a random scatter as seen in figure 5. However, if any trends appear blocking and randomization can help to improve the analysis.

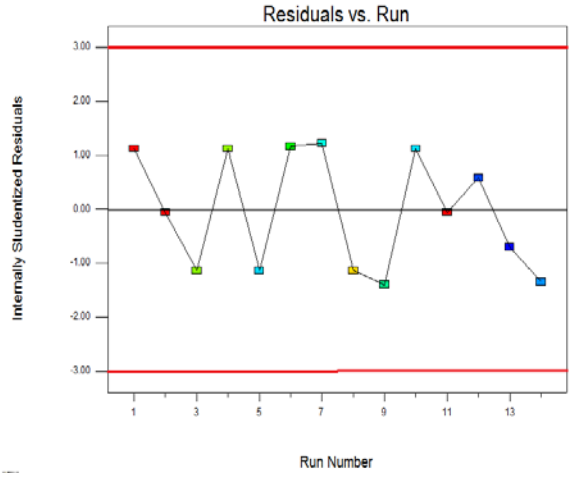


**Figure 5 The residuals versus run.**

**The predicted vs. actual plot**

The predicted versus actual plot compares the measured data points to the predicted values from the model. The measured data points should be spread evenly and close to the graph. Cluster of data points under and above the line, as shown in the right plot below in figure 6, indicates problems of over or under predicting. This means the data point cannot be predicted very precisely by the selected model, which can be corrected by a transformation or another model should be evaluated.

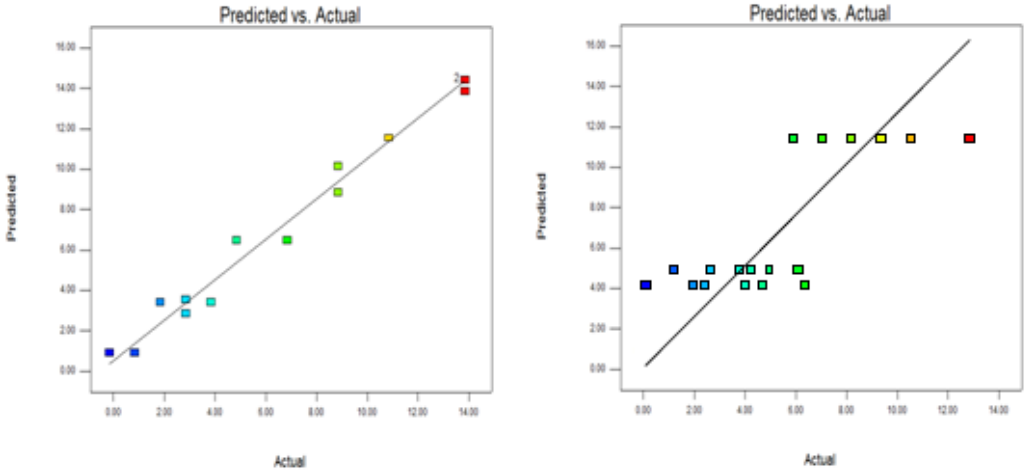


**Figure 6 The predicted versus actual plot.**

**The Box-Cox plot**

The response data are being analysed as they are entered into the program, however transformation may be required to make the assumptions in the analysis of variance valid. This means the entered response data must undergo a mathematical transformation to obtain a normal distribution with a constant variance.

The Box-Cow plot is meant as a guideline to check if the response data needs to undergo a transformation, and the recommended transformation will be given. The green line shows the optimal transformation. The blue line represents the response data without transformation, and as long as the blue line is in between the two red lines, there is no need for transformation (figure 7).

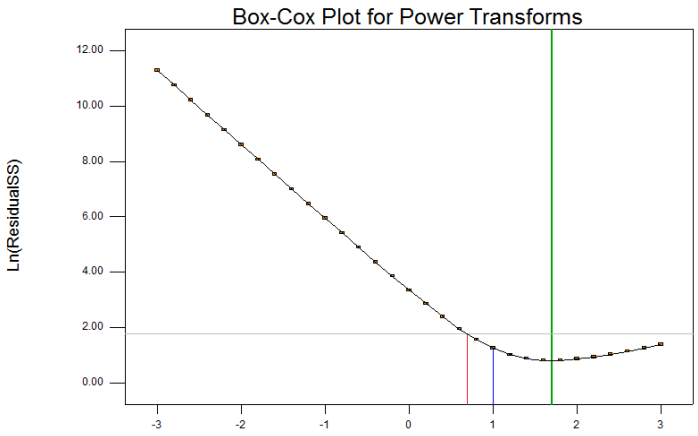


**Figure 7 The Box-Cox plot.**

**The residuals vs. factor plot**

A plot of residuals versus factors checks the residuals against a selected factor of choice to see if there are factors not accounted for by the model. However in mixture design all the factors are correlated with one another, meaning when a factor is changed this lead to changes in another factor, since the sum of proportion for the factors adds up to a fixed sum [1]. This makes it difficult to interpret the factors individually, therefore the residuals vs. factor plot are not been considered in this thesis.

## *2.3.2 Diagnostics-analysis of Influence Plots*

In the influence section of diagnostics, there are different plots used to check if there are any points in the experiments that are outliers, that is distinguishes from the rest of the data points. The analysis will provide measures of the influence for either potential or actual values of individual runs. These plots can therefore be very helpful in finding problems in the design, and give an indication of which responses should be removed or replaced.

**The externally studentized residuals**

The plot of the externally studentized residuals versus the run number is used to identify outlier data points in the model, which are the points outside the red lines (figure 8). The outlier points are the measured points that do not fit the selected model well. The outlier point should be investigated to

try and find the cause of their occurrence, if they are wrong or the model is wrong, in which case they may be removed or a replicate of the data point performed.

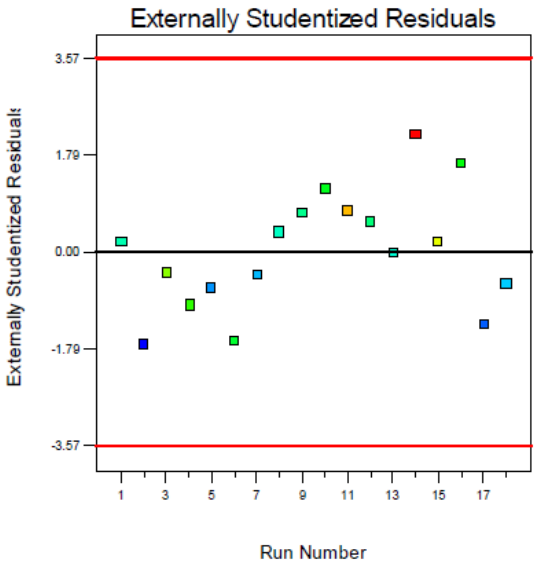


**Figure 8 The externally studentized residuals plot.**

**The leverage vs. run**

The leverage of a point is measured between 0 and 1, and indicates how much a point influence the models predicted values. The higher a leverage value a point have, the more influence the point have on the model. A leverage value of 1 means that the predicted value for that experiment will be the same as for the measured value found in the experiments, meaning the residual will be 0. The model will go through the point with leverage 1, even though it may deviate from the rest of the data points. A data point with leverage near 1 should therefore be checked, and a replicated may ensure no error has occurred for the point.

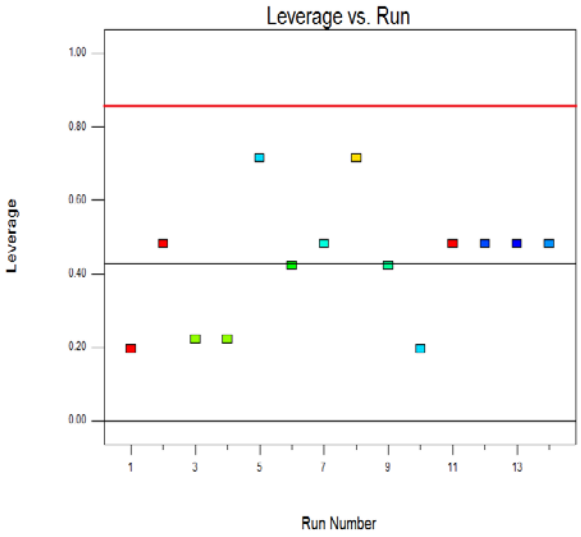


**Figure 9 The leverage versus run plot.**

**The difference in fits vs. run**

Difference in fit (DFFITS) measure the influence each data point have on the predicted value in the selected model. It is found by measuring the change in predicted values that occurs when a response is deleted. The DFFITS versus run plot will show the data points that will a high influence on the model, and are those points outside the redlines (figure 10). The higher the DFFITS value is for a point, the more influence the point will have on the model.

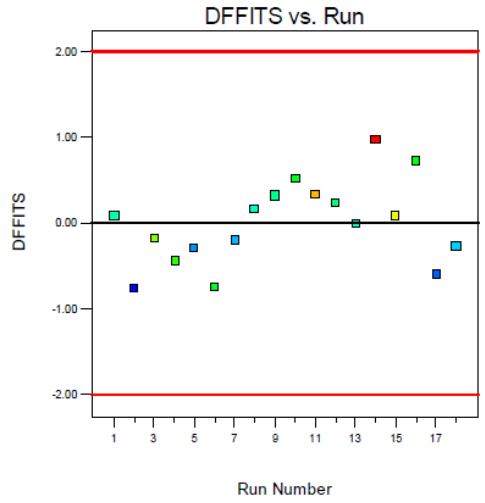


**Figure 10 The DFFITS versus run plot.**

**The difference in BETAS (DFBETAS) vs. run**

The difference in BETAS versus run plot measures the influence each point has on each regression coefficient for the model. The plot can be useful in identifying the data points which have high influence on the individual components importance in the formulation. The higher value of difference in BETAS a point has, the more it will influence the factor (figure 11).

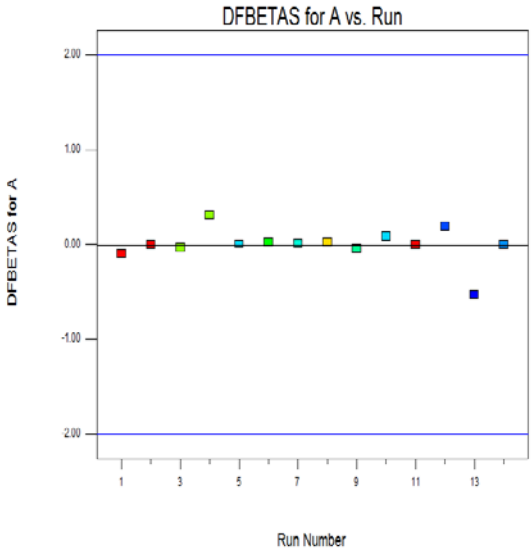


**Figure 11The DFBETAS versus run plot for factor A.**

**The Cook's distance**

The Cook's distance is a measure of how much the regression would have changed if a point with high influence had been deleted from the analysis. The Cook's distance plot will show the points that may influence the regression (figure 12). Points that have large distance values should be study further, to check if it is caused by mistake in the recording, an incorrect model, or a design point far from the rest of the design points. A large point value is normally considered 2-3 times larger than the other points, or points over the red line.

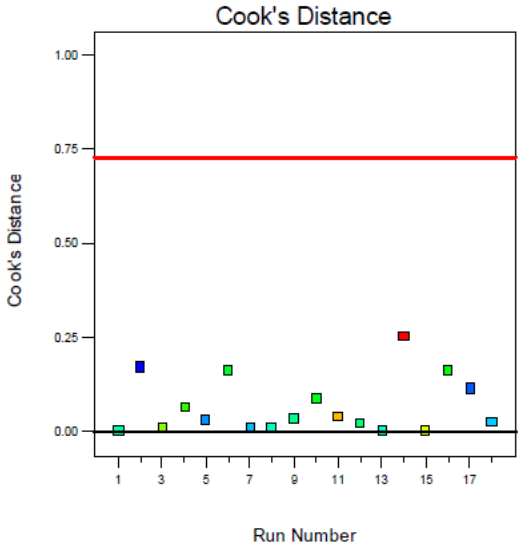


**Figure 12 The Cook's distance plot.**

## *2.3.3 Model graphs*

The result of the statistical analysis and model selection will lead to a model graph, showing the response data plotted as a function of the different components in a mixture. The most important plots are the contour map and 3-dimensional plot, as seen in figure 13. From these plots the best interaction between the different components can easily be observed, where the red colour indicates the best interaction and the blue colour the worse.

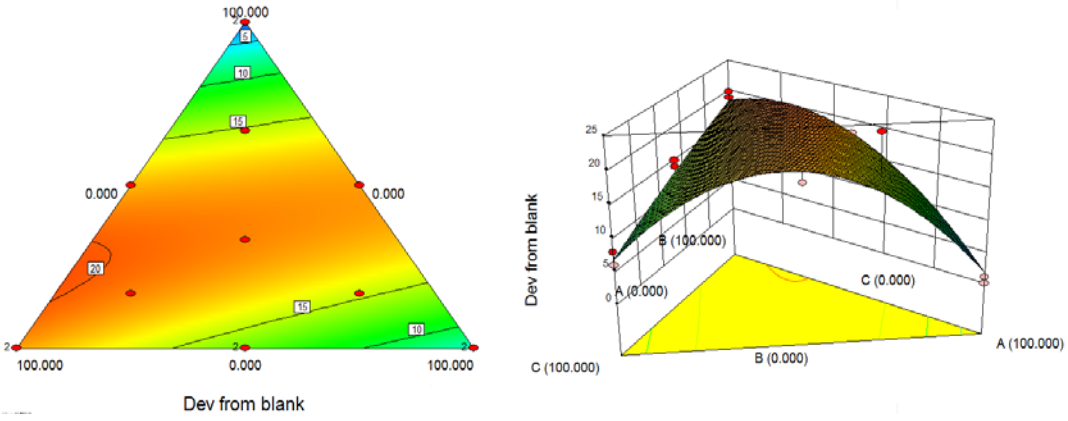


**Figure 13 The contour map and 3-dimensional graph showing the response surface for the components.**

## *2.4 Optimization*

Numerical optimization is preformed to find the maximum response value in the response surface graph for the different components in a mixture. The optimization maximum point is the highest point in the surface graph. The program will start seeking for the maximum point once the goal is defined. The maximum point will be marked on the contour map and the 3-dimensional graph (figure 14), and the precise formulation for the components in the mixture is provided. When the formulation for the optimization point is defined, there should be performed a new experiment to check the accuracy of the optimization point.

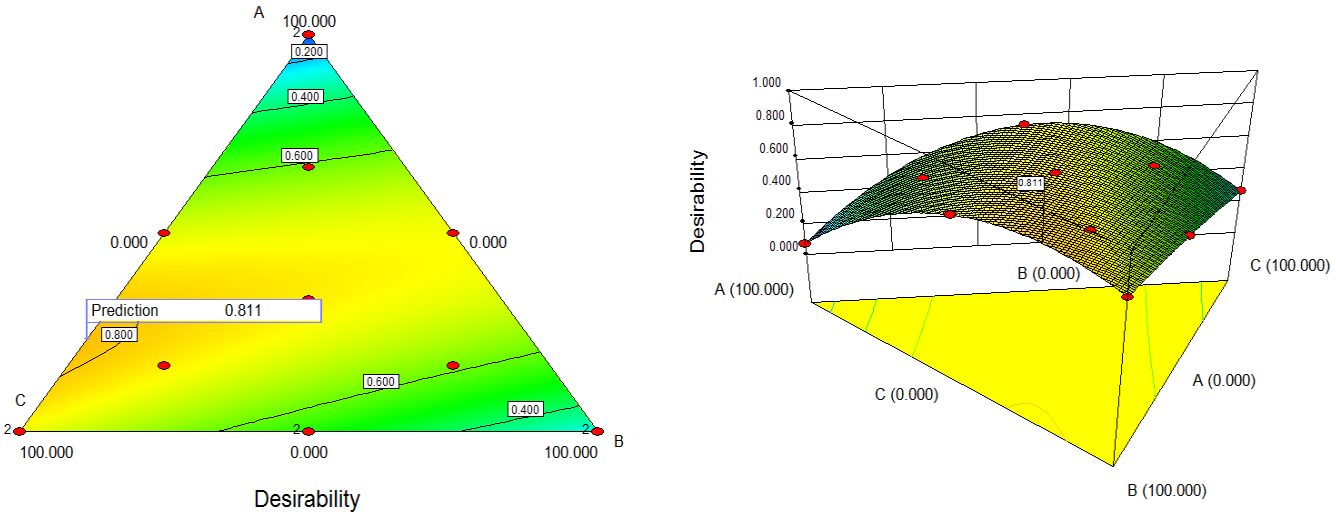


**Figure 14 The optimization point marked in the contour map and the 3-dimensional graph.**

# References:


1. Smith, W.F., *Experimental design of formulation*2005, Pittsford, New York: siam.
2. Franceschini, G. and S. Macchietto, *Model-based design of experiments for parameter precision: State of the art.* Chemical Engineering Science, 2008. **63**(19): p. 4846-4872.
3. Anderson, M.J. and P.J. Whitcomb, *Mixture DOE uncovers formulations quicker.* Rubber and Plastics News, 2002: p. 16-18.
4. Anderson, M.J. and P.J. Whitcomb, *Computer-aided tools for optimal mixture design.* Paint and Coatings Industry, 1999.
5. Batra, P. and R. Parsad, *EXPERIMENTS WITH MIXTURES.*
6. Scheffé, H., *Experiments with mixtures.* Journal of the Royal Statistical Society. Series B (Methodological), 1958: p. 344-360.
7. Woie, K., *Modellering og optimalisering av formuleringer ved hjelp av eksperimentell design*, in *Biologisk kjemi*2008, Universitet i Stavanger: Stavanger. p. 127.
8. 8.0, D.E., *DX8 topic help*, State-ease.
9. *NIST/SEMATECH e-Handbook of Statistical Methods*, 2003, NIST/SEMATECH.

# 3. Viscosity measurements

The intention with the viscosity measurements are to test the different mixture formulations of the PPDs, consisting of polymers with three different alkyl side chains length, which are defined and formulated in the DOE analysis in the next chapter. The viscosity measurements are used to find the optimum PPDs formulation, which will provide the best wax preventing performance.
The different PPDs are made based on the experimental plan from the simplex-lattice design, defined in chapter four. The chapter three will mainly focus on the performance of the experiments. While chapter four involve the processes of Design Expert software program, which includes the planning phase of the experiments, and analysis and interpretation of the data obtained from the experiments.

## 3.1 Introduction to viscosity measurements

When wax begins to precipitate in the pipelines, this will become notable by an increase in the viscosity of the well stream fluid. A high viscosity or gelling of the well stream fluid can be difficult to transport, therefore chemical inhibitors called pour point depressants (PPDs) have been developed to reduce and prevent the gelling of the crude. A viscometer may be used to measure the crude oils resistance to flow.
Fluids are normally divided into two types, Newtonian and non-Newtonian fluids. Newtonian fluids are liquids continuing to flow, despite of the force acting on them. While non-Newtonian fluids are viscous, and are in general dependent on the shear rate. The shear rate is a velocity gradient in a flowing material, caused by friction. Waxy crude oils will behave as Newtonian fluids when the temperatures are high and above the WAT. However when the temperature decreases below the WAT, the crude oils behave as non-Newtonian fluids, and are shear thinning, meaning the viscosity reduces when the shear rate increases [1].
In a viscometer the change in viscosity of a crude oil is measured by determining the fluid resistance as the temperature is decreased. A sample of the crude oil is put in a small container with a spindle immersed into the sample. When the test start the spindle is being rotated with a constant speed. The viscometer measures the torque required to rotate the spindle as the viscosity or flow resistance increases, during a decreasing temperature rate.
A computer software program is connected to the viscometer, which will collect and process the viscosity and temperature data. The collected data is used to make a plot showing the changes of viscosity versus the temperature. The plot may therefore be helpful to predict the WAT for crude oils [2].
The performance of the PPDs on a crude oil can be measured with a viscometer. The viscometer measures the increase in the viscosity of a sample, as the temperature of the sample is reduced with a constant rate. The viscosity of a crude oil will start to increase as the temperature comes below the WAT. The plot over the viscosity against the temperature can indicate at what temperature the wax begins to precipitate, shown by a steep increase in the viscosity graph. Comparing the viscosity graphs for a crude oil with and without PPDs, will give an indication on how well the PPDs manage to displace the temperature at which gelling of the crude oils occurs.

## *3.2 Viscosity measurements on Pour point depressants performance*

Viscosity measurements are used to evaluate the performance of a group of PPDs known as acrylate ester polymers. The polymers are design to contain a polymer backbone where different length alkyl side chains are attach onto, which will either be of 16 carbons, 18 carbons, 22 carbons, or a combination of these. These alkyl side chains are meant to interfere with the wax crystals in the crude oil, and reduce further growth of the wax crystals.

DOE is used to find the optimal formulation of a mixture containing different percentages of the different alkyl side chains on the polymers. There will be performed two different analysis with the acrylate ester polymers, where they will differ in the way the samples of the PPDs are prepared:

- In the first experiment there are synthesized acrylate ester polymers with different percentage of 16 carbons, 18 carbons and 22 carbons length alkyl side chains on the polymer backbone.
- In the second experiment there are synthesized three acrylate ester polymers, where one polymer has alkyl side chains of 16 carbons length, another polymer with 18 carbons length alkyl side chains, and the last polymer with 22 carbons length alkyl side chains (figure 2). Samples with different percentage of each of the polymers are made by mixing them together in xylene.

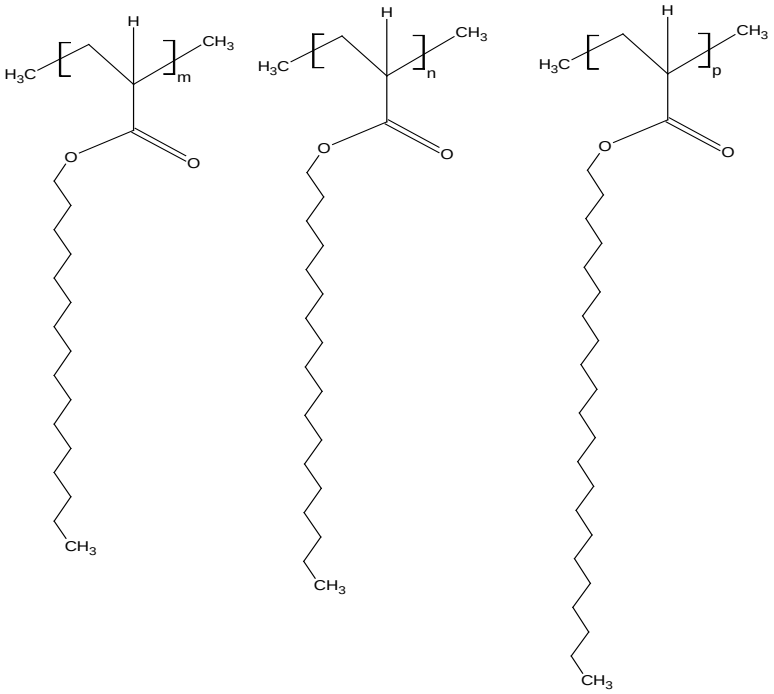


**Figure 2 The acrylate ester polymers with respectively 16, 18 or 22 length alkyl side chains.**

The polymer products are solid materials in room temperature, and therefore need to be dissolved before they can be applied. All the samples are made in solution of 25% active chemical, dissolved in xylene. The samples were put in an oven at around 60°C, to properly dissolve the sample.

## *3.3 The Experimental procedure for viscosity measurements*

The viscosity measurements were performed by using a Brookfield viscometer, called DV-III Ultra, as shown in figure 4 on the next page. The principle of the viscometer is to drive a spindle, which is immersed in a test cell containing the sample of crude oil, through a calibrated spring. The spring will measure the resistance against the spindle caused by the fluid.
A computer software program, called Rheocalc, is used to collect the viscosity and temperature data. The temperature is regulated by a water bath, by cooled fluid which is circulating through the jacket of the sampler container. A program is set for the water bath to decrease the temperature in a constant rate. In Rheocalc, all the parameters for the viscosity tests are set in a standard program, including the rotational speed, spindle size, and the time interval between readings. The standard settings used for the viscosity measurements were:

- Spindle size 21
- Rotational speed of 20 rpm
- Cooling rate ≈ 0.60 °C
- 30 second time interval between readings

Rheocalc plots the viscosity in centipoises (cP), against the temperature. Figure 3 below shows a viscosity graph for the crude Videle. The data collected can be transferred to excel for further analysis.


**Figure 3 Viscosity test for crude Videle shown in Rheocalc.**

Before the crude oil can be tested on the viscometer it has to be preheated to 90°C for a couple of hours, to ensure the complete dissolution of the wax crystal and remove the memory of previous wax formation [3]. The crude oil is then stored in an oven at 60°C until tested.
It is important that the experimental procedure for the viscosity measurements is performed as similar as possible each time, to ensure the same conditions for all the results.

The general procedure for the viscosity measurements:

- The water bath was turned on, and the start temperature set at 60°C.
- The Brookfield viscometer (figure 4) and Rheocalc were started, and the viscometer is auto zeroed.
- The sample container and the spindle were placed into the jacket, and thereby preheated to 60°C by the water bath. This is to avoid wax precipitation on the surfaces of the equipment before the tests start, due to cold surfaces.
- A 10 ml sample of the heated crude oil was made, and added 8 µl of the chemical solution, 25% in xylene. The concentration of the active chemical was 200 ppm.
- The sample was shaken well in approximately 30 second, before placed in the oven at 60°C for 15 min. After this it was shaken for approximately 30 seconds again, and added to the heated test cell, until the spindle was fully submerged.
- The Rheocalc program was started, and then the temperature program
- The test was finished when the graph had reached a steep increase in the viscosity, shows an exponential growth.
- The collected data was transferred to excel, where they can be plotted in a new graph for further analysis and comparisons.


**Figure 4 The Brookfield viscometer and water bath.**

## *3.4 Results and discussion*

There were performed viscosity measurements on two different crude oils:

- Crude Videle, which is a very black and viscous crude oil.
- Crude Malakai, which is a brown and light crude oil, more similar to condensate.

The viscosity measurements with the different PPDs tested on the crude oils are divided into two sets, due to their differences in the preparation of the samples.

- **The first set** contains 10 chemicals of arylate ester polymers, where one polymer have different percentage of the alkyl side chains of length 16, 18 and 22 carbons, attached to the backbone.
- **The second set** contains 10 chemical mixtures of different percentage of acrylate ester polymers, where each polymer contains either 16, 18 or 22 length alkyl side chains. These chemicals are normally referred to as EPT-2454 (C16), EPT-2455 (C18) and EPT-2456 (C22).

The percentages for the different chemical combinations found in set one and two are defined in chapter four, in the experimental plan obtained by the simplex-lattice design. The table 1 and 2 below contains an overview of the different chemical found in the two sets, with their different chemical percentage formulations.

**Table 1 Chemical set 1 of PPDs.**

| Chemical name | Component 1: Percentage of EPT-2455 | Component 2: Percentage of EPT-2455 | Component 3: Percentage of EPT-2456 |
|---|---|---|---|
| **EPT-2454 (C16)** | 100 | 0 | 0 |
| **EPT-2455 (C18)** | 0 | 100 | 0 |
| **EPT-2456 (C22)** | 0 | 0 | 100 |
| **CdId 325** | 16,667 | 16,667 | 67,666 |
| **CdId 326** | 50 | 0 | 50 |
| **CdId 327** | 16,667 | 67,666 | 16,667 |
| **CdId 328** | 50 | 50 | 0 |
| **CdId 329** | 0 | 50 | 50 |
| **CdId 330** | 67,666 | 16,667 | 16,667 |
| **CdId 331** | 33,333 | 33,333 | 33,333 |

In table 2 below for set 2, the chemical names for the different mixture combinations are just named as the run number, which was provided in Design-Expert. The table will also include the four replicates that were given in the experimental plan.

**Table 2 Chemical set 2 of PPDs, with the 4 replicates.**

| Run | Component 1 A:EPT-2454 percent | Component 2 B:EPT-2455 percent | Component 3 C:EPT-2456 percent |
|---|---|---|---|
| 1 | 16.667 | 66.666 | 16.667 |
| 2 | 0.000 | 100.000 | 0.000 |
| 3 | 33.333 | 33.333 | 33.333 |
| 4 | 66.666 | 16.667 | 16.667 |
| 5 | 50.000 | 0.000 | 50.000 |
| 6 | 0.000 | 50.000 | 50.000 |
| 7 | 0.000 | 0.000 | 100.000 |
| 8 | 50.000 | 50.000 | 0.000 |
| 9 | 0.000 | 50.000 | 50.000 |
| 10 | 16.667 | 16.667 | 66.667 |
| 11 | 0.000 | 100.000 | 0.000 |
| 12 | 100.000 | 0.000 | 0.000 |
| 13 | 100.000 | 0.000 | 0.000 |
| 14 | 0.000 | 0.000 | 100.000 |

### *3.4.1 Crude videle viscosity measurements*

The viscosity measurements were first performed on the crude oil Videle, which is regared as a waxy crude oil. The first viscosity measurements performed was blank tests with crude Videle alone. The graph in figure 5 shows the plot for the blank crude Videle test. From this graph the WAT for the waxes is around 35-40 °C, which are found where the diversion of the lineraty in the graph occurs. The interception point in the graph at the viscosity value around 2700 cP, occurs as a result of the sample becomming to viscous for the spindle to rotate in and thereby shear off.
The blank viscocity measurement is used furter to compare with the effects for the PPDs viscosity measurements.

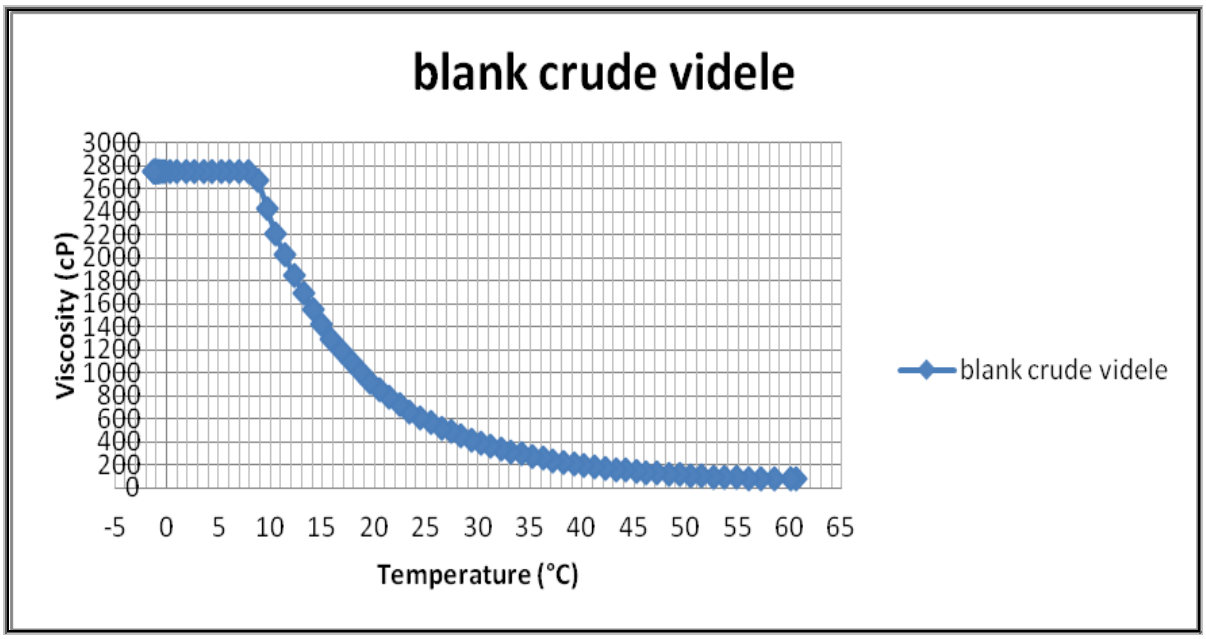


**Figure 5 Viscosity measurement with blank crude Videle.**

There were performed viscosity measurements for some of the PPDs from the set 1. The different chemicals tested from set 1 were randomly chosen, and were CdId 327, CdId 323 and CdId 329. The viscosity results were plotted in a graph together with the blank Videle result, to easier compare their effectiveness, as shown in the figure 6.

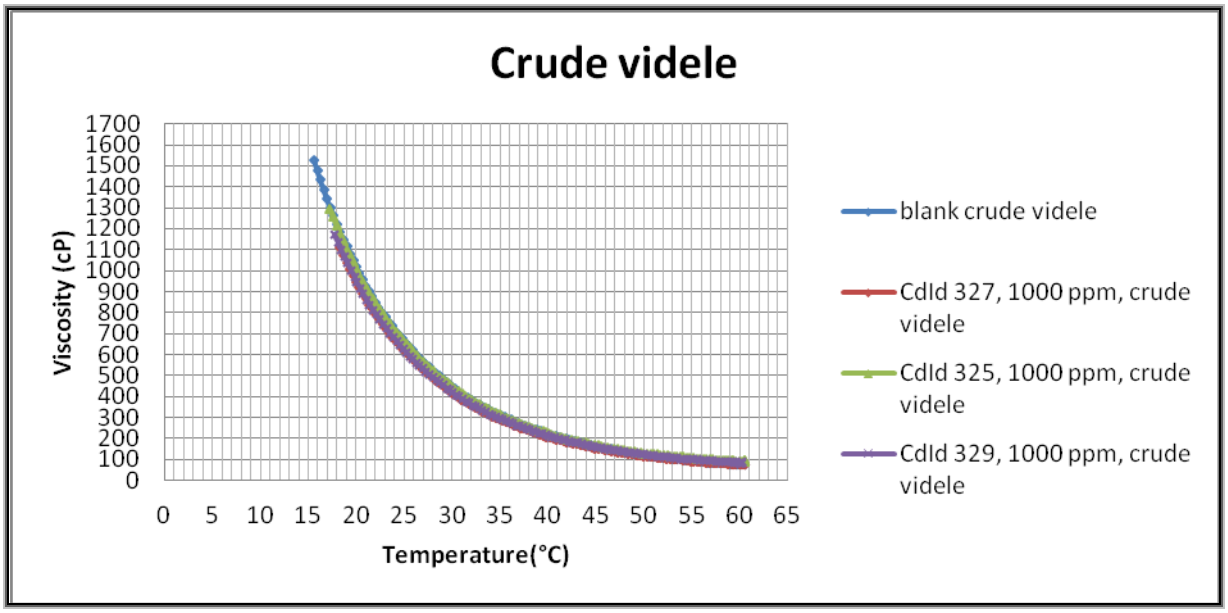


**Figure 6 The viscosity measurements for the different chemicals from set 1, compared with the blank.**

The chemicals from the set 1 tested on crude Videle, did not manage to displace the temperature for when the viscosity increased. All the chemicals experienced the same viscosity increase tendencies at the same temperature, as the blank crude Videle test had given.

There were therefore performed a viscosity measurement where the concentration of chemical CdId 325 (randomly chosen) were increased. The concentration of CdId 325, 25% in xylene, in the first viscosity measurement was at 1000 ppm, while in the second viscosity measurement the concentration of the CdId 325 solution was increased to 2000 ppm.
However doubling the concentration of the chemical CdId 325, did not lead to any better effect for the chemical, as seen in the figure 7. The same viscosity curve was observed for both the concentrations.

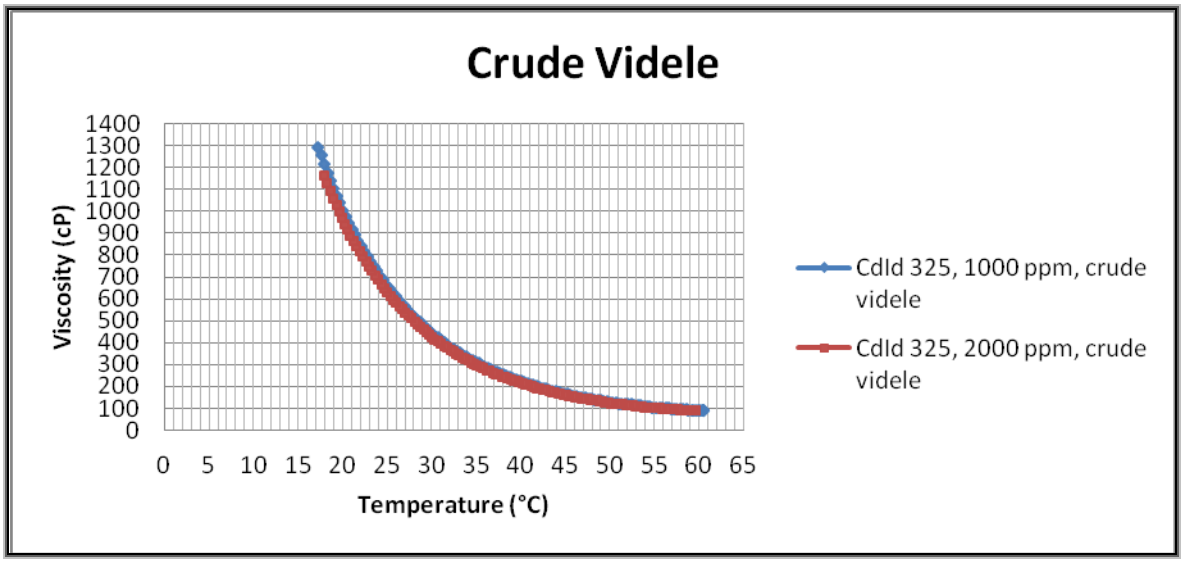


**Figure 7 The viscosity measurements for CdId 325 at different concentrations.**

Since the viscosity results for the chemicals tested on crude Videle gave no response, compared to the blank curde videle test, it was decided to try the chemicals on a different crude oil.
The reason there was not any effect with the chemcials, can be that the length on the alkyl side chains on the PPDs polymer are not of the right size to interferre with wax crystals in the crude oil. The length of the alkyl side chains should be of similar size as the length of the wax alkane chains found in the crude oil, to get the best interaction and to reduce further wax growth.

### *3.4.2 Crude Malakai viscosity measurements*

The second crude oil used for the viscosity measurements, was crude Malakai, which is a light crude oil. The viscosity measurements with crude Malakai were done over a larger temperature range, because the displacements of the viscosity were observed at much lower temperature for some of the chemicals. This required therefore a better water bath, Julabo FP50, which was able to decrease the temperature down to -20°C. The first water bath, Julabo 50, could only decrease the temperature down to -10°C.

The change of the water baths caused a little variation in the viscosity graphs. The viscosity measurements done with the first chemicals on the first water bath, started on a slightly higher viscosity, around 20-30 cP higher, compared to the chemicals tested with the last water bath. However the graphs showed to follow the same viscosity increasing trends at the same temperature for both the water baths, as seen in figure 8. Figure 8 compares the blank viscosity measurements for crude Malakai with the different water baths.

The new water bath, Julabo FP50, caused a small vibration in the bench on where the viscometer was placed on. However, a calibration of the viscometer indicated no effect of the vibration on the results from the viscosity measurements.

The prediction of the WAT from the blank viscosity graph for crude Malakai was found at 17 °C.

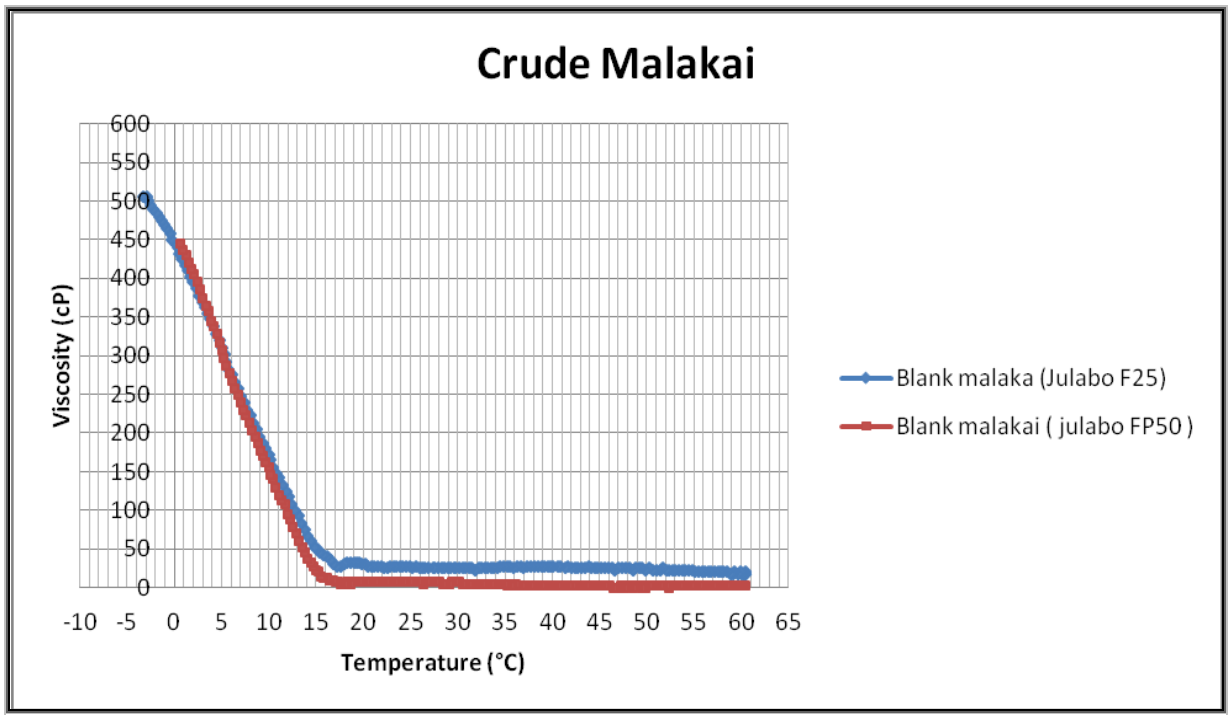


**Figure 8 The blank viscosity measurements for crude Malakai, preformed with the different water baths.**

## *Viscosity measurements with chemical Set 1 for crude Malakai*

Viscosity measurements were performed on the Crude Malakai with the chemicals from set 1. There were in total 10 chemicals tested, and all the viscosity results are plotted in the same graph together with the blank viscosity result, shown in figure 9 on the next page.

The results of the viscosity measurements by the chemicals from set 1, gave in general good effects on the displacement of the viscosity curves at lower temperatures, compared to the blank viscosity curve.

The chemical EPT-2454 gave the poorest displacement, and began the steep viscosity increasing at 1 °C below the blank. EPT-2456 gave a better displacement of the curve, with a viscosity increasing temperature at 9°C, which is 8 °C temperature displacement of the graph compared to the blank. However both EPT-2454 and EPT-2456 were the chemicals that lead to the least temperature displacement.

The chemical that gave the best temperature displacement was CdId 330, which gave a temperature displacement of 22 °C compared to the blank. The steep increase in the viscosity did not start before the temperature had reach -5°C. There were performed three replicates for the CdId 330 viscosity tests, which all gave similar graphs, as seen in figure 10.

The other chemicals that showed a good displacement for the temperature were EPT-2455 and CdId 331, which gave displacement in temperature at 20°C and 19°C compared to the blank.

The other chemicals gave a steep increase in the viscosity at temperatures between 2°C-5°C, which is also good compared to the blank at 17 °C.

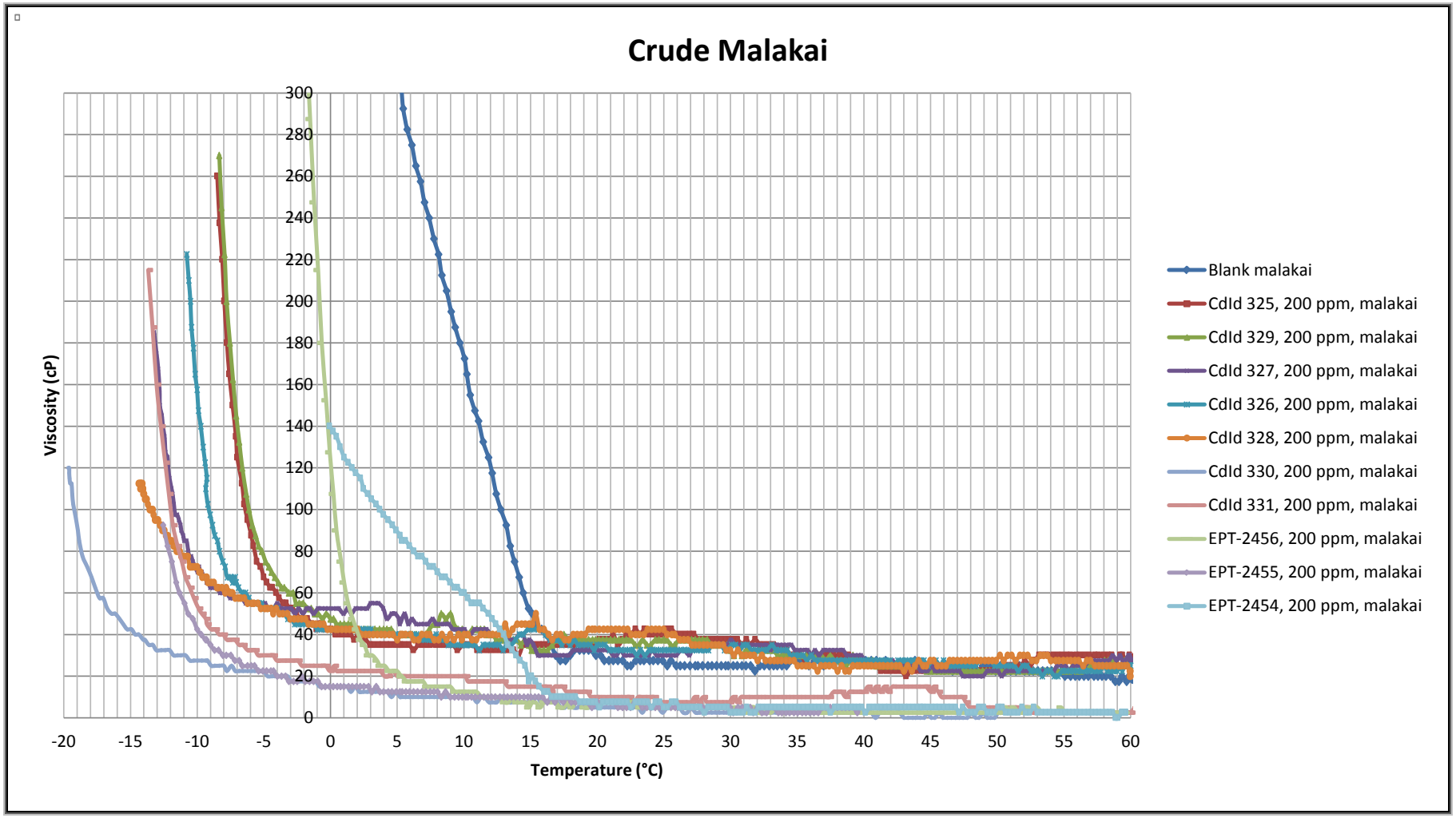


**Figure 9 The viscosity measurements for all the chemicals in set 1, compared with the blank Malakai viscosity measurement.**

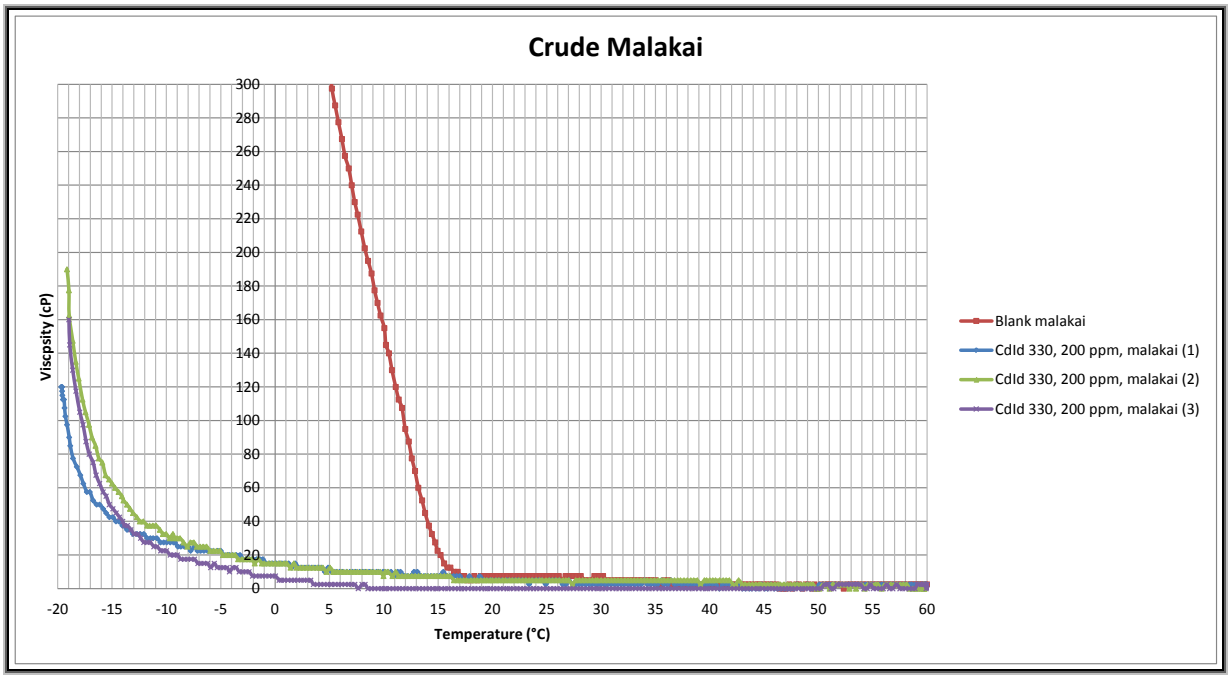


**Figure 10 The viscosity measurements for CdId 330, compared with the blank.**

## *Viscosity measurements with chemical set 2 for crude malakai*

There were performed viscosity measurements for all the chemicals in the set 2, which are shown in figure 11 on the next page. The viscosity results for the set 2 gave in general a large decrease in the temperature for when the steep viscosity increased occurred for most of the chemicals, compared to the blank.

The chemical EPT-2454, EPT-2455 and EPT-2456, are the same chemicals used in set 1, which gave similar viscosity results. EPT-2454 and EPT-2456 gave also in set 2 the poorest displacements of the temperatures, compared to the other chemicals, such as seen in set 1.

EPT-2455 gave one of the best displacements of the temperature for the set 2 compared to the blank. Figure 12 compares three viscosity measurements done for EPT-2455 compared to the blank, where similar viscosity graph were obtain for all three measurements.

The other chemical which gave the best displacement of temperature was for run 1 at 14°C, compared to the blank. The temperature for when the steep increase in the viscosity occurred for run 1 was at 3°C.

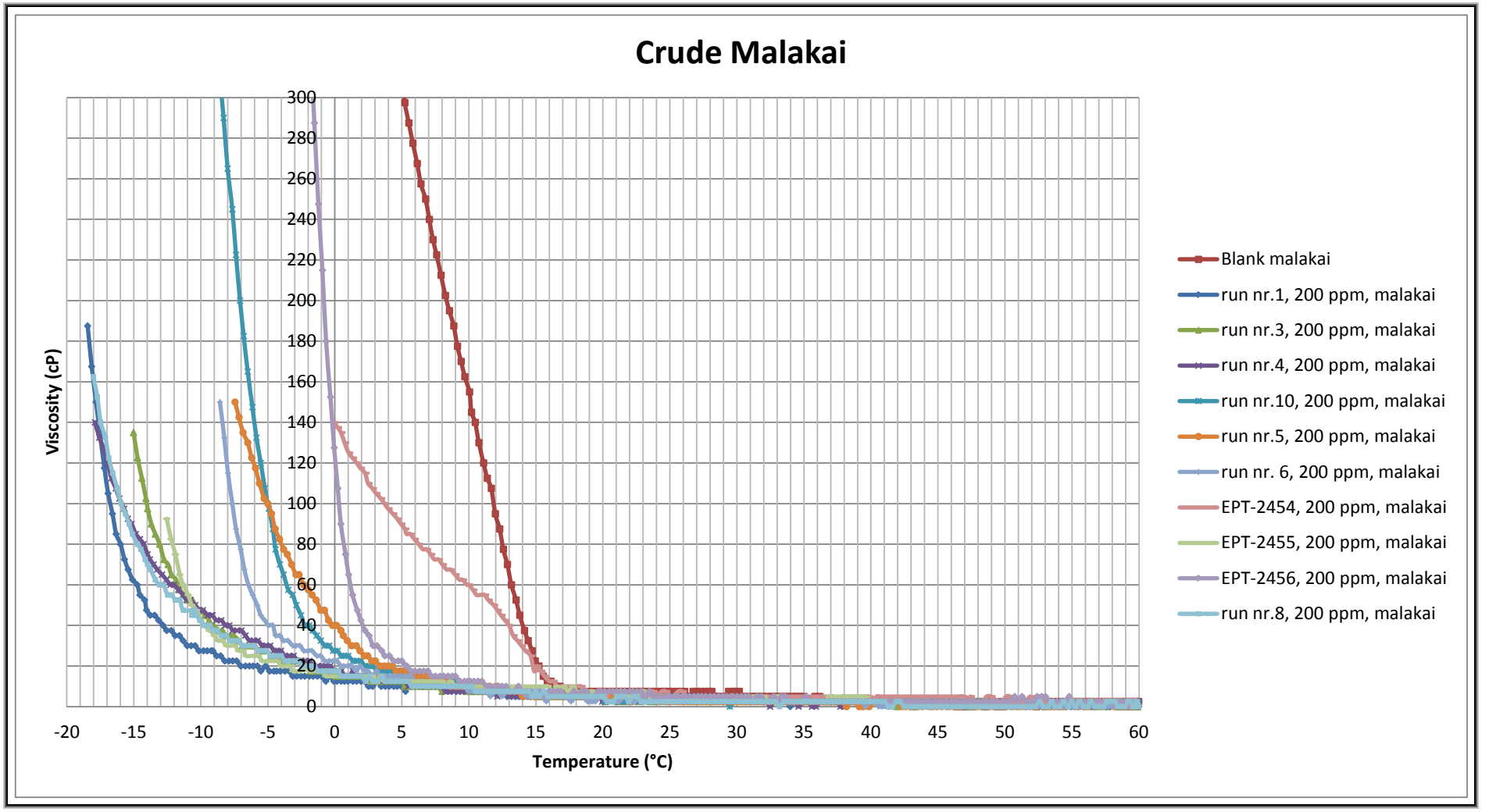


**Figure 11 The viscosity measurements for the chemicals in set 2, compared with the blank.**

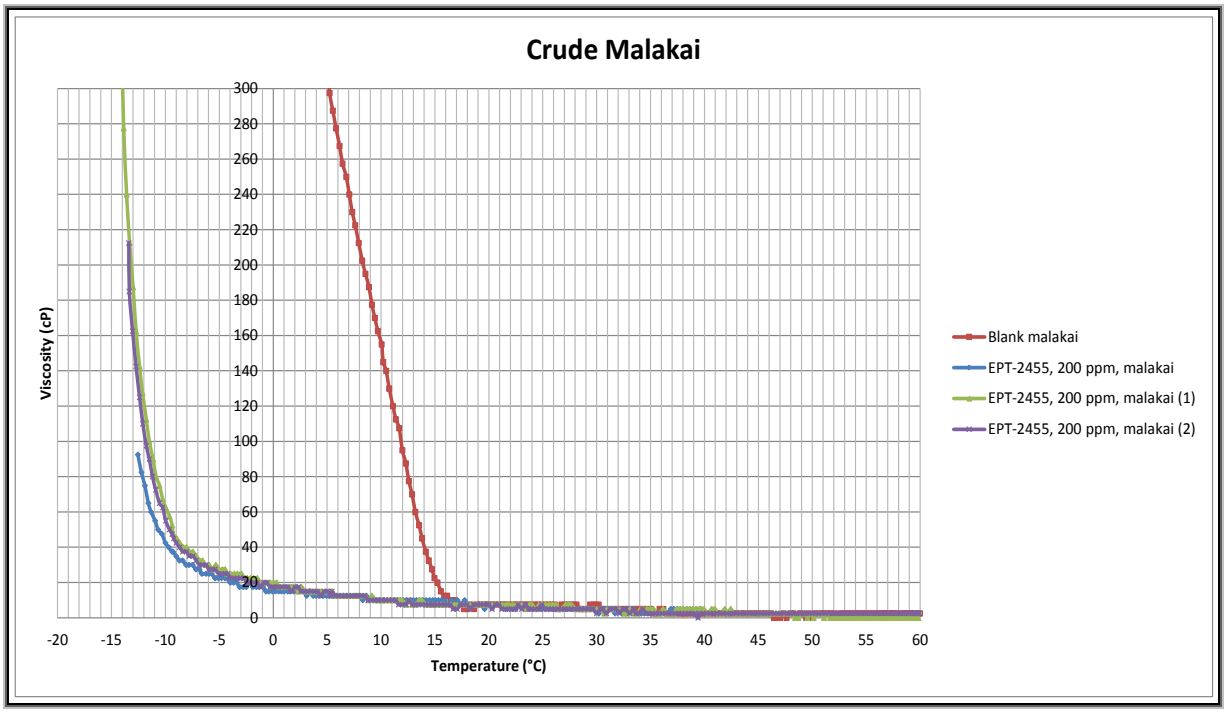


**Figure 12 Viscosity measurements for EPT-2455 compared with the blank.**

There were performed three viscosity measurements for EPT-2454, where the viscosity graph indicated a similar displacement of the temperature for all the graphs, as seen in figure 13 below.

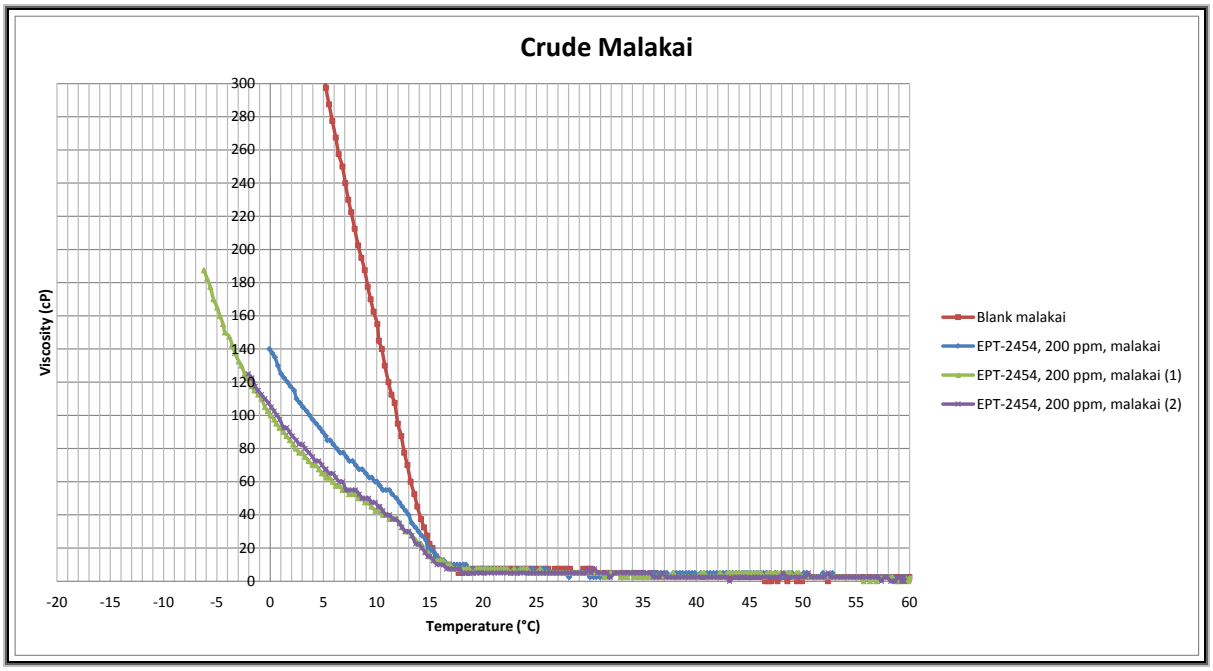


**Figure 13 Viscosity measurements for EPT-2454, compared with blank.**

## *3.5 Conclusion*

The chemicals from set 1, tested on the crude oil Videle, gave no difference in results on the viscosity measurements compared to the blank. The chemicals viscosity graph experienced the same tendencies as was found for the viscosity graph for the blank crude Videle test, indicating no effect as PPDs for these chemicals for this specific crude oil. This can be due to little interaction occurring between the PPDs alkyl side chains with the wax alkane chains in the crude oil.

The viscosity measurements performed on crude Malakai with chemical set 1 and 2, gave in general large displacements of the temperature for when the steep increase in viscosity occurred, compared to the blank viscosity measurements. However, the chemicals in set 1 gave better viscosity results compared to the chemicals in set 2. Meaning the PPDs polymers where the different length of alkyl side chains are varied on one polymer backbone, performed better than the mixtures of polymers, which vary in the percentage of the three polymers with different length alkyl side chains.
In both set 1 and 2 the PPDs polymer called EPT-2455, showed good effect in displacing the temperature compared to the blanks. EPT-2455 consists of acrylate ester polymers, with 18 carbons length alkyl side chains.
In set 1 the largest displacement of the temperature was by CdId 331, which gave a steep increase in the temperature at approximately -5°C. This is a large displacement compared to the blank, which gave a steep increase in the viscosity at approximately 17°C.
In set 2 the largest displacement was for run 1 and EPT-2455, which both gave the steep increase in temperature at approximately 3°C.

The viscosity measurements results from set 1 and 2 are further analysed in chapter four, as a part of the DOE analysis.

## *References:*


1. Venkatesan, R. and J.L. Creek, *Wax deposition and rheology: progress and problems from an operator*, in *Offshore Technology Conference*2010: Houston, Texas, USA.
2. Zhu, T., J.A. Walker, and J. Liang, *Evaluation of Wax Deposition and Its Control During Production of Alaska North Slope Oils*, 2008, University of Alaska.
3. Tiwary, D. and A.K. Mehrotra, *Measurement of Rheological Properties of Highly Paraffinic "Waxy " Mixtures ™*, in *Canadian International Petroleum Conference*2002, Petroleum Society of Canada: Calgary, Alberta.

# *4. Design of experiments with design-expert 8.0*

Design of experiments (DOE) is a statistic method used to make it easier to carry out experiments. The mixture design is a DOE process used to determine the optimum combination of components in a mixture, by applying the minimum number of experimental runs. Design-Expert is a software program created to make it easier to use the DOE technique. Design-Expert is a proven to be an effective and simple tool in chemistry experiments for screening, modelling and optimization [1, 2]. In this thesis Design-Expert is used to find the best formulation in two mixture designs containing different polymers used as PPDs, called acrylate ester polymers. There are made two different chemical sets for the mixture designs, which differ in the preparation of the samples, as was explained earlier in chapter 3.2.

- **Set 1** contains acrylate polymers with different percentage of 16 carbons, 18 carbons, and 22 carbons length alkyl side chain on the polymer backbone.
- **Set 2** contains mixtures of different percentages of acrylate polymers having either 16 carbons, 18 carbons or 22 carbons length alkyl side chains.

Viscosity measurements are the experimental method used to test the effects of the different PPDs combinations in set 1 and 2, which were performed in chapter three.
The different combinations of the components in set 1 and 2, were decided in the experimental plan provided by the simplex-lattice design, as seen in figure 1. The simplex-lattice design comes up with 14 experimental runs, which is the minimum number of experiments needed to make a response surface graph for the components interaction. Four of the experimental runs are replicates, needed to estimate the pure error. The 10 other experiments consists of different combinations of the components in the mixture, marked as red dots in the simplex-lattice shown in figure 1.

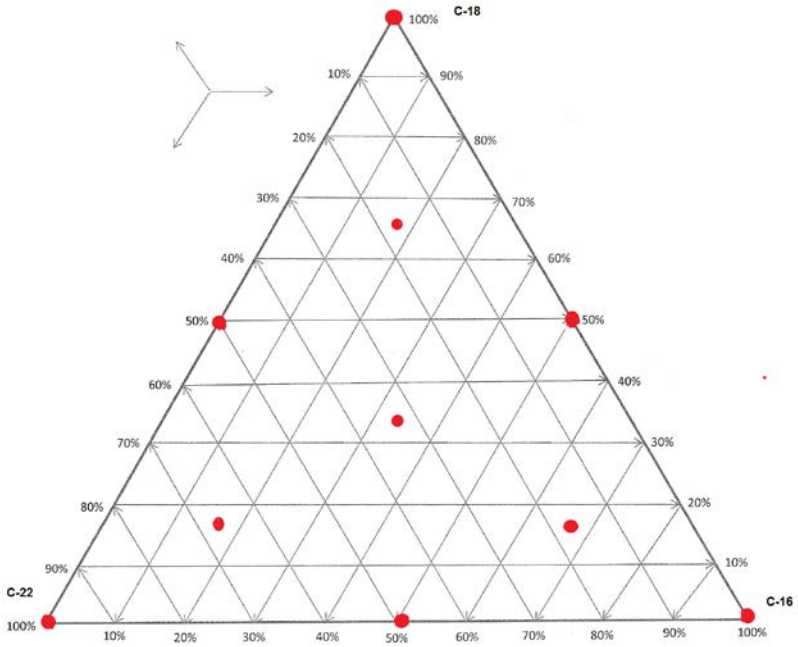


**Figure 1 The simplex-lattice design shows the experiments needed for a mixture design with three components.**

## *4.1 Definition of the responses*

From the experimental runs there have to be defined and measured a response, in order to make a response surface graph for the best combinations of the components in a mixture.
In the viscosity measurements the response for the different PPDs are how much they manage to displace the temperature before the steep viscosity increasing occurs, compared to the blank viscosity measurement. The temperature points can however be read of the viscosity graph in two different ways, which are the responses used in the DOE analysis:

- **Response 1: Deviation from blank**
  The temperature for when the steep increase of the viscosity occurs in the crude oil with the PPDs, compared to the blank viscosity measurement. The blank viscosity graph starts to increases in the viscosity at a temperature of 17°C, as pointed out in figure 2. The response measurement for the PPDs is the absolute value between temperature of the steep increase in viscosity for the PPDs, and the blank temperature value at 17°C.

- **Response 2: 50 centipoise (cP) limit**
  The viscosity value for the linear curve in the beginning of the viscosity measurements are found, which is the viscosity value that have the longest range of linearity before the viscosity starts to deviate. This viscosity value is then added 50 cP, and a temperature is found where this new viscosity value intercepts the viscosity curve. The temperature for the PPDs is further used to compare with the temperature value for the blank. The response 2 value for the blank is found in figure 2, and is at 14 °C. The response values for the PPDs are the absolute value between the PPDs 50 cP limit value and the blank 50 cP limit value.

The temperature for when the steepening of the viscosity curve occur will be a subjective interpretation, however to get valid results the most important thing is to always use the same method for interpreting the viscosity graphs in the experimental design plan.

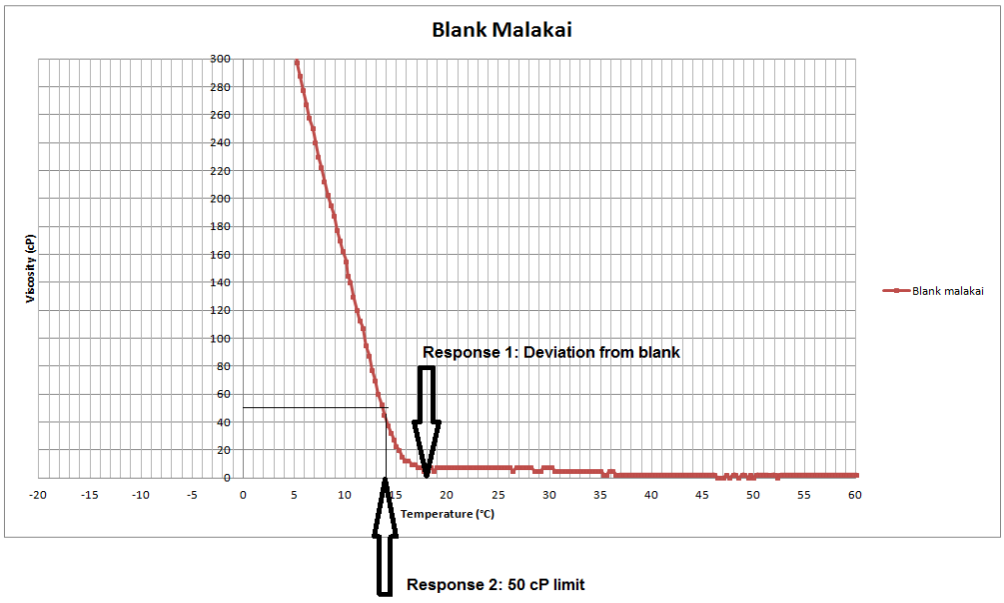


**Figure 2 The defined responses are found from the viscosity measurements, and compared with the blank crude Malakai, where the response 1 is at temperature 17°C, and response 2 at temperature 14°C.**

The experimental runs, combination of the components and the measured responses are all found in table 1 and 2 below, which tables are made in Design-Expert. The measured responses are filled into the tables after the viscosity measurements have been performed.

**Table 1 The experimental plan and viscosity measurement results for the chemical set 1, with crude Malakai.**

| Run | Component 1 A:C-16 percent | Component 2 B:C-18 percent | Component 3 C:C-22 percent | Response 1 Dev from blank C | Response 2 50 cP limit C |
|---|---|---|---|---|---|
| 1 | 16.667 | 16.667 | 66.667 | 14 | 20 |
| 2 | 0.000 | 50.000 | 50.000 | 15 | 18 |
| 3 | 100.000 | 0.000 | 0.000 | 1 | 4 |
| 4 | 16.667 | 66.667 | 16.667 | 13 | 24 |
| 5 | 0.000 | 0.000 | 100.000 | 8 | 12 |
| 6 | 0.000 | 100.000 | 0.000 | 20 | 25 |
| 7 | 50.000 | 0.000 | 50.000 | 17 | 22 |
| 8 | 66.667 | 16.667 | 16.667 | 22 | 29 |
| 9 | 0.000 | 100.000 | 0.000 | 19 | 25 |
| 10 | 0.000 | 0.000 | 100.000 | 6 | 12 |
| 11 | 33.333 | 33.333 | 33.333 | 19 | 24 |
| 12 | 100.000 | 0.000 | 0.000 | 0 | 6 |
| 13 | 50.000 | 50.000 | 0.000 | 18 | 25 |
| 14 | 0.000 | 50.000 | 50.000 | 14 | 19 |

**Table 2 The experimental plan and viscosity measurement results for the chemical set 2, with crude Malakai.**

| Run | Component 1 A:EPT-2454 percent | Component 2 B:EPT-2455 percent | Component 3 C:EPT-2456 percent | Response 1 Dev. from bla... C | Response 2 50 cP limit C |
|---|---|---|---|---|---|
| 1 | 16.667 | 66.666 | 16.667 | 14 | 28 |
| 2 | 0.000 | 100.000 | 0.000 | 14 | 25 |
| 3 | 33.333 | 33.333 | 33.333 | 9 | 24 |
| 4 | 66.666 | 16.667 | 16.667 | 9 | 24 |
| 5 | 50.000 | 0.000 | 50.000 | 3 | 15 |
| 6 | 0.000 | 50.000 | 50.000 | 7 | 20 |
| 7 | 0.000 | 0.000 | 100.000 | 4 | 12 |
| 8 | 50.000 | 50.000 | 0.000 | 11 | 25 |
| 9 | 0.000 | 50.000 | 50.000 | 5 | 19 |
| 10 | 16.667 | 16.667 | 66.667 | 3 | 17 |
| 11 | 0.000 | 100.000 | 0.000 | 14 | 24 |
| 12 | 100.000 | 0.000 | 0.000 | 1 | 3 |
| 13 | 100.000 | 0.000 | 0.000 | 0 | 1 |
| 14 | 0.000 | 0.000 | 100.000 | 2 | 11 |

When all the design information needed for the mixture design is collected, Design-Expert will start the DOE analysis, where it will find the best model to describe the response surface graph for the mixture components. DOE analysis for chemical set 1 and 2 for crude oil Malakai are performed, and for the two different measurement responses. In total four DOE analysis are done, and they will be discussed in the next sections.

## *4.2 Doe for the chemical set 1 with response 1: Deviation from blank*

Based on the information given in table 1, Design-Expert will compare the different scheffè polynomial model equations against the response data, in the fit summary section.
The models which manage to describe the response data best, with the least variations between the measured data and the predicted data from the model, are the one suggested for the mixture design. A quadratic model was suggested for the chemical set 1 with response 1.

**Diagnostics**

In the diagnostics plots some important statistics analyses are applied to the response data, to see how the well the measured points fit the model. The different plots are briefly described in the next section.

**Normal plot**

The normal plot of residuals for set 1 with response 1 (figure 3), shows that the measured response data follow a normal distribution. The residuals are randomly scattered, and follow the red line. There is a slight tendency of a S-form in the residuals, however the Box-Cox plot gave no suggestions about transformation required.

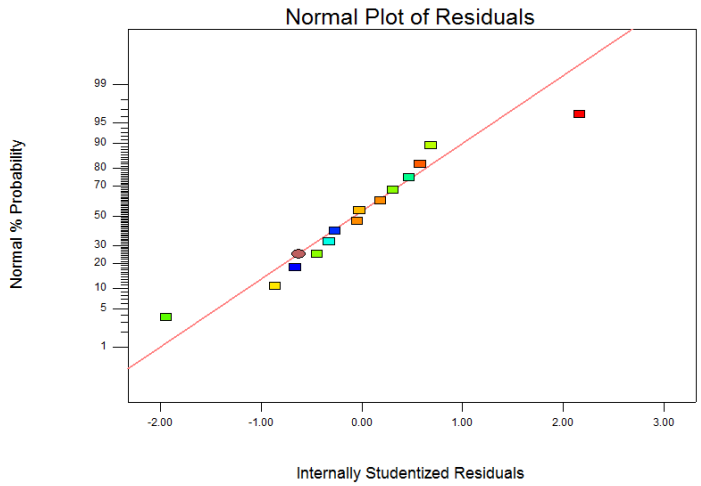


**Figure 3 The normal plot of residuals for set 1 with response 1.**

**Residuals vs. predicted plot**

The residuals versus predicted plot for the measured response data compared to the predicted response values of the model, shows a small tendency of the residuals to increase from left to right (figure 4). This may imply a higher uncertainty with the higher response values, which means higher uncertainties in the results with higher temperatures. However all the residuals are inside the red boundary lines, and the transformation given are within the limits.

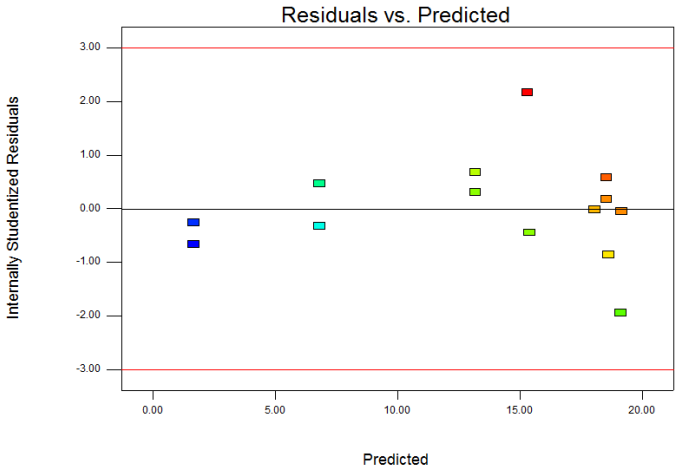


**Figure 4 The residuals vs. predicted plot for set 1 with response 1.**

### Residuals vs. run plot

The residuals versus the experimental run order plot, shows in general an even scatter in the experimental run order for the residuals. There are two points which are a bite high and low compared to the other points, but they are still inside the red lines, and there are no special trends formed in the plot (figure 5).

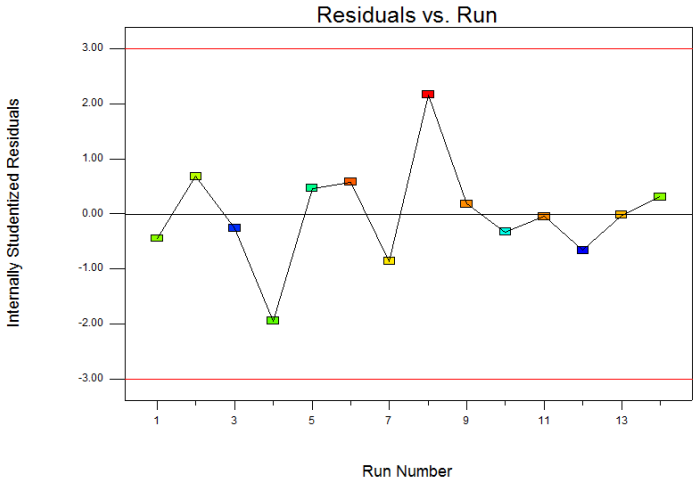


**Figure 5 The residuals vs. run plot for the set 1 with response 1.**

### Predicted vs. actual plot

In figure 6 the measured response data are plotted against the predicted response values from the suggested model. The measured response values are in general scattered randomly around the model line, however there are found a cluster of data points at higher values, but a transformation were not recommended in the Box-Cox plot.

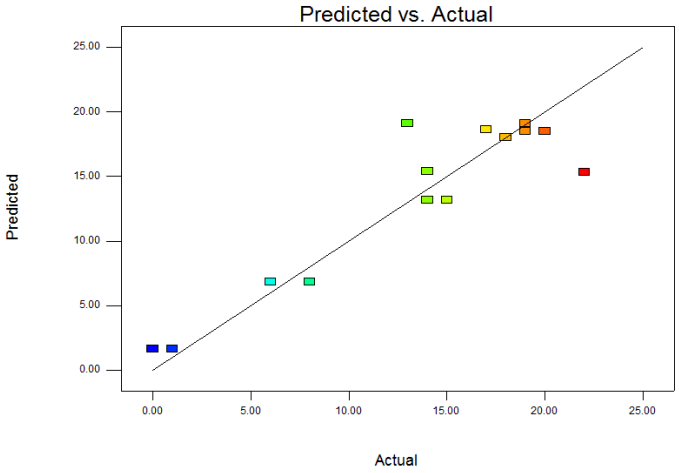


**Figure 6 The predicted vs. actual plot for the set 1 with response 1.**

### Box-Cox plot

The Box-Cox plots recommends no transformation for the measured response data, which is illustrated in figure 7 below, where the blue line is between the red boundary lines.

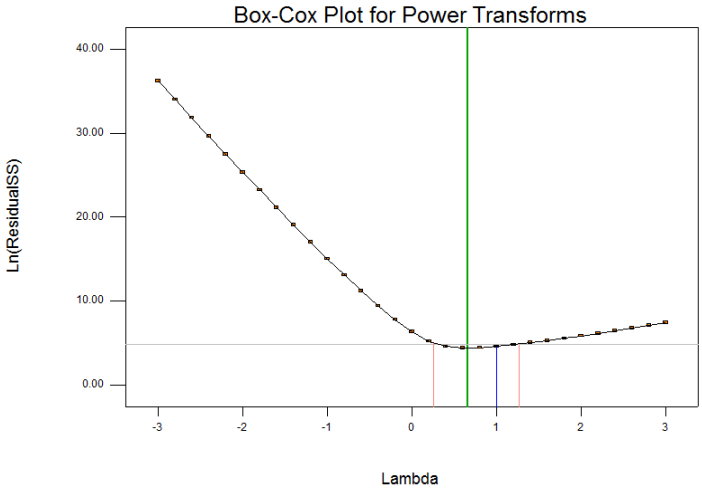


**Figure 7 The Box-Cox plot for the set 1 with response 1.**

### Influence

The influence plots in the diagnostic section checks if there are any measured response data that do not fit well with the suggested model. If there are such outlier points, they will be found outside the boundary levels for the plot, i.e. red lines.

All the measured data point for set 1 with response 1, were inside the boundary lines, which means that there are no concern with any outlier points that can influence the model (figure 8).

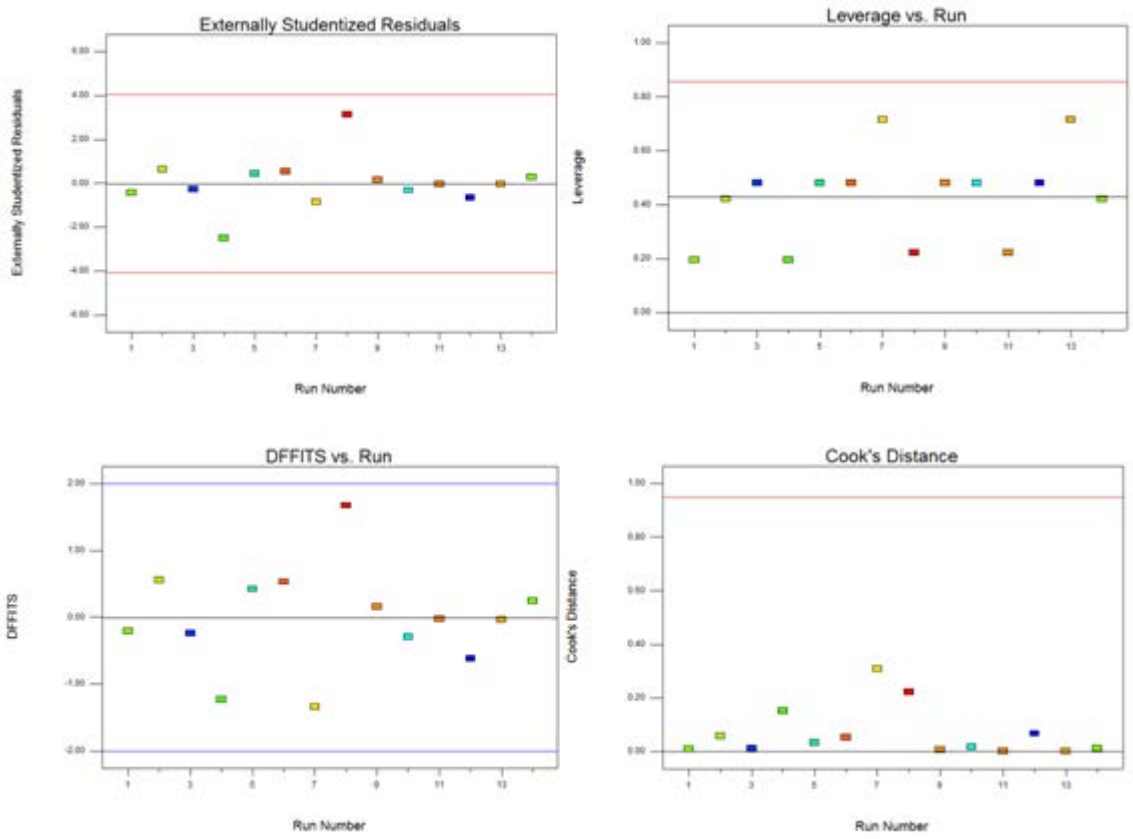


**Figure 8 The different influence plots for set 1 with response 1.**

**Model Graphs**

The different diagnostics plots did not show any trends or measure point, which did not fit well with the suggested model. The suggested quadratic model can therefore be used to make the response surface graphs for the different combinations of the components in the set 1. The graphs below in figure 9 show the contour map and the 3-dimentsional response surface graph. From these plots the best interactions between the components seem to incline towards the component B, which is the chemical EPT-2455 alone. EPT-2455 was one of the PPDs which gave the best temperature displacement of the viscosity curve in the viscosity measurements, therefore the interactions in the model response surface graph seems to correspond well with experimental data.

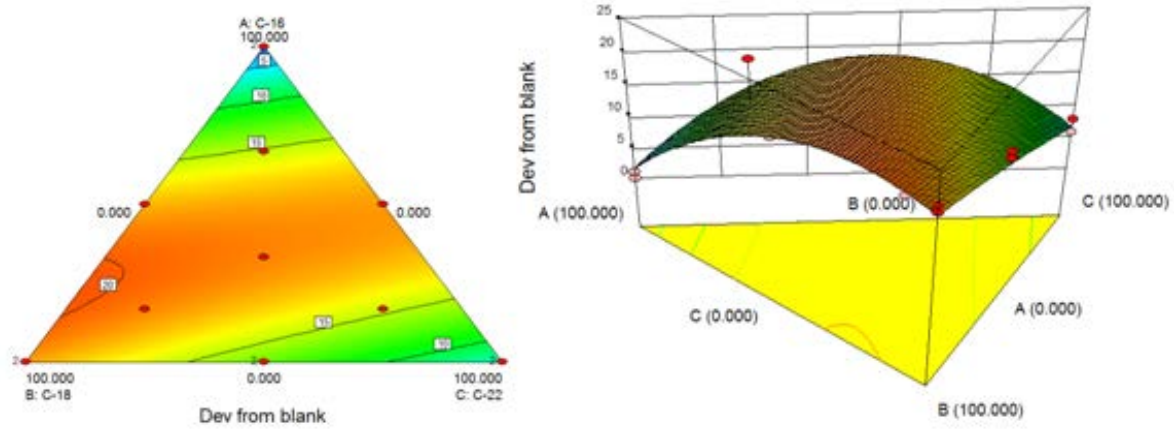


**Figure 9 The response surface graphs, contour map and 3-dimensional graph, for the set 1 with response 1.**

## Optimization

Numerical optimization was performed on the response surface graph, to provide a precise formulation of the optimum combination of the components in the set 1 with response 1. The precise formulation is given in table 3 below. The optimization point was found close to component B, and was a mixture of polymer with alkyl side chains length of C16 and C18.

**Table 3 The precise formulation of the optimization point for set 1 with response 1.**

| Solutions | | | | | | |
|---|---|---|---|---|---|---|
| Number | C-16 | C-18 | C-22 | Dev from blar | Desirability | |
| 1 | 23.438 | 76.562 | 0.000 | 20.2791 | 0.811 | Selected |

The optimization point for the set 1 with response 1, are marked on the contour map and the 3-dimensional response surface graph in figure 10 and 11.

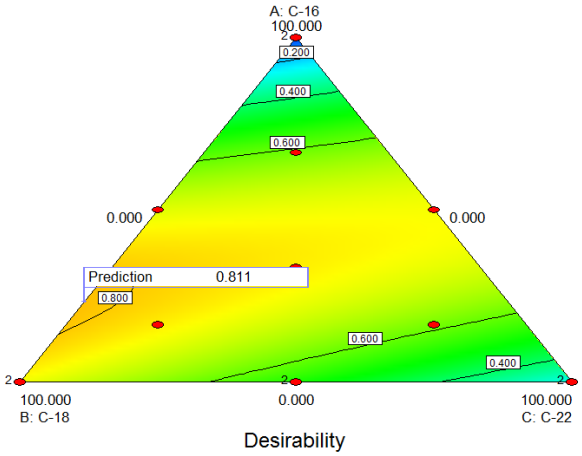


**Figure 10 The contour map showing the optimization point for the set 1 with response 1.**

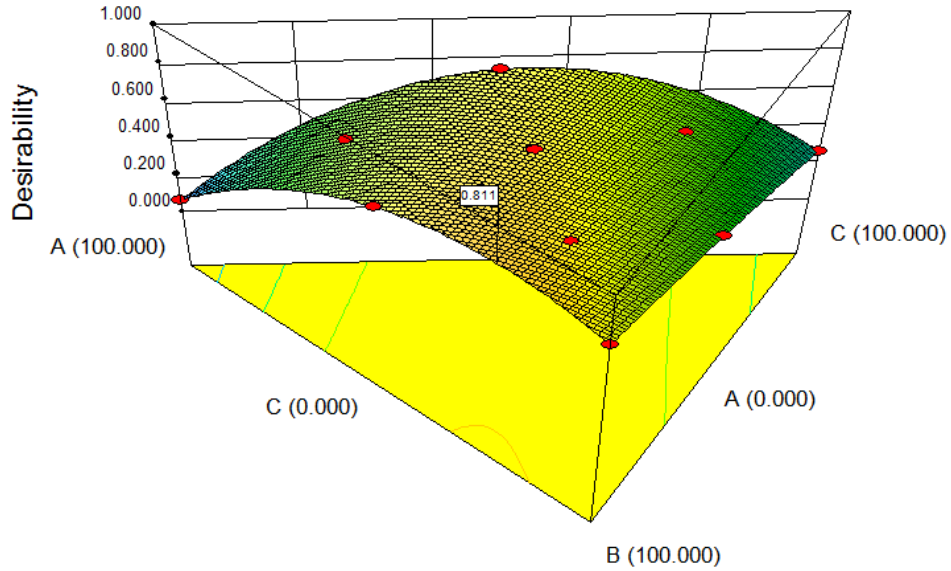


**Figure 11 The optimization point marked on the response surface graph, for set 1 with response 1.**

To test the accuracy of the response surface graph, the optimum formulation was made and a viscosity measurement was performed. The new PPD was called 397, and the graph from the viscosity measurement is seen in figure 12.
The viscosity graph for the optimization point for set 1 with response 1, gave a much poorer displacement of the temperature in viscosity graph, compared to the results from the best PPDs found, CdId 330 and EPT-2455, in the experimental plan. The temperature where the steep increase in viscosity occurred for CdId 397 was found at 5°C, while for CdId 330 the temperature was found at -5°C, which is a relatively large difference between the two chemicals.

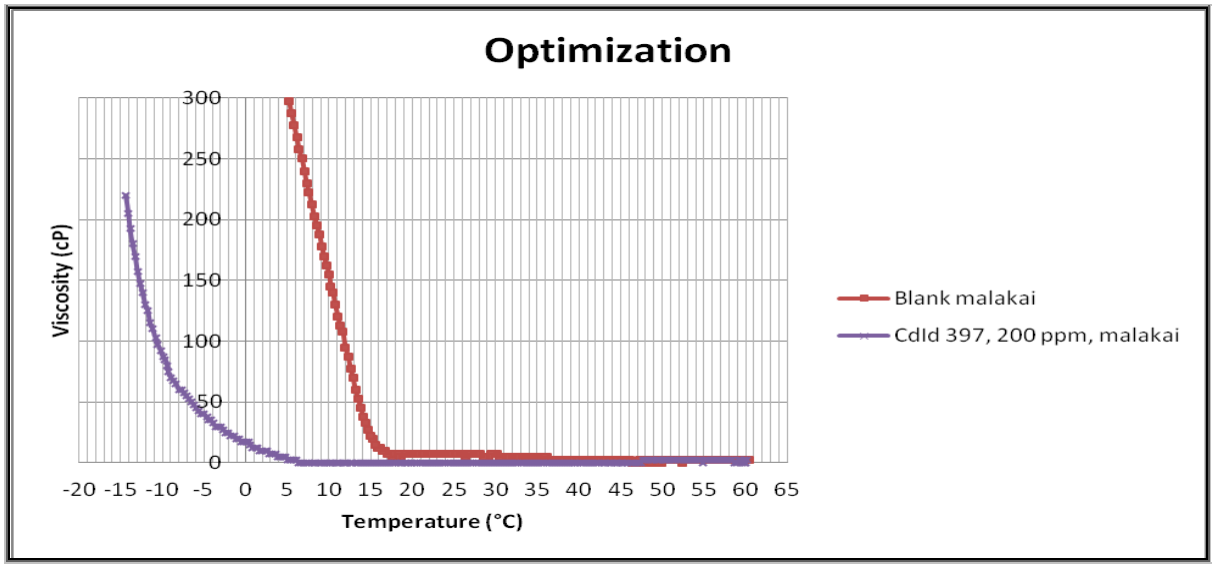


**Figure 12 The viscosity measurement for the optimization point of the DOE analysis for set 1 with response1.**

The response data obtained from the viscosity measurement for the optimum formulation chemical, CdId 397, was put into the Design-Expert, to be able to see how the response data for CdId 397

change the response surface graph. The contour map and the 3-dimensional response surface graph are shown in figure 13 and 14.

The low response value obtained from the viscosity measurements made the response surface graph decline near the area with component B. The adding of the new response data lead to a new optimization point towards component A, which is mainly of EPT-2454. However EPT-2454 gave the poorest response values in all the viscosity measurements for the sets, which therefore weaken the reliability for the new optimization point.

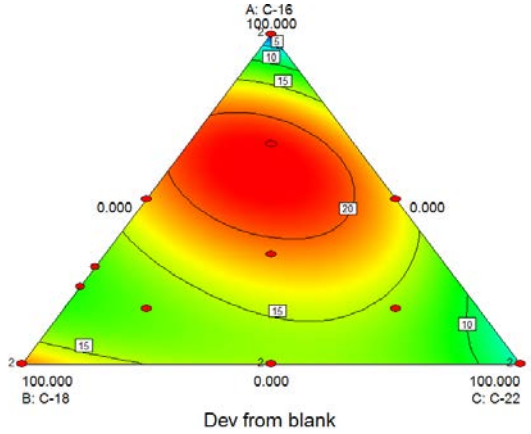


**Figure 13 The contour map changes after optimum PPD was added, for the set 1 with response 1.**

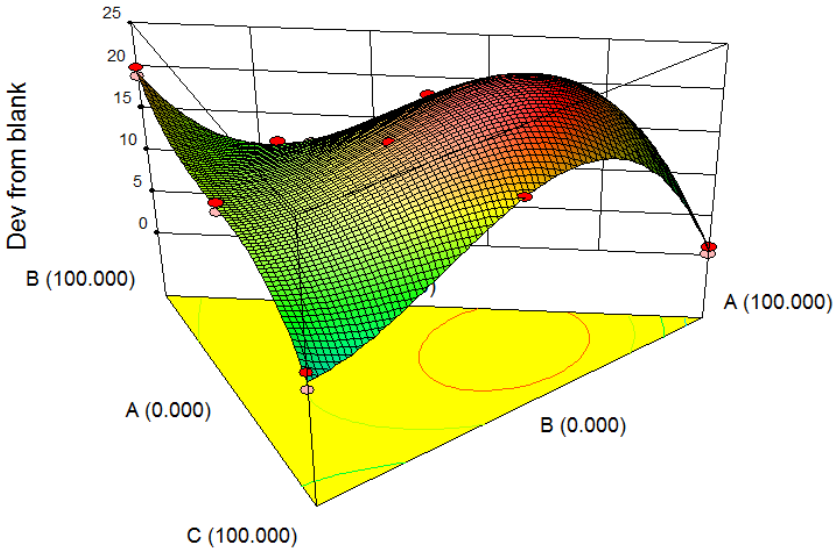


**Figure 14 The change of the response surface graph after optimum PDD was added, for set 1 with response 1.**

## *4.3 Doe for the chemical set 1 with response 2: 50 cP limit*

The DOE analysis for the chemical set 1 for response 2 is performed in this section.
The DOE analysis started with finding the best model to describe the measured response data for the set 2, in the fit summary section. The model suggested by Design-Expert was the quadratic.

**Diagnostics**

Statistics analyses are performed on the suggested quadratic model for chemical set 1 with response 2 in the diagnostic section, to show how well the model describes the measured response data.

**Normal plot**

The normal plot of residuals shows that almost all the measured response data are located closed to the line, expect for one point, as seen in figure 15 below. This response data point is run 8, the chemical CdId 330, which is the PPD that gave the best displacement temperature for the viscosity measurements. There have been performed three replicates for the viscosity measurements for CdId 330, so there should be no error with the response data obtained.
The normal plot shows also a tendency of a S-form, however transformation were not recommended by the Box-Cox plot.

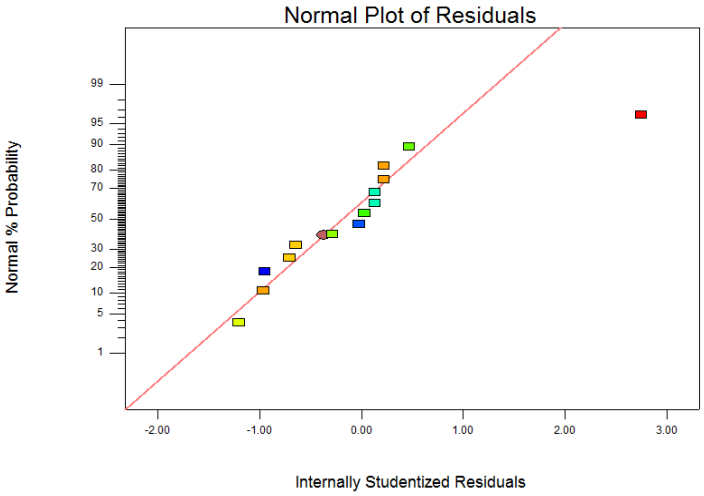


**Figure 15 The normal plot of residuals for set 1 with response 2.**

**Residuals vs. predicted plot**

The residuals versus the predicted plot in figure 16, shows a random scatter of the residuals, which indicates that the residuals fit the suggested model well. The red residual data point represents the chemical, CdId 330, which also in this plot deviates slightly from the rest of the residual points, however the point is inside the boundary lines.

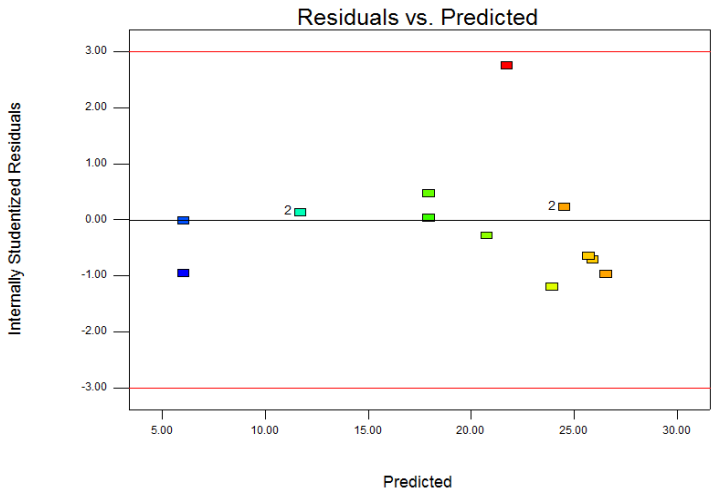


**Figure 16 The residuals vs. predicted plot for the set 1 with response 2.**

### Residuals vs. run plot

The residuals versus the run order plot shows in general a random scatter for the experimental run order, where all the residuals are found inside the boundary lines. Again the run 8, i.e. CdId 330, varies compared to the rest of the residuals, as seen in figure 17 below.

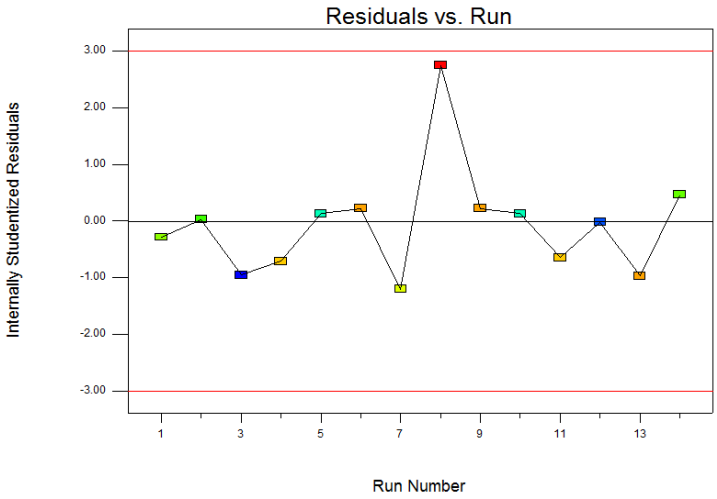


**Figure 17 The residuals vs. run plot for the set 1 with response 2.**

### Predicted vs. actual plot

The predicted versus the actual plot indicates that the measured response points are in general randomly scattered and follows the predicted values for the suggested model. However there are more measured response data points found at higher values (figure 18).

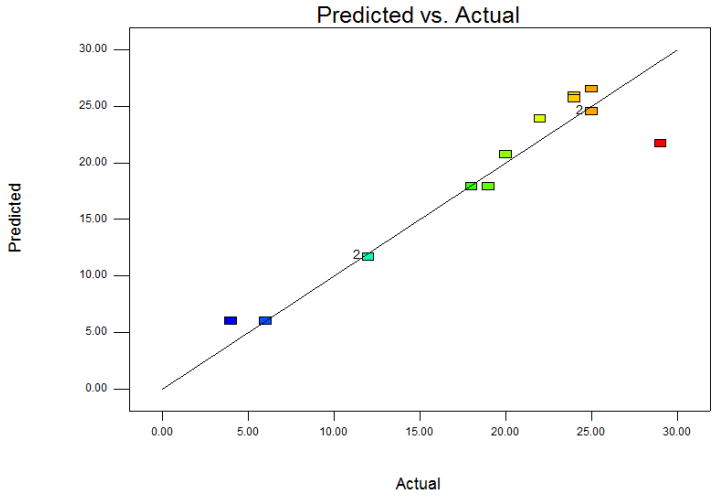


**Figure 18 The predicted vs. actual plot for the set 1 with response 2.**

### Box-Cox plot

The Box-Cox plot below in figure 19, shows that there is no need for any transformation for the measured response data, and they can be used as entered.

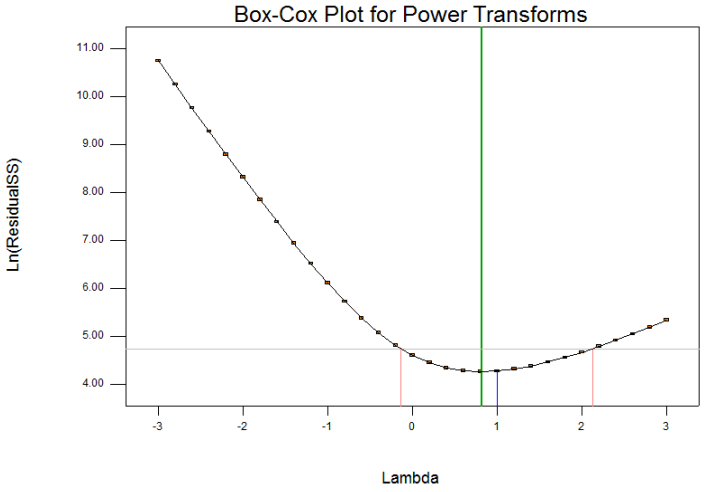


**Figure 19 The Box-Cox plot for the set 1 with response 2.**

### Influence

The different influence plots are found in figure 20 on the next page. The externally studentized residual plot and the DFFITS versus run plot, shows that the response value for run 8 are an outlier point. The response point is high over the boundary line for both the plots, which means that this point will have a large influence on the suggested model. However the point has been investigated and new replicates made (figure 10 in chapter 4), which indicated no error related to the point. The effect of the PPD on the temperature displacement of the viscosity measurement are much higher compared to the other PPDs in the set 1, and therefore deviates from the other response values.

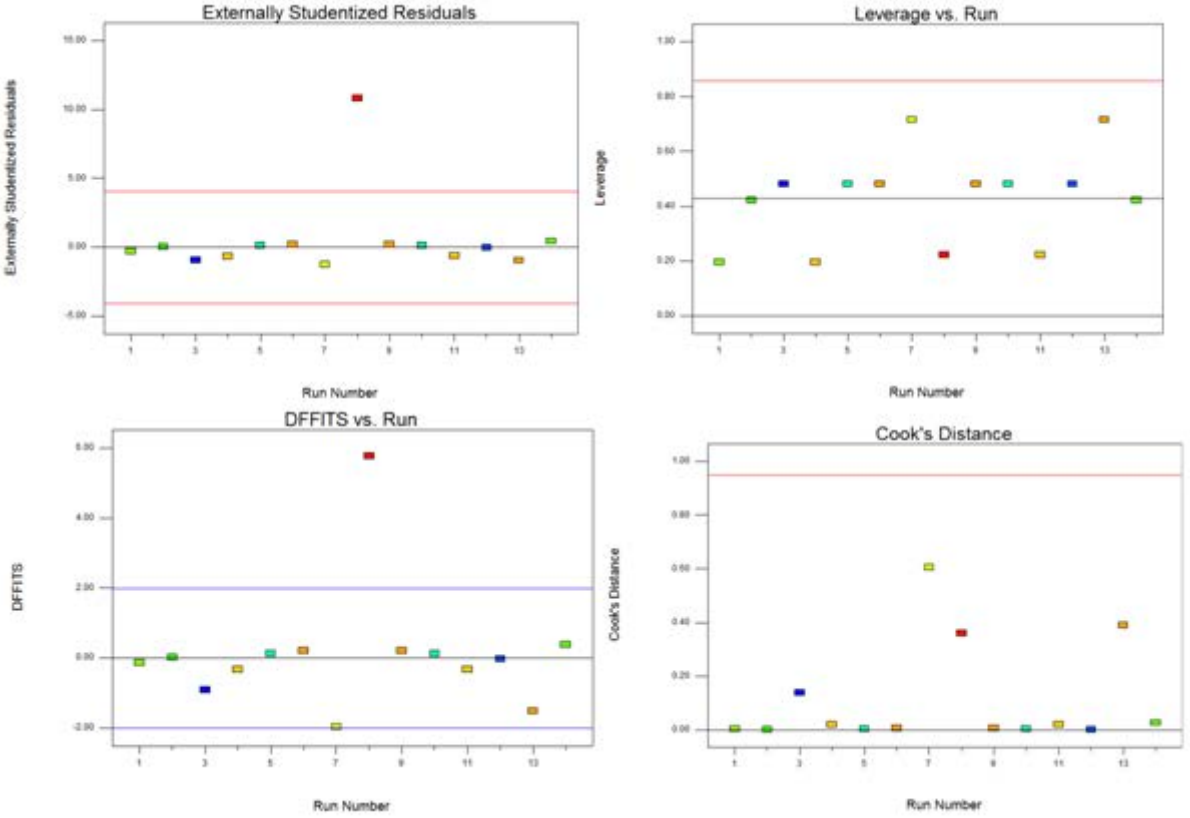


**Figure 20 The different influence plots for the set 1 with response 2.**

### Model graphs

The contour map and response surface graph for the suggested model are shown in figure 21 below. The figures indicates that the best interaction of the different components in the set 1 are between component A and B, i.e. EPT-2455 and EPT-2454, however the graph incline more towards component B, EPT-2455. This is similar to the result found from the first set with response 1, which implies that the different responses correlate to each other, as assumed.

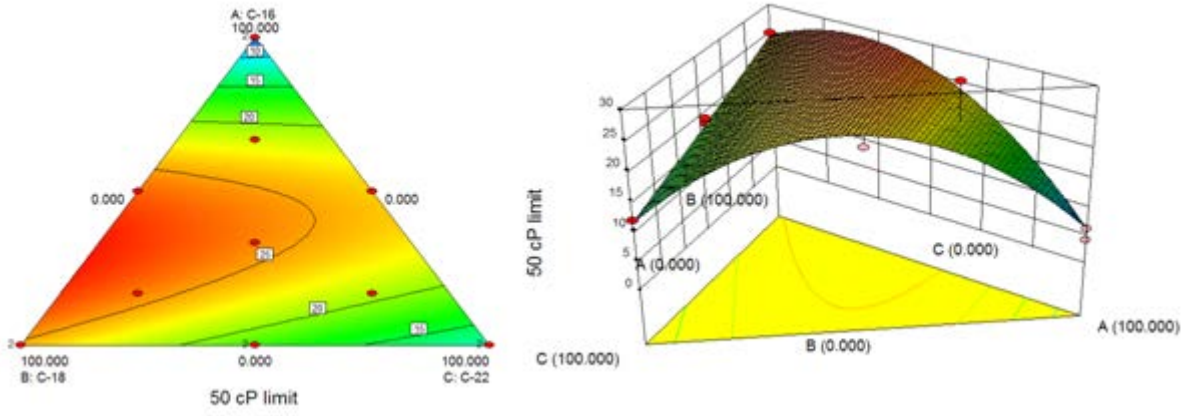


**Figure 21 The contour map and the response surface graph, for set 1 with response 2.**

**Optimization**

The optimization of the response surface graph gave an optimum formulation of the PPD with alkyl side chains of 29,48% of C16 and 70,52% of C18 length, on the polymer backbone (table 4). The optimum formulation for response 2, do not differ much from the optimum formulation found for response 1, which was 23,44% for C16 and 76,56% for C18, for set 1.

The optimum point is marked on the contour map in figure 22 and on the response surface graph in figure 23.

**Table 4 The formulation of the optimum point from the response surface graph, for set 1 with response 2.**

| Solutions | | | | | | | |
|---|---|---|---|---|---|---|---|
| Number | C-16 | C-18 | C-22 | Dev from blar | 50 cP limit | Desirability | |
| 1 | 29.478 | 70.522 | 0.000 | 20.1634 | 28.4365 | 0.873 | Selected |

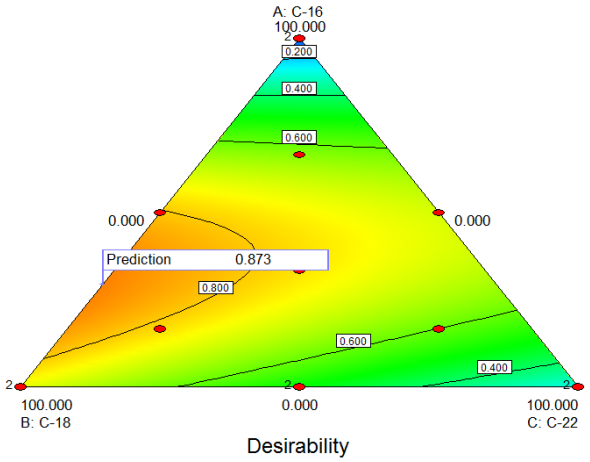


**Figure 22 The optimization point marked on the contour map, for set 1 with response 2.**

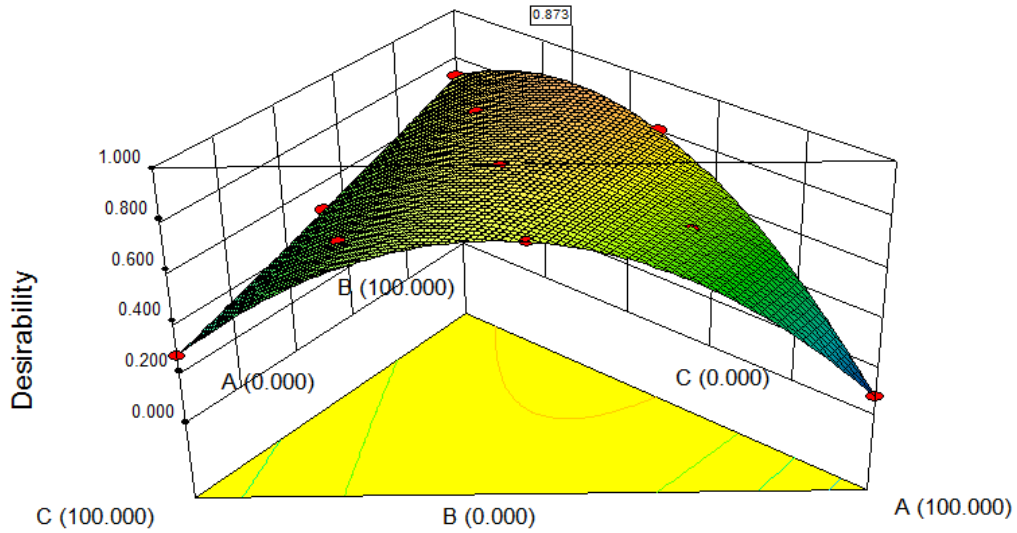


**Figure 23 The optimization point marked on the response surface graph, for set 1 with response 2.**

The optimal formulation found from the optimization of the response surface graph, for set 1 with response 2, was made and tested on the viscometer. The viscosity result for the optimal formulation, called CdId 398, is shown in the viscosity graph in figure 23.
The 50 cP limit for the optimal formulated PPD, compared to the blank 50 cP limit, is 21°C. This value is much lower compared to the best PPD found in the experimental plan, which was CdId 330, and had a 50 cP limit of 29 °C, compared to the blank.

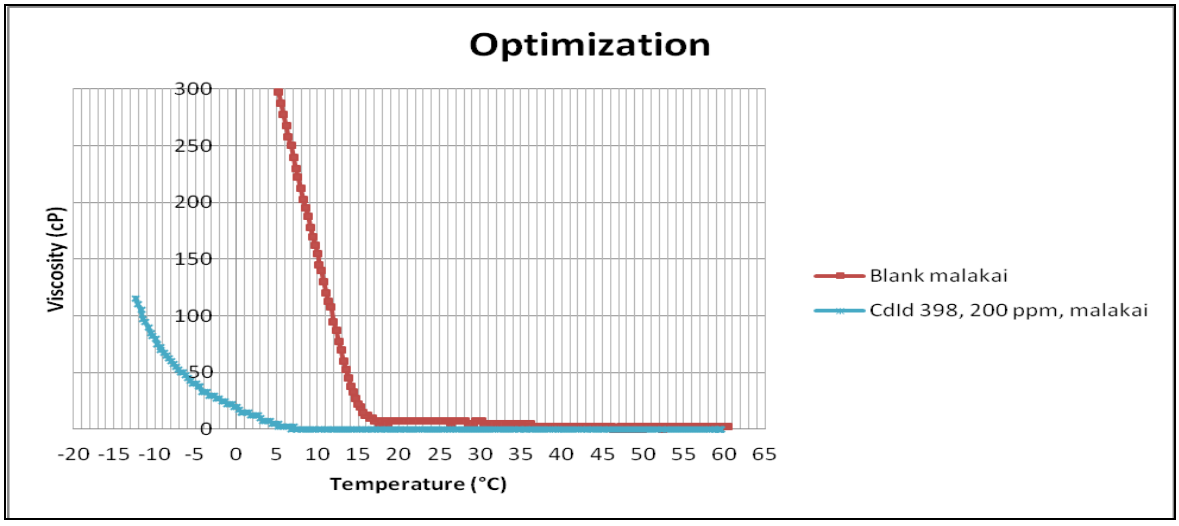


**Figure 23 The viscosity measurement for the optimal formulation for set 1 with response 2.**

The new response value for the optimal PPD, CdId 398, was added to the experimental plan in Design-Expert. From this a new surface graph was made, where the optimal PPD was included. The contour map (figure 24) and the response surface graph (figure 25) with the optimal PPD, caused a decrease in the formulation effects towards the component B, i.e. EPT-2455. The new optimization point seems to incline in the middle of the response surface graph and up towards component A, EPT-2454, which was the same trend shown for set 1 with response 1.

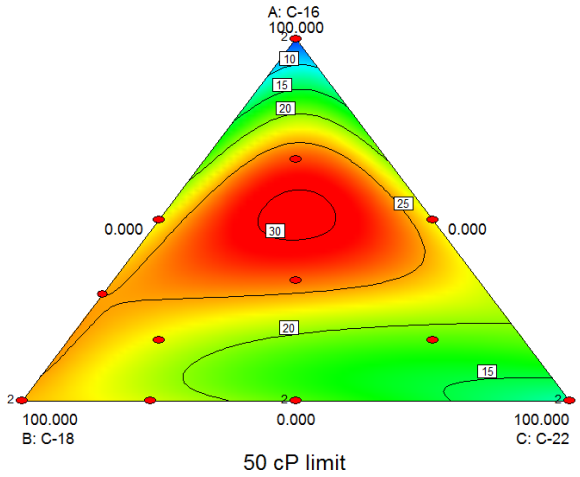


**Figure 24 The change of the contour map when the optimal response value was included, for set 1 with response 2.**

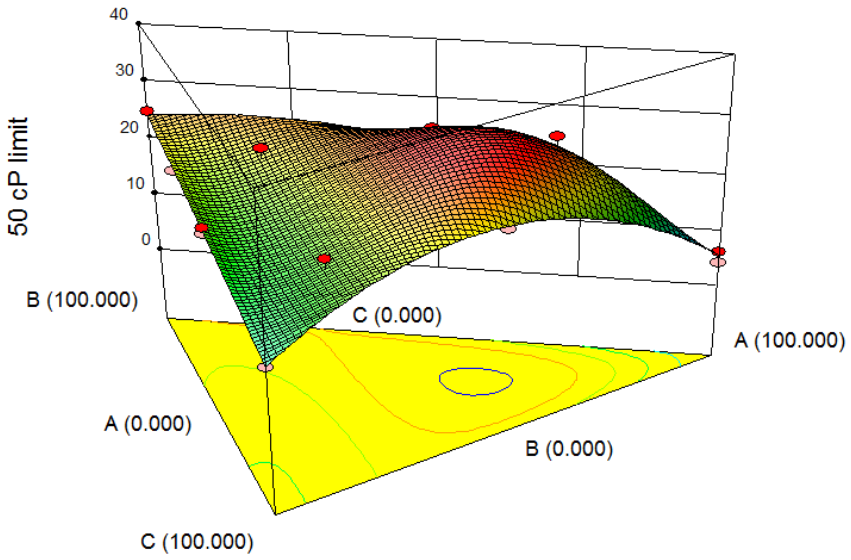


**Figure 25 The change in the response surface graph, when the optimal response value was included, for set 1 with response 2.**

## *4.4 DOE for the chemical set 2 with Response 1: Deviation from blank*

The DOE analysis for the chemical set 2, consisting of different combination of the PPDs polymers EPT-2454, EPT-2455, and EPT-2456, which have respectively the alkyl side chain length of C16, C18 and C22. The different component combinations tested in the experimental plan and responses measured were given in table 2 earlier.
The suggested model to describe the response data was provided in the fit summary section, and was the quadratic model.

**Diagnostics**

The different diagnostic plots are briefly described in this section, and will show how well the measured responses fit the selected model.

**Normal plot**

The normal plot of residuals is evenly and randomly spread around the line, which indicates that they are normally distributed, as seen in figure 26.

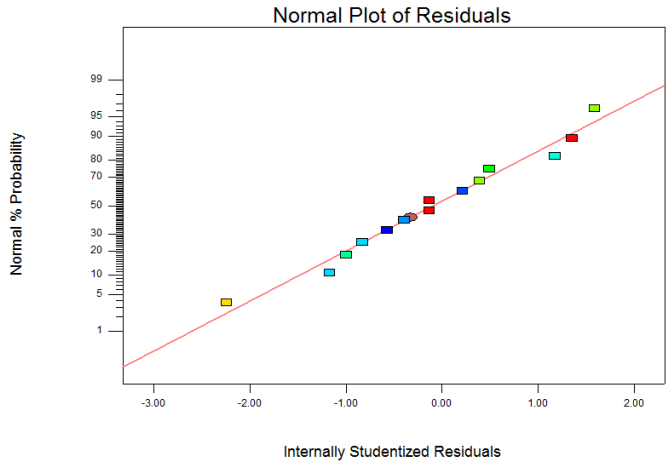


**Figure 26 The normal plot of residuals for set 2 with response 1.**

**Residuals vs. predicted plot**

The residuals versus predicted plot shows that the measured response data points are randomly and evenly spread around the predicted values for the selected model (figure 27). The assumption of a constant variance is then valid.

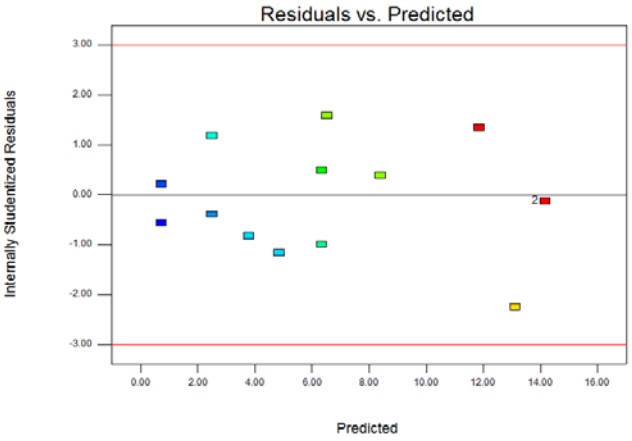


**Figure 27 The residuals versus the predicted plot for set 2 with response 1.**

### Residuals vs. run plot

The residuals plotted with the experimental run order, shows a small decreasing trend in the performance of the experiments, mainly due to the low value for the yellow point (figure 28). However all the residuals are in between the boundary lines, therefore of little concern.

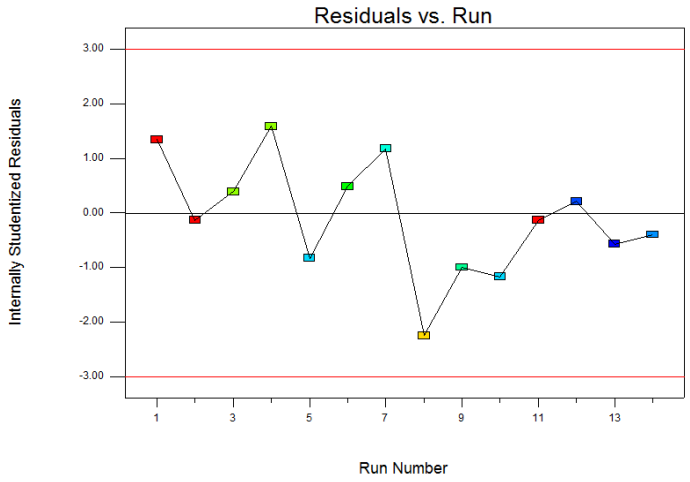


**Figure 28 The residuals versus run order plot for set 2 with response 1.**

### The predicted vs. actual plot

The measured response data points are spread evenly and randomly around the predicted values for the suggested model, as seen in figure 29. The plot indicates that the model selected manage to describe the measured response data well.

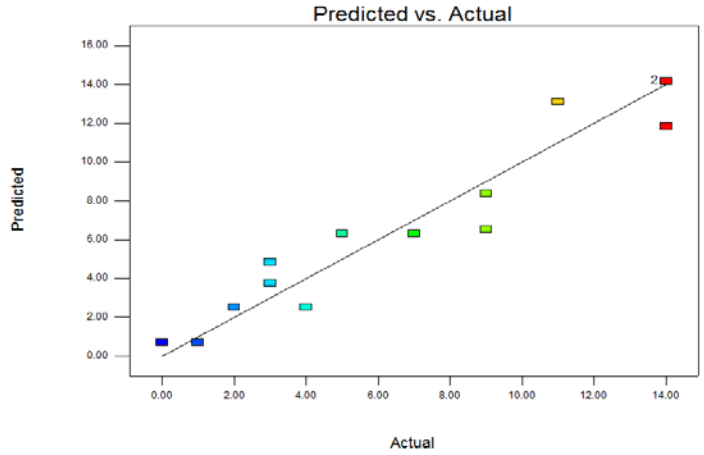


**Figure 29 The predicted versus actual plot for set 2 with response 1.**

### Box-Cox plot

The Box-Cox plot illustrates that there is no need for transformation of the entered response data (figure 30).

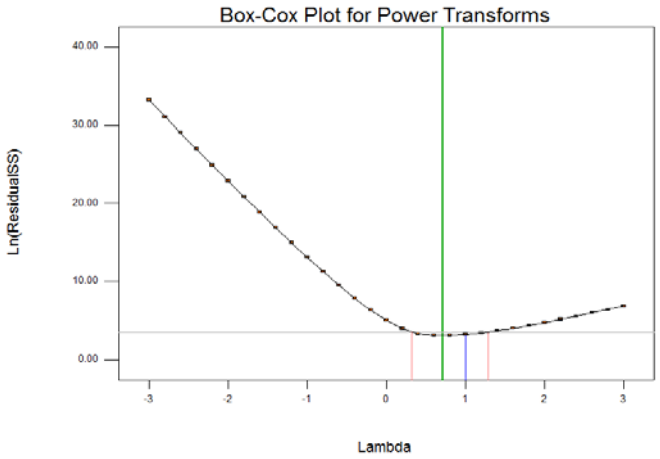


**Figure 30 The Box-Cox plot for set 2 with response 1.**

### Influence

From the influence plots there is one outlier point in the DFFITS in run plot and in the Cook's distance plot, which is located outside the boundary lines. The response data point are called run 1, which was the PPD that showed the best temperature displacement in the viscosity measurements, for set 2 with response 1. The high response temperature for the run 2 chemical, compared to the other chemicals in the set 2, is the reason for the influence of this point.

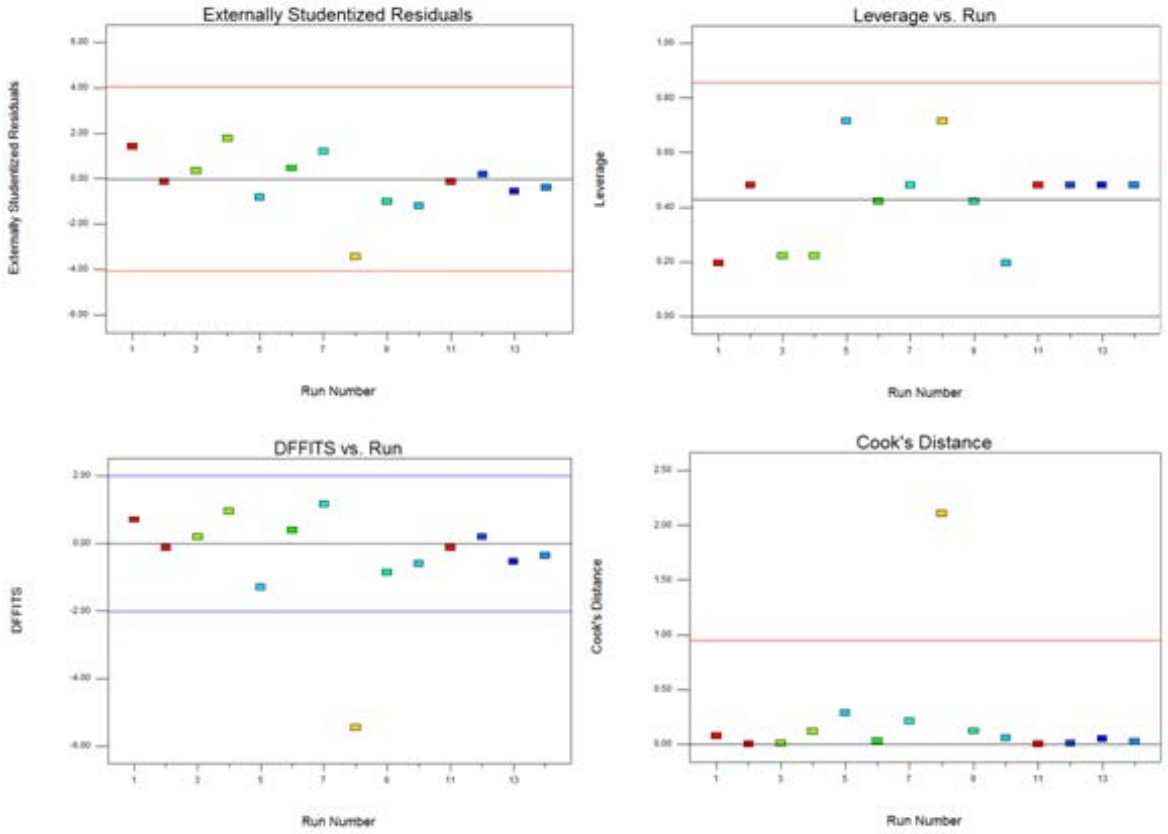


**Figure 31 The influence plots for set 2 with response 1.**

### Models graphs

The contour map and response surface graph for the selected model are shown in figure 32 below. The graphs indicates an optimal formulation of the components between A and B, respectively EPT-2454 and EPT-2455, however the incline is mostly towards the EPT-2455. This is the same trend that was found in the set 1 for both the responses.

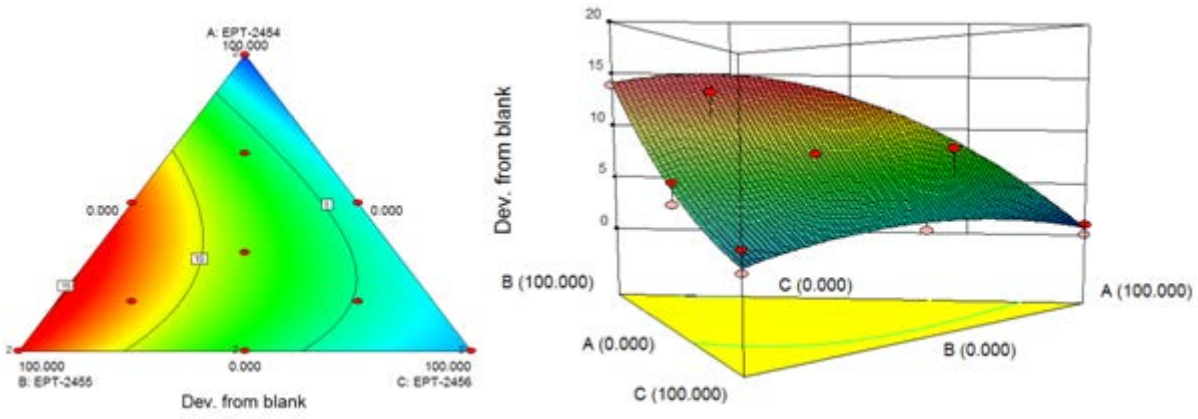


**Figure 32 The contour map and response surface graph for set 2 with response 1.**

**Optimization**

The optimization point from the response surface graph was a combination of 20,43% EPT-2454 and 79,66% of EPT-2455 (table 5). These values are similar to what was found for the set 1 and the responses. The optimization point is marked in the contour map and the response surface graph in figure 33 and 34.

The optimization point fits well with the measured response values found from the viscosity measurements, where EPT-2455 and run 1 gave the best PPDs effects.

**Table 5 The optimization point formulation for set 2 with response 1.**

| Solutions | | | | | | | |
|---|---|---|---|---|---|---|---|
| Number | EPT-2454 | EPT-2455 | EPT-2456 | Dev. from bla | 50 cP limit | Desirability | |
| 1 | 20.344 | 79.656 | 0.000 | 15.1095 | 29.1577 | 0.889 | Selected |

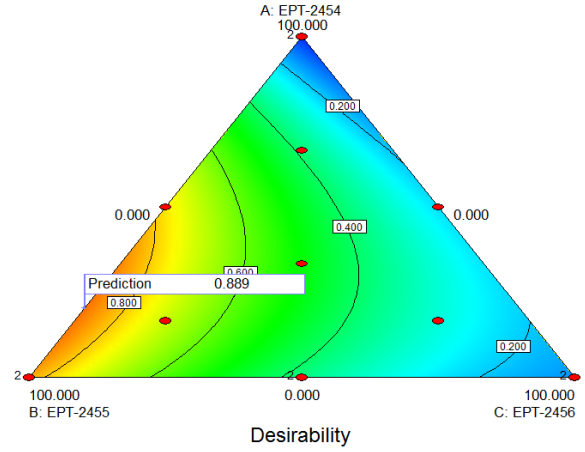


**Figure 33 The optimization point shown in the contour map for set 2 with response 1.**

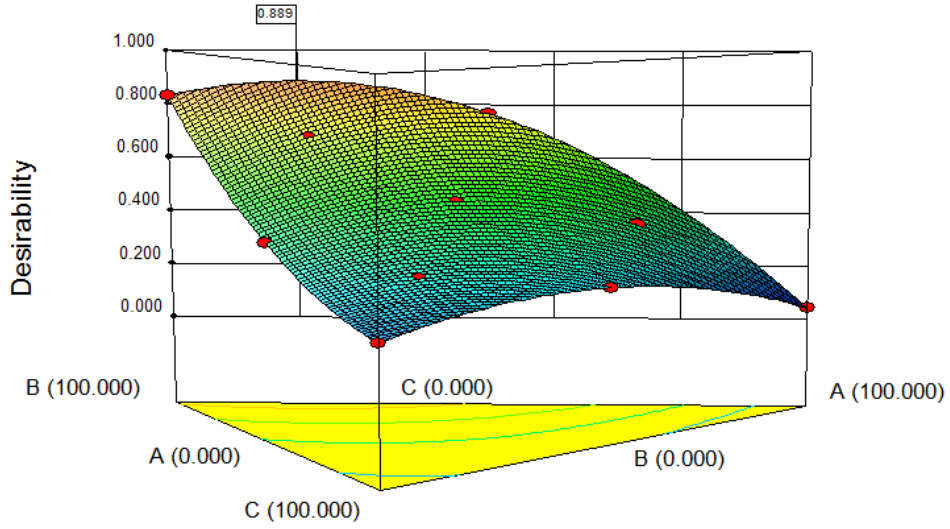


**Figure 34 The optimization point shown in the response surface graph for set 2 with response 1.**

The optimal formulation was made, and tested on the viscometer, as seen in figure 35 below. The optimal formulated PPD gave a temperature displacement of the viscosity curve of 13 °C, compared to the blank. The best displacement temperature where found for EPT-2455 and run 1, which was both at 14 °C, compared to the blank. The optimal formulated PPD are therefore not better then these two, however the point showed good effect as PPD, compared to the results from the other optimization points for the set 1.

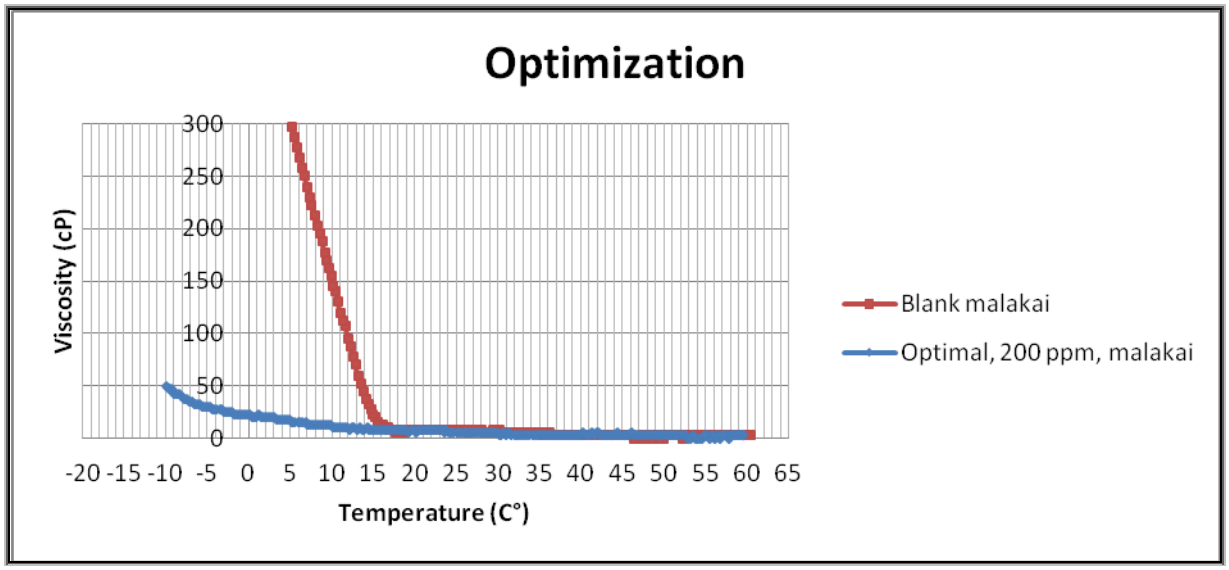


**Figure 35 The viscosity measurement for the optimal PPD for set 2 with response 1.**

The response value from the optimal PPD was added to the experimental plan, and the effect of the optimal PPD on the contour map and response surface graph is shown in figure 36 and 37 below. When the optimal PPD was added to the response surface graphs, it caused a larger incline of the optimization point towards the component B, i.e. EPT-2455.

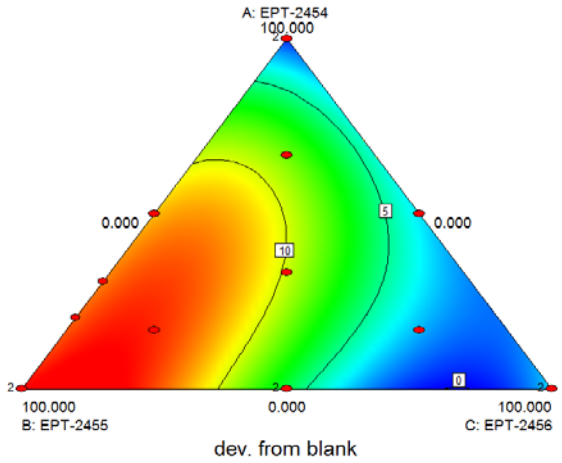


**Figure 36 The change in the contour map caused by the optimal PPD for set 2 with response 1.**

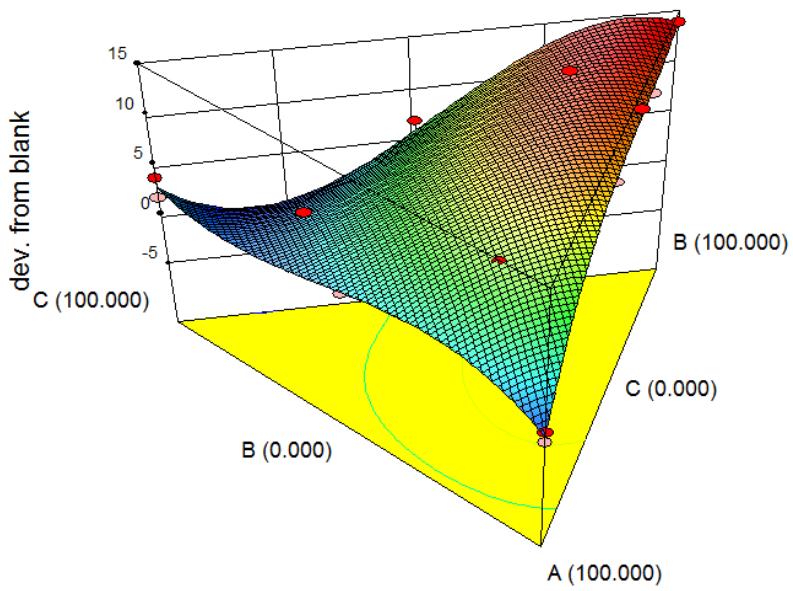


**Figure 37 The change in response surface graph caused by the optimal PPD for set 2 with response 1.**

## *4.5 DOE for the chemical set 2 with Response 2: 50 cP limit*

In this section the DOE analysis for the chemical combinations in set 2, for the response 2, are preformed. In the fit summary section the suggested model which fitted the measured response data best was the quadratic model.

**Diagnostics**

The measured response data are check to see if they fit the selected quadratic model well in the diagnostic section.

**Normal plot**

The normal plot of the residuals shows an evenly and random scatter where the measured data point in general follow the line well. However there is one point that deviates a little from the rest of the points, which is the yellow point at the right top corner. This point represent the measured response value for the run 4, which is a chemical solution containing 66,66% EPT-2454, 16,67% EPT-2455 and 16,67% EPT-2456. The measured response value for run 4 was 24°C for the 50 cP limit, compared to the blank. The high value for this mixture can be the reason this response point deviates from the other response points.

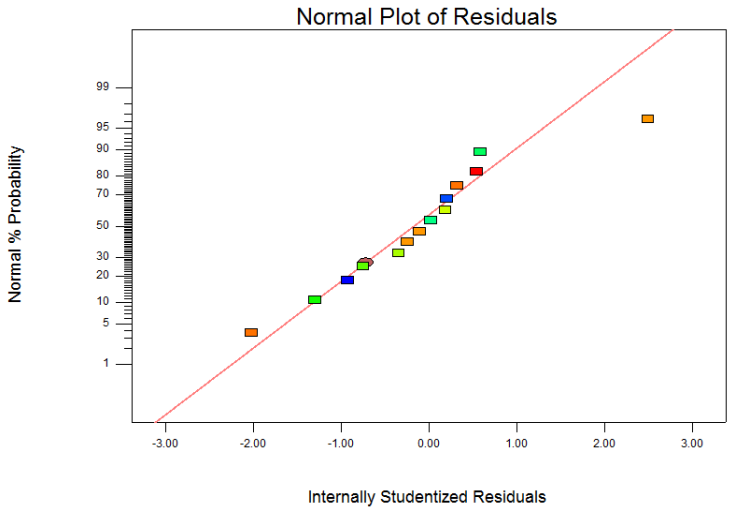


**Figure 38 The normal plot of residuals for set 2 with response 2.**

**Residuals vs. predicted plot**

The residuals versus predicted plot shows the residuals being randomly scattered (figure 39), and no sign of any trends are shown, which means the assumption of a constant variance is good.

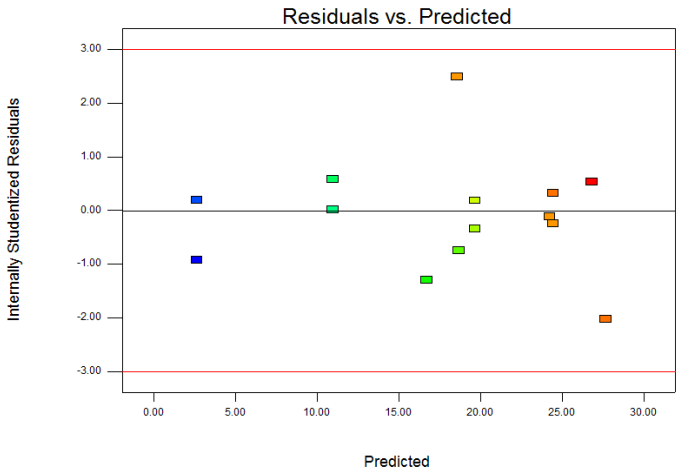


**Figure 39 The residuals versus predicted plot for set 2 with response 2.**

**Residuals vs. run plot**

The experimental run order for the residuals shows in general a random scatter within the boundary lines (figure 40), however also in this plot the run 4 shows are larger value compared to the other residuals.

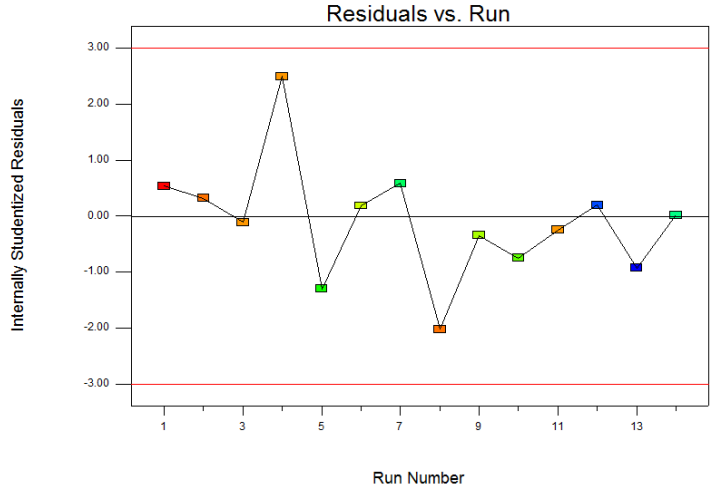


**Figure 40 The residuals versus the run order for set 2 with response 2.**

**Box-Cox plot**

The Box-Cox plot in figure 41 implies that the entered response data do not need any transformation.

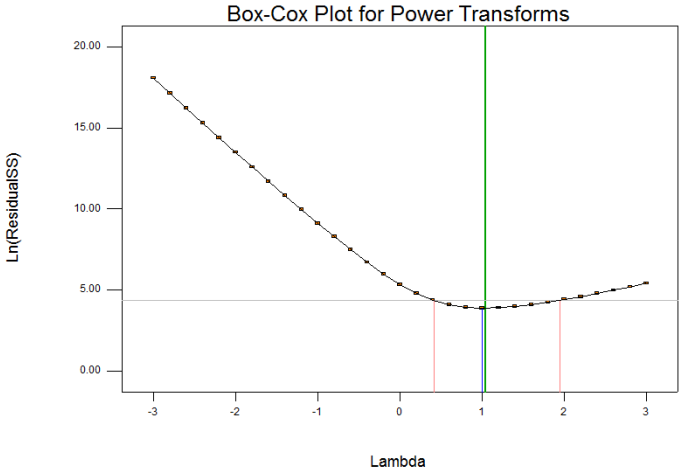


**Figure 41 The Box-Cox plot for set 2 with response 2.**

**Influence**

From the influence plots showed in figure 42, there are found some outlier points in the externally studentized residuals, DFFITS vs. run plot and the Cook's distance plot. The outlier points found are for the measured responses of run 1, 2 and 11. These measurements were checked, but showed no signs of error. Run 2 and 11 are the response values for EPT-2455, where run 11 is a replicate. The run 1 is a mixture of 16,67% EPT-2454, 66,66% EPT-2455 and 16,67% EPT-2456. These were the chemicals which gave the highest temperature values in the 50 cP limit, and can therefore cause more influence in the model.

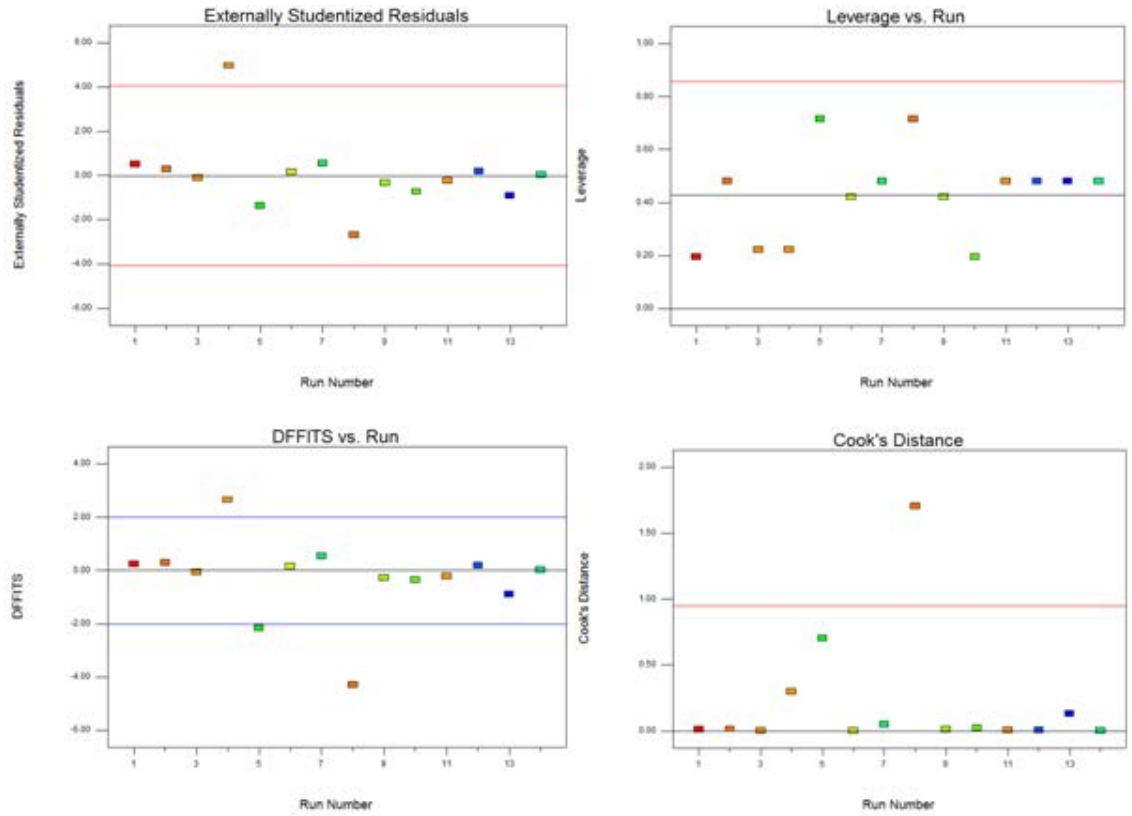


**Figure 42 The influence plots for set 2 with response 2.**

### Model graphs

The contour map and the response surface graph for the selected model are shown in figure 43 below. From the graph the optimal formulation point for the components are found between component A and B, and inclining towards the component B, which is the EPT-2455.

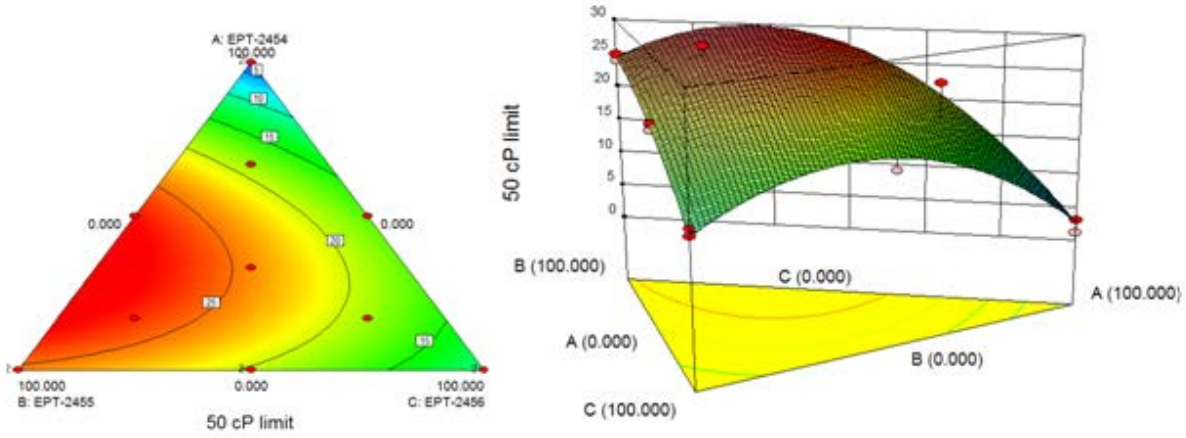


**Figure 43 The contour map and the response surface graph for set 2 with response 2.**

**Optimization**

The optimization point found from the response surface graph are a mixture with 30,72% EPT-2454 and 69,28% EPT-2455 (table 5), which is similar to the optimization points found for the other sets and responses.

**Table 5 The optimization point formulation for set 2 with response 2.**

| Solutions | | | | | | | |
|---|---|---|---|---|---|---|---|
| Number | EPT-2454 | EPT-2455 | EPT-2456 | Dev. from bla | 50 cP limit | Desirability | |
| 1 | 30.719 | 69.281 | 0.000 | 14.8658 | 29.7652 | 0.959 | Selected |

The optimization point is marked in the contour map and the response surface graph shown in figure 44 and 45.

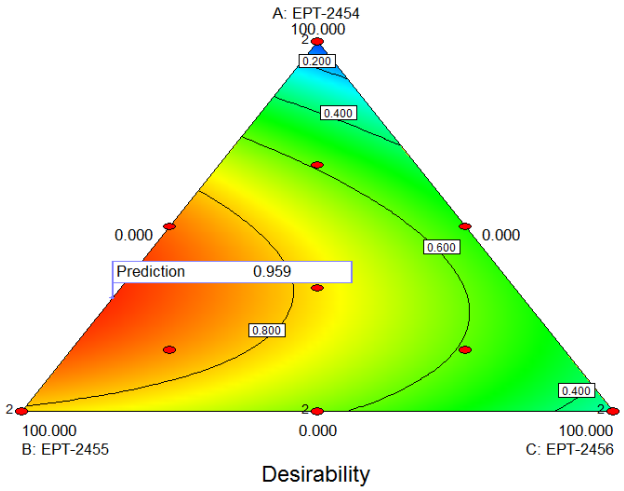


**Figure 44 The optimization point marked in the contour map for set 2 with response 2.**

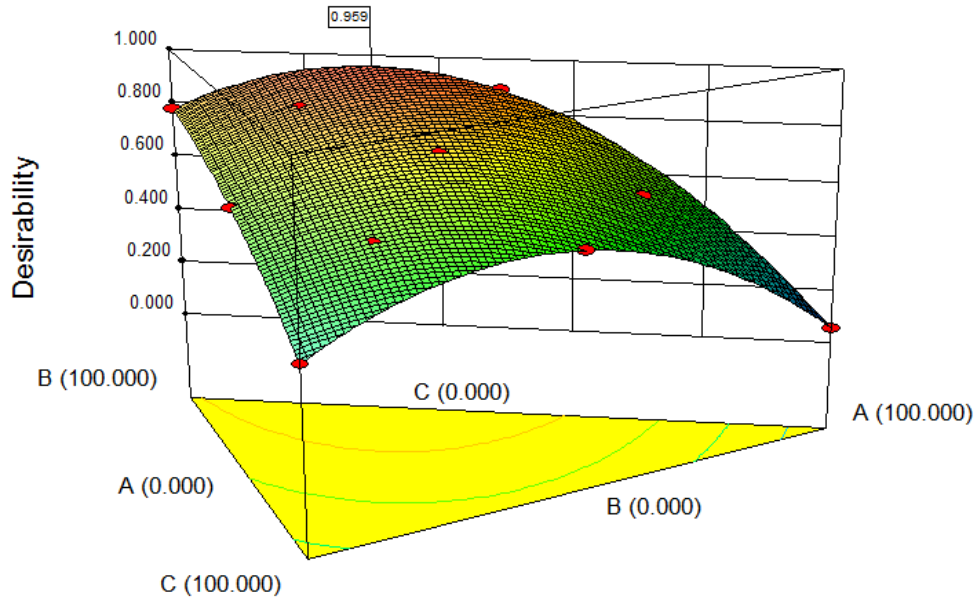


**Figure 45 The optimization point marked in the response surface graph for set 2 with response 2.**

The optimal formulation point for the response 2 was made, and tested on viscometer (figure 46). The viscosity measurements for the optimal PPD gave a response value of 24°C for the cP 50 limit, compared to the blank. The PPD in the experimental plan in set 2 with response 2, which gave the best cP limit value, was run 1, with 28 °C. This is higher value than compared to with the optimal PPD.

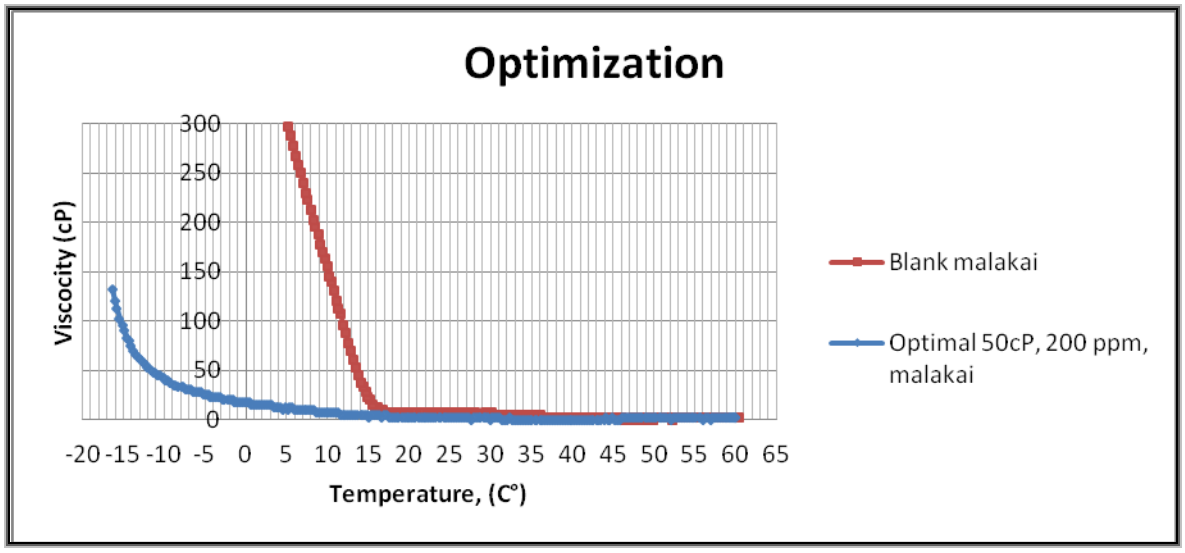


**Figure 46 The viscosity graph for the optimal PPD compared with the blank, for set 2 with response 2.**

The optimal formulation PPD was added to the experimental plan, and the changes this made in the contour map and the response surface graph are seen in figure 47 and 48.
The adding of the optimal PPD to the response surface graph did not lead to any large changes. The new optimal point is still between the component A and B, however it is slightly more towards the component B now, i.e. the EPT-2455. The result is similar to the result found in the response 1 for set 2, which indicates that there is little change in the response surface graph for the different ways of reading the temperature displacement of the viscosity graphs.

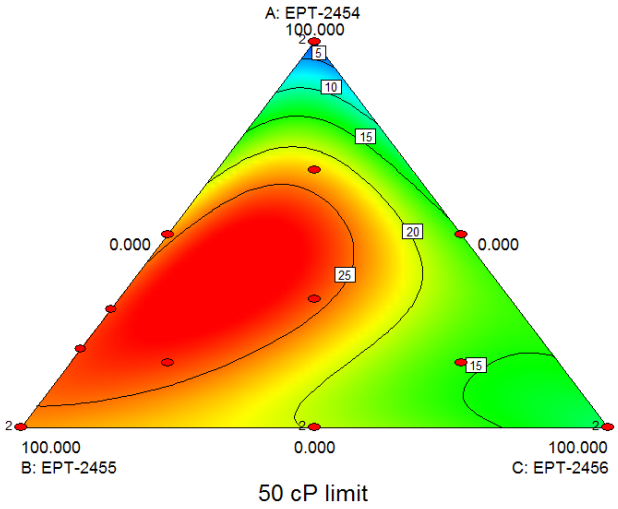


**Figure 47 The change in the contour map caused by adding the optimal PPD response value, for set 2 with response 2.**

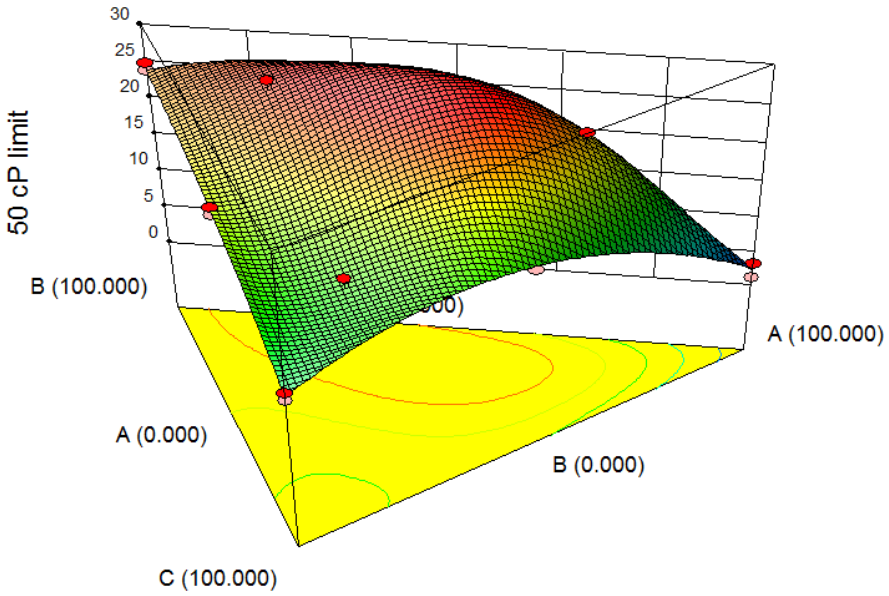


**Figure 48 The change in the response surface graph caused by the added optimal PDD response value, for set 2 with response 2.**

## *4.6 Conclusion*

DOE suggested the quadratic model for the different chemical sets and the responses. The model managed to describe the measured responses good, with little variation from the predicted values from the model compared to the measured response values. There were some outlier points in the influence plot, but they were usually caused by the response data points with the highest temperature displacement in the viscosity measurements.

The results from the response surface graphs and the optimization points for the different DOE analysis showed similar results, both for the different sets and the responses. It appears that the different ways the two mixture design was prepared, did not make much changes on the response surface graph results. In general for both sets, the tendencies for the measured responses showed an optimal formulation of the different components between EPT-2454 and ETP-2455, where the optimum increased towards EPT-2455.

The optimization points found from the response surface graph were made and tested on the viscometer. Some of the mixture combinations of the different components in the sets appeared to have an optimal PPD performance. However, the result obtained from the viscosity tests for the optimal formulated chemicals did not correspond well with the optimization points found from the response surface graphs. The optimization points were in general much lower than expected from the response surface graphs, and lead to new optimization points. The new points suggested were either towards EPT-2454, which in generally was a worse PPD, or towards the EPT-2455, which in all cases appeared to be one of the best PPDs used in the experiments.

Overall the different DOE analysis did not seem to find an optimal combination for the different components in the sets, which were any better than EPT-2455 alone, when tested on crude Malakai. However Design-Expert has shown to be an effective and simple method for performing experiments where the main objective is to find the optimal formulation in a mixture.

## *References*


1. Alben, K.T., *Books and Software: Design, analyze, and optimize with Design-Expert.* Analytical Chemistry, 2002. **74**(7): p. 222 A-223 A.
2. Solvason, C.C., et al., *Efficient Visual Mixture Design of Experiments using Property Clustering Techniques.* Industrial & Engineering Chemistry Research, 2009. **48**(4): p. 2245-2256.